ADSORPTION OF ACID RED 1 ON SILICA- AND

POLYMER-BASED ADSORBENTS

Kanlayanee Kajsanthia

A Thesis Submitted in Partial Fulfillment of the Requirements for the

Degree of Doctor of Science in Chemistry

Suranaree University of Technology

Academic Year 2018

การดูดซับแอซิดเรด 1 บนตัวดูดซับจากซิลิกาและพอลิเมอร์

นางสาวกัลยาณี กาจสันเทียะ

วิทยานิพนธ์นี้เป็นส่วนหนึ่งของการศึกษาตามหลักสูตรปริญญาวิทยาศาสตรดุษฎีบัณฑิต

สาขาวิชาเคมี

มหาวิทยาลัยเทคโนโลยีสุรนารี

ปีการศึกษา 2561

ADSORPTION OF ACID RED 1 ON SILICA- AND

POLYMER-BASED ADSORBENTS

Suranaree University of Technology has approved this thesis submitted in partial fulfillments of the requirement for the Degree of Doctor of Philosophy.

Thesis Examining Committee
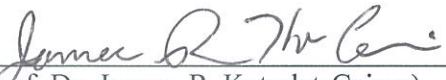
_____
(Prof. Dr. James R. Ketudat-Cairns)

Chairperson

_____
(Asst. Prof. Dr. Sanchai Prayoonpokarach)

Member (Thesis Advisor)
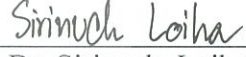
_____
(Asst. Prof. Dr. Sirinuch Loiha)

Member

_____
(Prof. Dr. Jatuporn Wittayakun)

Member

_____
(Asst. Prof. Dr. Theeranun Siritanon)

Member

_____   _____
(Prof. Dr. Santi Maensiri)   (Assoc. Prof. Dr. Worawat Meevasana)

Vice Rector for Academic Affairs   Dean of Institute of Science

and Internationalization

กัลยาณี กาจสันเทียะ : การดูดซับแอซิดเรด 1 บนตัวดูดซับจากซิลิกาและพอลิเมอร์ (ADSORPTION OF ACID RED 1 ON SILICA- AND POLYMER-BASED ADSORBENTS) อาจารย์ที่ปรึกษา : ผู้ช่วยศาสตราจารย์ ดร. สัญชัย ประยูรโภคราช, 129 หน้า.

ในงานวิจัยนี้มีจุดมุ่งหมายหลักในการศึกษาการดูดซับของแอซิดเรด 1 โดยใช้ตัวดูดซับ ต่างๆ ได้แก่ มีโซพอรัสซิลิกาที่ดัดแปรด้วยหมู่อะมิโน อนุภาคซิลิกาที่มีรอยพิมพ์ประทับโมเลกุล และไนลอน/ซิลิกาคอมโพสิท   นำตัวดูดซับที่เตรียมได้ไปพิสูจน์เอกลักษณ์ด้วยกล้องจุลทรรศน์ อิเล็กตรอนแบบส่องผ่าน กล้องจุลทรรศน์อิเล็กตรอนแบบส่องกราด การเลี้ยวเบนของรังสีเอ็กซ์ การดูดซับและการคายซับของไนโตรเจนและสเปกโทรสโกปีฟูเรียร์ทรานส์ฟอร์มอินฟราเรด การ ทดลองการดูดซับทำโดยใช้ตัวดูดซับ 0.035 กรัม โดยได้มีการปรับเปลี่ยนความเข้มข้นของสีย้อม พี เอชของสารละลายสีย้อม เวลาในการดูดซับ และอุณหภูมิที่ใช้ในการทดลอง

มีโซพอรัสซิลิกาที่ดัดแปรด้วยหมู่อะมิโนสังเคราะห์ขึ้นด้วยกระบวนการโซล-เจล   แหล่ง ของซิลิกาที่ใช้คือเตตระเอทิลออโธซิลิเกท (ทีอีโอเอส)   แม่แบบมีโซพอรัสที่ใช้คือเซทิลเมทิล แอมโมเนียมโบรไมด์ อนุภาคที่ได้นำไปดัดแปรด้วย 3-อะมิโนโพรพิลไตรเอทอกซีไซเลน (เอพีทีอี เอส) ขนาดของอนุภาคมีเส้นผ่าศูนย์กลางประมาณ 1 ไมโครเมตร การดูดซับแอซิดเรด 1 ที่ 25.0 องศาเซลเซียสเข้าสู่สมดุลที่เวลา 1 ชั่วโมง พีเอชที่เหมาะสมเท่ากับ 2.0 และค่าความจุการดูดซับ เท่ากับ 139.6 มิลลิกรัมต่อกรัม การดูดซับเป็นไปตามแบบจำลองไอโซเทอร์มแบบฟรุนดลิชที่ช่วงสี ย้อมความเข้มข้นต่ำ และเป็นไปตามแบบจำลองไอโซเทอร์มแบบแลงเมียร์ที่ช่วงสีย้อมความเข้มข้น สูง   กระบวนการการดูดซับเกิดได้เองและเป็นกระบวนการดูดความร้อน   ระบบมีความไม่เป็น ระเบียบสูงขึ้นเมื่อเข้าสู่สมดุล จลนพลศาสตร์การดูดซับเป็นไปตามแบบจำลองปฏิกิริยาอันดับสอง เทียม

เพื่อเพิ่มความเลือกสรรของตัวดูดซับ ได้สังเคราะห์ตัวดูดซับมีโซพอรัสซิลิกาที่ดัดแปรด้วย หมู่อะมิโนที่มีรอยพิมพ์ประทับโมเลกุลด้วยวิธีโซล-เจล พื้นผิวของตัวดูดซับดัดแปรด้วยเอพีทีอีเอส ก่อนจะนำไปใช้ในกระบวนการรอยพิมพ์ประทับโดยใช้แอซิดเรด 1 เป็นแม่แบบ ตัวดูดซับที่ไม่มี รอยพิมพ์ประทับสังเคราะห์ด้วยขั้นตอนที่เหมือนกัน โดยปราศจากการเติมแม่แบบ ขนาดของตัวดูด

ซับที่ได้อยู่ที่ประมาณ 100 นาโนเมตรและกระจายตัวได้ดี การดูดซับของตัวดูดซับที่มีรอยพิมพ์
ประทับเป็นไปตามแบบจำลองไอโซเทอร์มแบบแลงเมียร์ กระบวนการการดูดซับเกิดได้เองและ
เป็นกระบวนการคายความร้อน ระบบมีความไม่เป็นระเบียบต่ำลงหลังจากการดูดซับเข้าสู่สมดุล
จลนพลศาสตร์การดูดซับเป็นไปตามแบบจำลองปฏิกิริยาอันดับสองเทียม ค่าความจุการดูดซับที่
25.0 องศาเซลเซียสของตัวดูดซับที่มีรอยพิมพ์ประทับและตัวดูดซับที่ไม่มีรอยพิมพ์ประทับเท่ากับ
36.9 และ 28.3 มิลลิกรัมต่อกรัม ตามลำดับ ค่าแฟคเตอร์การแยกของตัวดูดซับที่มีรอยพิมพ์ประทับ
สำหรับแอซิดเรด 1 เปรียบเทียบกับทาร์ทราซีน ซินคอน และซัลฟาซาลาซีนเท่ากับ 30.5 2.22 และ
1.78 ตามลำดับ ผลที่ได้แสดงให้เห็นว่าตัวดูดซับที่มีรอยพิมพ์ประทับสามารถจับกับสีย้อมเป้าหมา
ยได้อย่างเลือกสรร

      ไนลอน/นาโนซิลิกาคอมโพสิทถูกเตรียมโดยใช้ไนลอน 6 และนาโนซิลิกา แอซิดเรด 1 ถูก
ใช้เป็นแม่แบบในการสังเคราะห์เพื่อตรวจสอบผลของรอยพิมพ์ประทับ ได้มีการทดสอบผลของ
เวลาที่ใช้ในการไฮโดรไลซิสของไนลอนและเวลาในการผสมของซิลิกากับไนลอน เวลาในการ
ไฮโดรไลซิสและเวลสในการผสมที่เหมาะสมอยู่ที่ 2 และ 16 ชั่วโมง ตามลำดับ อนุภาคถูกเคลือบ
ด้วยไนลอนแต่อนุภาคไม่ได้แยกออกจากกันทั้งหมด ค่าความจุการดูดซับของไนลอน/ซิลิกาคอม-
โพสิทที่ถูกสังเคราะห์กับแม่แบบเท่ากับ 23.4 มิลลิกรัมต่อกรัม และของไนลอน/ซิลิกาคอมโพสิทที่
ถูกสังเคราะห์โดยปราศจากแม่แบบเท่ากับ 16.0 มิลลิกรัมต่อกรัมที่ 25.0 องศาเซลเซียส ค่าแฟค
เตอร์รอยพิมพ์ประทับน้อยกว่า 1 แสดงว่ากระบวนการทำรอยพิมพ์ประทับไม่ประสบความสำเร็จ

สาขาวิชาเคมี   ลายมือชื่อนักศึกษา___กัลยาณี ทฅลัานเทพน___
ปีการศึกษา 2561   ลายมือชื่ออาจารย์ที่ปรึกษา_____

KANLAYANEE KAJSANTHIA : ADSORPTION OF ACID RED 1 ON
SILICA- AND POLYMER-BASED ADSORBENTS. THESIS ADVISOR :
ASST. PROF. SANCHAI PRAYOONPOKARACH, Ph.D. 129 PP.

ACID DYES/ ADSORPTION/ MESOPOROUS SILICA/NYLON-SILICA
COMPOSITE/SELECTIVE RECOGNITION

In this research, the main goal was to study the adsorption of acid red 1 to various adsorbents. The adsorbents were amino-functionalized mesoporous silica, molecularly imprinted silica-based particles, and nylon/silica composite. The prepared adsorbents were characterized by transmission electron microscopy (TEM), scanning electron microscopy (SEM), X-ray diffraction (XRD), nitrogen adsorption-desorption analysis, and Fourier transform infrared (FTIR) spectroscopy. Adsorption experiments were performed with 0.035 g adsorbent. The dye concentration, pH of dye solutions, adsorption time and temperature were varied.

Amino-functionalized mesoporous silica was synthesized by a sol-gel process. Tetraethylorthosilicate (TEOS) was used as a silica source and cetyltrimethylammonium bromide was used as a mesoporous template. The particles were functionalized with 3-aminopropyltriethoxysilane (APTES). The size of the particles was ~1 µm in diameter. The adsorption of acid red 1 reached equilibrium in 1 h. The optimum pH for the adsorption was 2.0 and the maximum adsorption capacity was 139.6 mg/g. Adsorption isotherms followed the Freundlich model in the low dye concentration range and followed a Langmuir model in the high concentration range. The adsorption processes were spontaneous and endothermic.

After the equilibrium adsorption, the systems were in a higher state of randomness. Adsorption kinetics followed a pseudo-second order model.

To enhance selectivity of the adsorbents, the molecularly imprinted adsorbent was synthesized by the sol-gel method. The adsorbent surface was functionalized with APTES before its use in the imprinting process. Acid red 1 was used as a template. A nonimprinted adsorbent was synthesized with the same procedure without adding template. The sizes of the adsorbents were ~100 nm and well distributed. The adsorption of the imprinted adsorbent followed the Langmuir isotherm model. The adsorption processes were spontaneous and exothermic. After the equilibrium adsorption, the systems were in a lower state of randomness. Adsorption kinetics followed a pseudo-second order model. The adsorption capacities of the imprinted and nonimprinted adsorbent were 36.9 and 28.3 mg/g, respectively. Values of a separation factor of the imprinted adsorbent for acid red 1 compared to tartrazine, zincon, and sulfasalazine were 30.5, 2.22, and 1.78, respectively. The results demonstrate that the imprinted adsorbent can selectively bind the target dye.

Nylon/silica composite was prepared using nylon 6 and nanosilica. Acid red 1 was also used as the template in the synthesis to investigate the imprinting effect. The optimum hydrolysis time and mixing time were 2 and 16 h, respectively. The obtained particles were coated with nylon but were not totally separated from each other. The adsorption capacity of the nylon/silica composite synthesized with the template was 23.4 mg/g and without was 16.0 mg/g. Values of imprinting factors were less than 1, indicating that the imprinting process did not succeed.

School of Chemistry   Student's Signature _____

Academic Year 2018   Advisor's Signature _____

ACKNOWLEDGEMENTS

In the first place I would like to record my deep and sincere gratitude to Assist. Prof. Dr. Sanchai Prayoonpokarach for his patience, motivation, enthusiasm, immense knowledge supervision, advice, and guidance from the very early stage of this research as well as giving me extraordinary experiences throughout the work.

I would like to acknowledge scholarship, Science Achievement Scholarship of Thailand (SAST), from the Thai government. I wish to thank all lecturers of the School of Chemistry for their good attitudes and useful advice, all staffs at the Center for Scientific and Technological Equipment for their assistance and suggestion for the use of instruments. Thank you to all of my good friends in Material Chemistry Research Unit and other friends for their friendship and all their help.

I also want to express my appreciation for my deceased boyfriend, Frank Wai-Fung Wong, who sustains my life in every way. Thanks for his enduring love, support, patience, encouragement, believing in me long after I had lost belief in myself, putting up with me throughout the toughest time to reach the goal of my doctoral and life journeys and always showing how proud he is of me. Rest In Peace Frank. You will be in my heart and soul forever.

Last, but not least, a note of thanks goes to my parents, Mr. Udomsak and Mrs. Petai Kajsanthia, my younger brother, Mr. Parinya Kajsanthia, and other family members for their unconditional love, encouragement and supporting me spiritually during my education and throughout my whole life. I am everything I am today because of them.

<div align="right">Kanlayanee Kajsanthia</div>

CONTENTS

CONTENTS (Continued)

CONTENTS (Continued)

CONTENTS (Continued)

CONTENTS (Continued)

CONTENTS (Continued)

CONTENTS (Continued)

CONTENTS (Continued)

LIST OF TABLE

LIST OF TABLES (Continued)

LIST OF FIGURES

LIST OF FIGURE (Continued)

LIST OF FIGURE (Continued)

CHAPTER I

INTRODUCTION

1.1 Significance of the study

Dyeing is an important process in making fabric products. This process could eventually lead to a wastewater containing dyes with intense color. If the wastewater is released into the environment water, it could cause problems to aquatic lives and human health. Dyes are important pollutant and difficult to treat because of their high water solubility and complex molecular structures (González-Vargas et al., 2014).

Nowadays, various existing treatment processes for removing dye from wastewater have been investigated. Several techniques, such as adsorption (Shan et al., 2015), degradation by bacteria (Sheng et al., 2017), electrocoagulation (El-Hosiny et al., 2018), and catalytic degradation by using H_2O_2 (Kayan et al., 2017) have been used. However, the efficiency of these methods is relatively moderate. Among these methods, adsorption has been found to be superior to other techniques in terms of low cost of operation and simplicity of adsorbents preparation.

In this work, acid red 1 was used as a model dye. A molecular structure of the dye is shown in Figure 1.1. This dye was listed by the U.S. Environmental Protection Agency (EPA) as one of the non-biodegradable azo dyes (Thomas et al., 2014). In 2007, acid red 1 was used as a baby food coloring and in foodstuffs such as breakfast sausages and burger meats (European Food Safety Authority (EFSA), 2007).
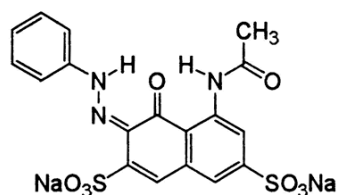
Figure 1.1 A structure of acid red 1.

In a latter-day, the Scientific Panel of the European Food Safety Authority (EFSA) raised the concern that this dye could be the cause of cancer (Villa and Conso, 2004). Moreover, this dye can be metabolized to aniline, which interferes with blood hemoglobin (González-Vargas et al., 2014). Nowadays, acid red 1 is one of many dyes used in the dyeing industry. The dye-containing wastewater released without treating can affect the environment in term of reducing oxygen on the surface water as the intense color of the dye could block the sunlight used for photosynthesis of aquatic plants.

Adsorbents are important components in adsorption processes. Their structures have strong influence on the adsorption of target compounds. Porous and functionalized-porous materials are commonly used for the adsorption. Various adsorbents have been used for acid red 1 removal, for example, coal fly ash (Hsu et al., 2008), cellulose grafted polymer with acrylic acid and acrylamide as monomers (Su et al., 2017), chitosan crosslinked with 7-ethyloctadecane diacid diglycidyl (Shimizu et al., 2003), saccharide-derived spherical biochar (Tran et al., 2017), activated carbon (Gómez et al., 2007), and organic-inorganic hybrid clay (Thue et al., 2017). Adsorption capacity and selectivity towards target compounds should be considered in the development of adsorbents for certain applications; however, it

would be a challenge to achieve both high adsorption capacity and selectivity for an adsorbent.

In this research, adsorption of acid red 1 was studied using various adsorbents. Adsorbents based on silica and nylon/silica composite were prepared with simple methods in order to obtain adsorbents with high adsorption capacity and/or high selectivity toward acid red 1. In Chapter III, mesoporous silica with and without the modification with aminopropyltriethoxysilane were synthesized, characterized, and used in the adsorption of acid red 1. Mesoporous silica was synthesized using a sol-gel process with tetraethylorthosilicate as a silica source and cetyltrimethylammoniumbromide as a template. Mesoporosity incorporated with amino functional groups were responsible for the high adsorption capacity. For conventional adsorbents, however, poor-selectivity, low reusability, and low adsorption capacity are the disadvantages.

Molecularly imprinted adsorbents (MIA) are alternative adsorbents for the removal of dyes. MIAs have gained some attentions because of several advantages such as high selectivity to target compounds and reusability (Zhang et al., 2014). In the synthesis of MIA, a target molecule is used as a template. After finishing the synthesis, it is extracted from the adsorbent, leaving sites that provide selectivity in size, shape and functionality to the target molecule (Vasapollo et al., 2011). However, molecular imprinting alone is insufficient to produce adsorbents with satisfactory adsorption selectivity and capacity. Functionalization is also required to produce adsorbents with better adsorption performance.

In Chapter IV, silica-based molecularly imprinted adsorbent and nonimprinted adsorbent (NIA) were synthesized, characterized, and used in the adsorption of acid

red 1. Preparation of nanosilica particles was based on the sol-gel process. Nanosilica particles were modified with aminopropyltriethoxysilane to yield adsorption sites for the dye. The amino-functionalized silica particles interacted with acid red 1 were coated with a mesoporous silica layer to form imprinted sites.

In Chapter V, nylon/silica composites were synthesized, characterized, and tested in the adsorption of acid red 1. Adsorption studies were carried out in solutions containing acid red 1, acid red 1 mixed with tratarzine, and acid red 1 mixed with nitroso-R.

1.2 Research objectives

The research objectives were as follows:

1.2.1 To synthesize mesoporous silica, molecularly imprinted silica, and nylon/silica composites, characterize the obtained adsorbents, and evaluate their performance in the adsorption of acid red 1.

1.2.2 To study the parameters that affect the adsorption capacity of the synthesized adsorbents such as pH of solutions, contact time, and temperature.

1.2.3 To explain adsorption behavior of some adsorbents based on thermodynamic and kinetic study.

1.3 Scope and limitations of the study

The scope and limitations of the study are listed:

1.3.1 Tetraethylorthosilicate was used as the only source of silica in the synthesis of silica-based adsorbents.

1.3.2 Aminopropyltriethoxysilane was the only reagent used to functionalize the surface of silica particles to provide -NH$_2$ groups.

1.3.3 nylon 6 was used to prepare adsorbents based on nylon/silica composites.

1.3.4 Acid red 1 was used as a dye model.

1.3.5 Performance characteristics of the synthesized adsorbents such as selectivity, adsorption capacity, and reversibility were studied in a batch system.

1.3.6 The adsorbents were characterized by X-ray diffraction (XRD), scanning electron microscopy (SEM), transmission electron microscopy (TEM), Fourier transform infrared spectroscopy (FT-IR), and nitrogen adsorption-desorption analysis.

1.3.7 The concentration of dyes in solutions with single dye component was determined by UV-Vis spectrophotometry.

1.3.8 The concentration of dyes in mixed dye solutions was determined by high performance liquid chromatography.

1.4 References

El-Hosiny, F. I., Abdel-Khalek, M. A., Selim, K. A., and Osama, I. (2018). Physicochemical study of dye removal using electro-coagulationflotation process. **Physicochemical Problems of Mineral Processing**. 54(2): 321-333.

European Food Safety Authority. (2007). Opinion of the scientific panel on food additives, flavourings, processing aids and materials in contact with food. **The EFSA Journal**. 515: 1-28. Parma, Italy.

Gómez, V., Larrechi, M. S., and Callao, M. P. (2007). Kinetic and adsorption study of acid dye removal using activated carbon. **Chemosphere**. 69(7): 1151-1158.

González-Vargas, C., Salazar, R., and Sirés, I. (2014). Electrochemical treatment of acid red 1 by electro-fenton and photoelectro-fenton processes. **International Journal of Electrochemical Science**. 4(4): 235-245.

Hsu, T. C. (2008). Adsorption of an acid dye onto coal fly ash. **Fuel**. 87: 3040-3045.

Kayan, B., Akay, S., Kulaksız, E., Gözmen, B., and Kalderis, D. (2017). Acid Red 1 and Acid Red 114 decolorization in H_2O_2-modified subcritical water: process optimization and application on a textile wastewater. **Desalination and Water Treatment**. 59: 248-261.

Shan, R. R., Yan, L. G., Yang, Y. M., Yang, K., Yu, S. J., Yu, H. Q., Zhu, B. C., and Du, B. (2015). Highly efficient removal of three red dyes by adsorption onto Mg–Al-layered double hydroxide. **Journal of Industrial and Engineering Chemistry**. 21: 561-568.

Sheng, S., Liu, B., Hou, X., Wu, B., Yao, F., Ding, X., and Huang, L. (2017). Aerobic biodegradation characteristic of different water-soluble azo dyes. **International Journal of Environmental Research and Public Health**. 15: 1-11.

Shimizu, Y., Taga, A., and Yamaoka, H. (2003). Synthesis of novel crosslinked chitosans with a higher fatty diacid diglycidyl and their adsorption abilities towards acid dyes. **Adsorption Science and Technology**. 21(5): 439-449.

Su, X., Liu, L., Zhang, Y., Liao, Q., Yu, Q., Meng, R, and Yao, J. (2017). Efficient removal of cationic and anionic dyes from aqueous solution using cellulose-g-p(AA-co-AM) bio-adsorbent. **BioResources**. 12(2): 3413-3424.

Thomas, S., Sreekanth, R., Sijumon, V. A., Aravind, U. K., and Aravindakumar, C. T. (2014). Oxidative degradation of acid red 1 in aqueous medium. **Chemical Engineering Journal**. 244: 473-482.

Thue, P. S., Sophia, A. C., Lima, E. C., Wamba, A. G.N., Alencar, W. S., Reis, G. S., Rodembusch, F. S., and Dias, S. L. P. (2018). Synthesis and characterization of a novel organic-inorganic hybrid clay adsorbent for the removal of acid red 1 and acid green 25 from aqueous solutions. **Journal of Cleaner Production**. 171(10): 30-44.

Tran, H. N., Lee, C. K., Vu, M. T., and Chao, H. P. (2017). Removal of copper, lead,methylene green 5, and acid red 1 by saccharide-derived spherical biochar prepared at low calcination temperatures: adsorption kinetics, isotherms, and thermodynamics. **Water Air and Soil Pollution**. 228(401): 1-16.

Vasapollo, G., Del Sole, R., Mergola, L., Lazzoi M. R., Scardino, A., Scorrano, S., and Mele, G. (2011). Molecularly imprinted polymers: present and future prospective. **International Journal of Molecular Sciences**. 12: 5908-5945.

Villa, A. F. and Conso, F. (2004). Aromatic amines. **EMC - Toxicologie-Pathologie**. 1: 161-177.

Zhang, C., Wang, Y., Zhou, Y., Guo, J., and Liu, Y. (2014). Silica-based surface molecular imprinting for recognition and separation of lysozymes. **Analytical Methods**. 6: 8584-8591.

CHAPTER II

LITERATURE REVIEW

2.1 Dyes

There are many ways to classify dyes based on, for example, their origins, chemical structures, and industrial applications. According to their charge, dyes can be classified as anionic (direct, acid, reactive), cationic (basic) and nonionic (disperse) dyes. Acid dyes are anionic dye commonly used for dyeing wool, animal fibers, and manufactured fibers. They contain sulfonate group ($-SO_3^-$) and usually are produced in the form of sodium sulfonate salts, which make them highly soluble in water. A dyeing process is usually carried out with a mixture of three dyes to produce various shades (Salaskar and Sahasrabudhe, 2003). As a result, wastewater originating from a dyeing reactor contains three dyes. In treating of the wastewater, all dyes might not be required to be removed from the water depending on their toxicity and concentration.

Basic dyes are water-soluble and are mainly used to dye acrylic fibers. They are mostly used with a mordant. A mordant is a chemical agent which is used to set dyes on fabrics by forming an insoluble compound with the dye. Basic dyes are used for cotton, linen, acetate, nylon, polyesters, acrylics, and modacrylics. Other than acrylic, basic dyes are not very suitable for any other fibers as they are not fast to light, washing or perspiration.

Nonionic dyes are water-insoluble. These dyes are finely ground and are available as a paste or a powder that gets dispersed in water. These dyes are used to dye nylon, cellulose triacetate, and acrylic fibers.

Dyes used in this work were acid red 1, tartrazine, sulfasalazine, and nitroso-R. Their structures are shown in Figure 2.1.

2.2 Acid dyes removal

Acid dyes contamination in water can be removed by various methods, for example, degradation by bacteria, electro-coagulation-flotation process, and catalytic degradation by using H_2O_2. Hu et al. (2007) used *Bacillus* sp. to remove acid red 1 and acid black 172. The results showed that both dyes could be decomposed by the biocatalyst in wastewater but the toxicity from the decomposition of the dye was not reduced. El-Hosiny et al. (2017) removed acid red 1 and other dyes using electro-flotation with aluminum electrodes. This method required a huge batch reactor, high electricity, and investment cost. Kayan et al. (2017) decolorized acid red 1 and acid red 114 in H_2O_2-modified subcritical water. Their degradation products were aniline, hydroquinone, benzoquinone, etc. These products are toxic to human health and the environment. Catalytic decomposition of dyes could lead to degraded products that could be more toxic than the initial dyes. Adsorption is one of the methods used for the removal of acid dyes. It has some advantages in terms of the low cost of operation, simplicity of adsorbents preparation, and reusability of adsorbents.

Acid red 1

Tartrazine

Zincon

Sulfasalazine
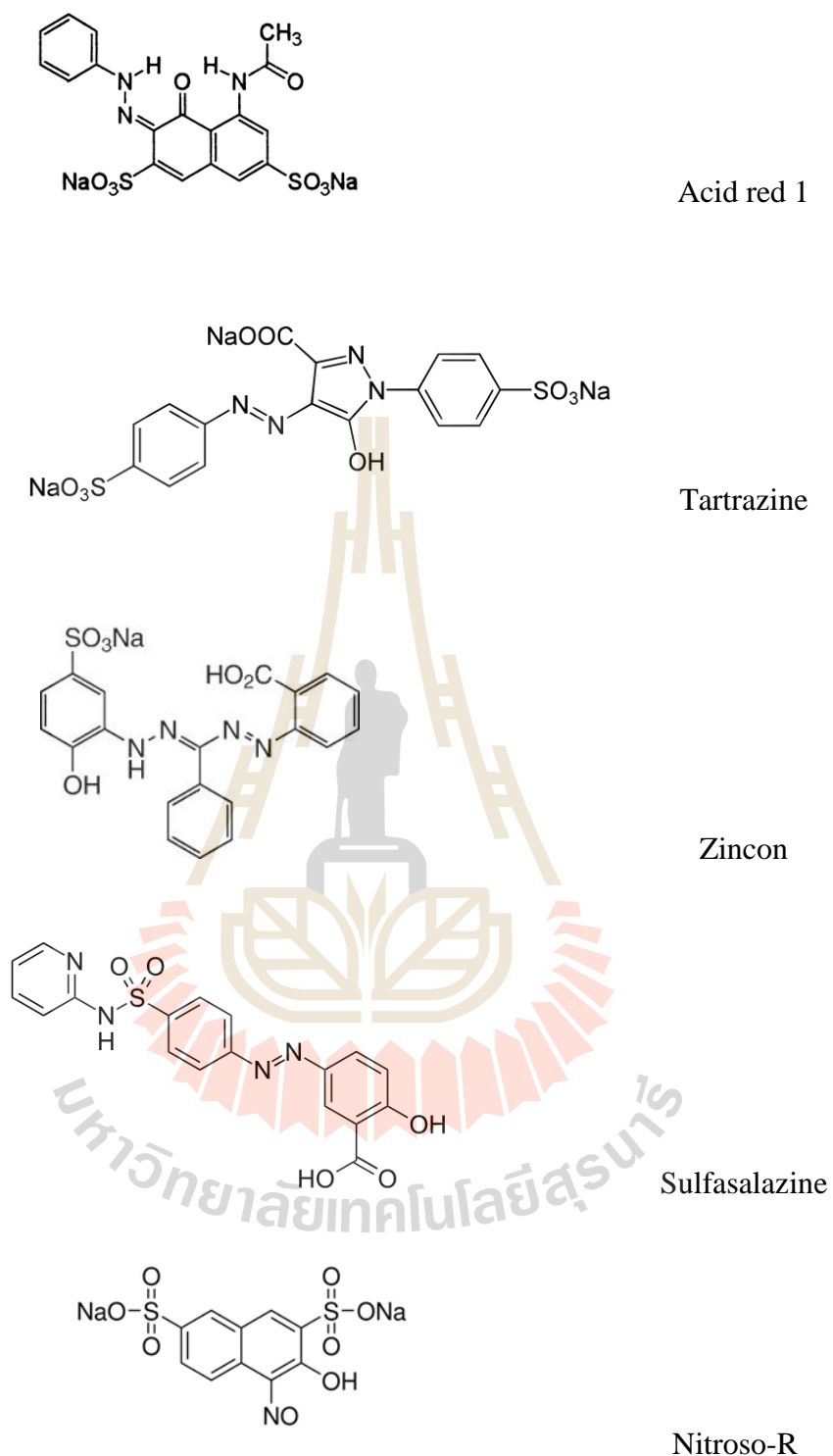
Nitroso-R

Figure 2.1 Structures of acid red 1, tartrazine, zincon, sulfasalazine, and nitroso-R. (https://en.wikipedia.org/wiki).

2.3 Adsorption

Adsorption is a process of accumulation of molecules on the surface of solids. The solid that accumulates other compounds on its surface is called adsorbent and the compound adsorbed on the adsorbent surface is called adsorbate. Adsorption can be classified into two types which are physical adsorption and chemical adsorption. Physical adsorption or physisorption occurs via weak intermolecular forces. Physical adsorption takes place with the formation of multilayer of the adsorbate on the adsorbent. The enthalpy change of the adsorption is lower than 40 kJ/mol (Masel, 1996). This type of adsorption takes place at a low temperature below the boiling point of the adsorbate and the adsorption decreases with the increase of the temperature. In chemical adsorption or chemisorption on the other hand, the adsorbate chemically bonds with the adsorbent. Chemisorption takes place with the formation of a monolayer of the adsorbate on the adsorbent. The enthalpy change of the adsorption is in the range of 60-400 kJ/mol (Masel, 1996). This type of adsorption can take place at all temperature.

2.3.1 Adsorption isotherms

Adsorption isotherms can provide principle information for the understanding of the adsorption process. There are several theoretical models developed to explain the adsorption process. The Langmuir and Freundlich adsorption isotherm models are commonly used to represent the experimental data.

2.3.1.1 Langmuir isotherm

The Langmuir isotherm is used to describe equilibrium adsorption based on three major assumptions (Do, 1998), which are:

1. The surface of the adsorbent is homogeneous; therefore, adsorption energy is constant for all sites,

2. Only one molecule or atom can be adsorbed on any one site and adsorption cannot occur beyond a monolayer and

3. There is no interaction between any of the adsorbed molecules or atoms.

The Langmuir adsorption equation can be represented as equation [2.1];

$$\frac{q_e}{q_m} = \frac{K_A C_e}{1 + K_A C_e}$$ [2.1]

where, q_e (mg/g) is the amount of the adsorbate adsorbed per gram of the adsorbent at equilibrium; q_m (mg/g) is the amount of the adsorbate adsorbed to form a monolayer coverage per gram of the adsorbents; K_A (L/mg) is the Langmuir adsorption equilibrium constant; C_e (mg/L) is the concentration of the adsorbate in a solution at equilibrium. q_e is described by equation [2.2];

$$q_e = \frac{V(C_0 - C_e)}{m}$$ [2.2]

where C_0 and C_e (mg/L) are the initial and equilibrium concentrations of the adsorbate in a solution, respectively, V is the volume of the solution (L) and m is the adsorbent mass (g).

Adsorption data can be fitted to the Langmuir isotherm in a linear form following equation [2.3];

$$\frac{C_e}{q_e} = \frac{C_e}{q_m} + \frac{1}{K_A q_m}$$ [2.3]

Maximum adsorption capacity (q_m) can be obtained from a linear plot of C_e/q_e against C_e. K_A can be calculated from the intercept value.

The suitability of the adsorbent to the adsorbate can be evaluated by using the Langmuir constant to calculate a value known as the constant separation factor, R_L as expressed in equation [2.4];

$$R_L = \frac{1}{1 + K_A C_0}$$ [2.4]

where, C_0 (mg/L) is the initial concentration of adsorbate in a solution. The value of R_L can be used to indicate the adsorption situations to be unfavorable ($R_L > 1.0$), linear ($R_L = 1.0$), irreversible ($R_L = 0$) and favorable ($0 < R_L < 1.0$) (Hall et al. 1966).

2.3.1.2 Freundlich isotherm

The Freundlich isotherm is another commonly used model. It has a general form as expressed by equation [2.5];

$$q_e = K_F C_e^{1/n}$$ [2.5]

where q_e and C_e are defined as in equation [2.1], K_F is the Freundlich constant, the indicative of the relative adsorption capacity of the adsorbent and $1/n$ is an empirical constant. A linear form of Freundlich isotherm is shown in equation [2.6].

$$\ln q_e = \ln K_F + \frac{1}{n} \ln C_e$$ [2.6]

When $\ln q_e$ is plotted against $\ln C_e$ and the data are treated by linear regression analysis, K_F and $1/n$ can be obtained from the intercept and the slope of the line, respectively. Freundlich model applies well to solid with heterogeneous surface properties.

2.3.2 Thermodynamics study

Thermodynamic parameters including Gibbs free energy change (ΔG), enthalpy change (ΔH) and entropy change (ΔS) are useful in providing information

about the adsorption process. The relationship among a distribution coefficient (K_D), ΔH and ΔS can be described by equation [2.7];

$$\ln K_D = \frac{\Delta S}{R} - \frac{\Delta H}{RT} \qquad [2.7]$$

where R is the universal gas constant (8.314 $Jmol^{-1}$ K^{-1}) and T is the absolute temperature (Kelvin). The values of ΔH and ΔS can be calculated from a slope and an intercept of a plot of $\ln K_D$ against 1/T. K_D can be calculated from equation [2.8];

$$K_D = \frac{q_e}{C_e} \qquad [2.8]$$

where q_e and C_e, defined as in equation [2.1]. ΔG provides information about the process spontaneity, which can be related to ΔH and ΔS as shown in equation [2.9];

$$\Delta G = \Delta H - T\Delta S \qquad [2.9]$$

The Gibbs free energy change can also be determined using equation [2.10];

$$\Delta G = -RT \ln K_D \qquad [2.10]$$

The effects of the enthalpy change, entropy change, and temperature on spontaneity of a reaction relating to ΔH, ΔS, and ΔG are summarized in Table 2.1.

2.3.3 Kinetic study

To describe the adsorption behavior with time. The obtained adsorption data were fitted with pseudo-first-order and pseudo-second-order models. These models are the most commonly used to describe the adsorption of dyes on adsorbents.

Pseudo-first order model is written as shown in equation [2.11];

$$\log (q_e - q_t) = \log q_e - (k_1 t / 2.303) \qquad [2.11]$$

Table 2.1 Relationship of enthalpy, entropy, and Gibbs free energy change to the occurrence of a reaction (Zumdahl and Zumdahl, 1989).

ΔH	ΔS	ΔG	Spontaneity of a process
$-$	$+$	$-$	Spontaneous at all temperature
$+$	$-$	$+$	Non-spontaneous
$+$	$+$	$-$	Spontaneous only at high temperature
$-$	$-$	$-$	Spontaneous only at low temperature

where q_e is the equilibrium adsorption capacity (mg/g), q_t is the adsorption capacity at time t (mg/g), k_1 is the pseudo first-order rate constant (min^{-1}), and t is the contact time (min).

Pseudo-second order model is written as shown in equation [2.12];

$$t/q_t = 1/k_2 q_e^2 + (1/q_e)t \qquad [2.12]$$

where k_2 is the pseudo second-order rate constant (g/mg.min), and t is the contact time (min).

2.4 Adsorbents for acid dyes removal

Adsorbents are important component in adsorption processes. Their structures have strong influence on the adsorption of target compounds. Various adsorbents have been used in adsorption of acid dyes.

2.4.1 Conventional adsorbents

Adsorbents with low surface area, but with suitable functional groups generated on their surface could be used for the adsorption of acid red 1. Hsu et al. (2008) used coal fly ash (CFA) to adsorb acid red 1. The CFA was treated in furnace

at a very high temperature at 600 ^{o}C. Su et al. (2017) synthesized cellulose grafted polymer using acrylic acid (AA) and acrylamide (AM) as monomers. The polymerization reaction was carried out at -18 ^{o}C for 24 h. The product had to be milled before use for the adsorption. Shimizu et al. (2003) synthesized crosslinked chitosan with 7-ethyloctadecane diacid diglycidyl (EODD) for acid red 1 and other dyes adsorption. The preparation process took about 68 h. In addition, the time for the adsorption to reach the equilibrium was relatively long that is 96 h at 30 ^{o}C and 72 h at 40 ^{o}C. Tran et al. (2017) prepared saccharide-derived spherical biochar for the removal of acid red 1 and other pollutants. Carbohydrate precursors were carbonized under hydrothermal condition at 190 ^{o}C and dried in an oven at 105 ^{o}C for 24 h. After that, the spherical biochars were calcined from 200 to 325 ^{o}C for 5 h and dried. The obtained adsorbents had negligible adsorption capacity for acid red 1 due to electrostatic repulsion. Thue et al. (2017) synthesized organic-inorganic hybrid clay adsorbent for the removal of acid red 1 and acid green 25. The adsorbent was grafted with 3-aminopropyltriethoxysilane (APTES) by refluxing at 75 ^{o}C for 24 h.

Porous solids are usually used in adsorption processes because high surface area and large pore volume are required to achieve high adsorption capacity. Ordered mesoporous structures such as MCM-41 (Lee et al., 2007) and SBA-3 (Anbia et al., 2010), have been used to remove acid dyes from wastewater. Calcined and uncalcined materials were investigated. High surface area and nanometer-sized pore sizes (from 20 to 100 Å) of the adsorbents offer a special environment for chemical separations of large molecules. Besides siliceous materials, hollow mesoporous carbon nanospheres (Konicki et al., 2013) has also been used for the adsorption of acid orange 8 and acid red 88 from aqueous solutions.

To enhance the adsorption performance, the mesoporous particles are functionalized with organosilanes. Wu et al. (2014) used MCM-41 functionalized with 3-aminopropyltriethoxysilane (APTES) in the mesoporous silica framework as the adsorbent for acid fuchsine and acid orange II. The surface area of the prepared adsorbent was 658 m^2/g. Other organosilanes also have been used to functionalize onto mesoporous materials. Lee et al. (2015) used various organosilanes including methyltriethoxysilane (MTES), phenyltriethoxysilane (PTES), and APTES to funcrionalize onto SBA-15 and the obtained adsorbents were used for the adsorption of acid orange 12 and acid red 73. The adsorption capacities of the dye increased with the increase amount of functionalized organosilanes.

For conventional adsorbents, low-selectivity to the target molecule, and high cost for reusability are the disadvantages. To improve adsorption selectivity, molecularly imprinted adsorbents have been investigated.

2.4.2 Molecularly imprinted adsorbents

Molecularly imprinted adsorbents (MIAs) are alternative adsorbents for the removal of dyes from wastewater. They have one prominent property that is high selectivity to target molecules. Typically, an imprinted adsorbent is formed by polymerization of monomers in the presence of a template molecule. This monomer-template complex is polymerized in the presence of a cross-linker to lock the orientation of the functional monomer and form a rigid polymer around the template. The template molecule after finishing the polymerization is extracted from the polymer, leaving sites that provide selectivity in size, shape, and functionality to the target molecule. (Vasapollo et al., 2011).

An imprinting process is schematically represented in Figure 2.2 (Algieri et al., 2014). Nonimprinted adsorbents were prepared using similar procedures as those for MIAs except that the template was not added.
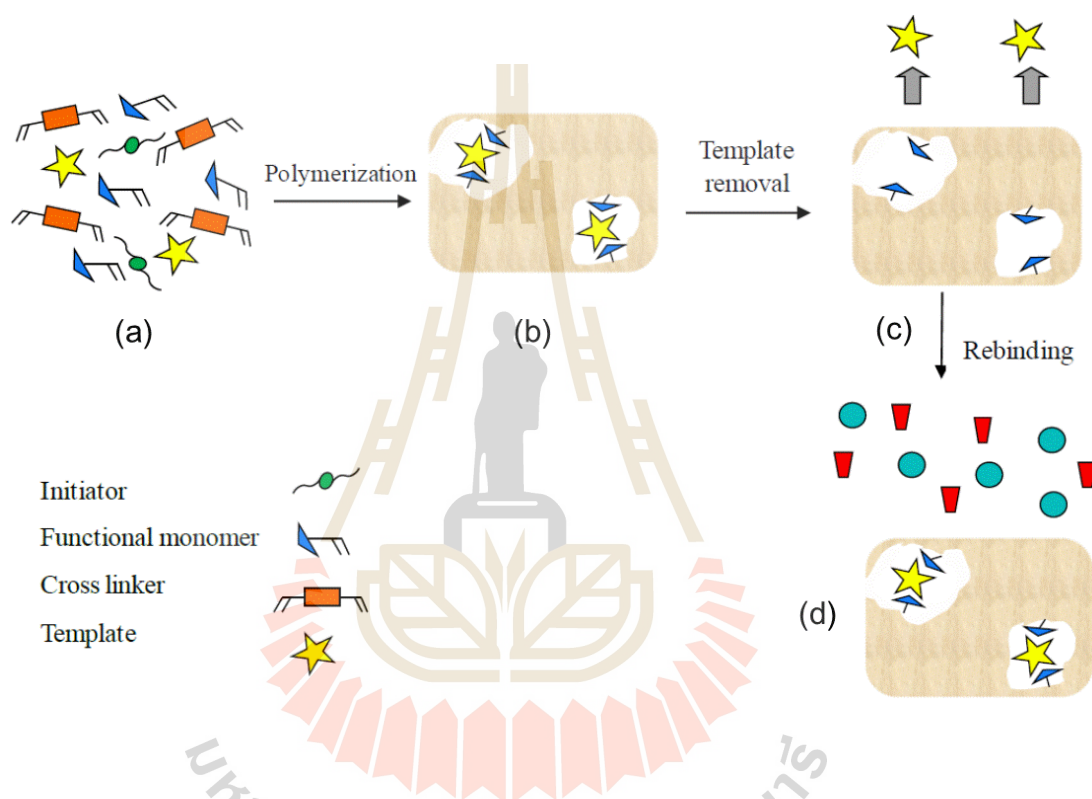
Figure 2.2 Representation of the molecular imprinting process. (a) Functional monomers interact with a template, (b) a template-monomers complex formed is polymerized in the presence of cross-linkers, (c) removal of the template from the formed polymer liberates binding sites, and (d) the polymer selectively rebinds with the target molecule (Algieri et al., 2014).

2.4.2.1 Separation factor and imprinting factor

2.4.2.1.1 Separation factor

Separation factor (α) is a measure of the strength of interaction of MIA towards the template molecule compared to another molecule. It is calculated using equation [2.13];

$$\alpha = K_{D1}/ K_{D2} \qquad [2.13]$$

K_D value is calculated according to equation [2.14];

$$K_D = \frac{q_e}{C_e} \qquad [2.14]$$

K_{D1} and K_{D2} are partition coefficients for molecule 1 and molecule 2 over the same adsorbent. Higher value of α corresponds to greater selectivity to dye 1. MIAs have no selectivity over any two dyes when the value of α is close to 1.0.

2.4.2.1.2 Imprinting factor

Imprinting factor (β) is a measure of the strength of interaction of MIA towards the template molecule compared with that of the NIA. The imprinting factor (β) can be represented as equation [2.15];

$$\beta = K_{D\,(MIA)}/K_{D\,(NIA)} \qquad [2.15]$$

$K_{D(MIA)}$ and $K_{D(NIA)}$ are the distribution coefficients of a target molecule for MIA and non-imprinted polymer, respectively. Higher value of β corresponds to greater difference in the interaction upon the target molecule between the two adsorbents. When β is equal to 1.0, it means that there is no difference in the adsorption character between MIA and NIA.

2.4.2.2 Molecularly imprinted adsorbents prepared by polymerization

In general, MIAs were produced by bulk polymerization methods. A bunch of monomers has been applied to interact with target templates. Commercial monomer such as methacrylic acid (MAA), 4-vinylpyridine (4-VP), acrylamide (AM), and 1-vinylimidazole (VI) are widely used as functional monomers to synthesize molecularly imprinted adsorbents for acid dyes (Karim et al., 2005). Foguel et al. (2017) synthesized molecularly imprinted polymer for acid green 16 adsorption using 1-vinylimidazole as a monomer. The selectivity of acid green 16 on the prepared adsorbent performance was compared to methyl green, basic red 9, acid red 1, and direct yellow 50. In addition, the synthesized monomers have been applied in order to obtain specific recognition sites with the template. Kyzas et al. (2009) used methacrylic acid and acrylamide as monomers to prepare molecularly imprinted polymers for the selective adsorption of reactive and basic dyes. Luo et al. (2011) used 1-(α-methyl acrylate)-3-methylimidazolium bromide (1-MA-3MI-Br) as a functional monomer to synthesize novel magnetic and hydrophilic molecularly imprinted polymers (mag-MIAs) for the adsorption of acid dyes such as amaranth, brilliant ponceau 5R, orange G, sunset yellow FCF, and tratarzine from contaminated water.

2.4.2.3 Drawbacks of molecularly imprinted adsorbents prepared by polymerization

MIAs prepared by bulk and solution polymerization have been shown to be applicable for the adsorption of the target dyes (Yan and Raw, 2006). However, the synthesized methods were time-consuming and yielded a moderate amount of imprinted sites. A big chunk of a polymer product was obtained. Grinding

of the product was required to obtain smaller particles. The grinding process could result in the heterogeneity of the adsorption sites, irregularity of the particle shapes, and the non-uniformity of the particle sizes. The number of recognition sites accessible to the target molecule could be low. In addition, the nonpolymerized monomer and solvent were difficult to remove from the polymer. These chemicals could degrade the bulk properties of the polymer. Moreover, MIAs face some serious problems such as poor rebinding in aqueous environments, heterogeneity of binding sites, slow mass transfer, and incomplete removal of the template.

To circumvent the drawbacks, other methods were considered. Molecular imprinting on nanopartilces is an effective approach to overcome this barrier and to remove the limitations of the traditional molecularly imprinted adsorbents.

2.4.2.4 Molecularly imprinted adsorbents prepared by sol-gel method

The sol-gel method was also utilized for the preparation of MIAs, by introducing an organosilane precursor into the sol-gel-based MIA synthesis mixture. Silica gel could be grafted with certain functional groups which could then interact with the imprinted molecules. The sol-gel process produces polymer materials that have a wide variety of applications in analytical chemistry (Wayne et al., 2005). MIAs prepared from the sol-gel process was proposed in order to form a confined and rigid structure so that superior binding specificity toward the target molecule could be achieved from such materials. An inorganic precursor, tetraethoxysilane (TEOS), was mixed with organic functional monomers, cross-linkers, and template molecules to produce imprinting sites. The chemical functionality was achieved and confined in the matrix via hydrolysis-condensation of

the sol-gel (Chang et al., 2009). Up to now, very few studies on the adsorption and separation of acid dyes using MIAs have been reported. Therefore, this work studied the preparation of silica-based molecularly imprinted adsorbents for acid red 1.

2.4.2.5 Composite adsorbents

From the advantages of conventional adsorbents and imprinted adsorbents prepared by the polymerization and sol-gel method as mentioned above. Combination of the conventional adsorbents and polymers to create composite materials can result in some interesting properties of the materials. Composites adsorbents have been studied to promote the adsorption capacity and selectivity of the adsorbents. Zhao et al. (2014) synthesized imprinted composite membranes using TiO_2/calcium alginate hydrogel as a matrix for the adsorption and photocatalytic degradation of sulfonic dye. Yang et al. (2017) prepared magnetic imprinted N-doped $P25/Fe_3O_4$-graphene oxide for catalytic degradation of sulfonic dye (congo red). However, those adsorbents were difficult to prepare and posed a problem due to low selectivity.

In recent years, nylon/silica composites have been reported. Tayebi et al. (2015) studied the adsorption of acid blue 62 on nylon 6 yarns composited with titania. However, the materials still have a low surface area. Chen et al. (2015) studied the mechanical properties of nylon 6-silica flake and clay sub-micro composites. Silica nanoparticle were incorporated in different polymers including nylon as reinforcement material and could be improved the properties of nylon, for example, enhance the surface area. Nakada et al. (2016) synthesized nylon-6,6 in cetyltrimethylammonium chloride reverse micelles adsorbed on silica surfaces and used as a stationary phase for the separation analysis. Reyes-Gallardo et al. (2017)

prepared silica nanoparticles-nylon 6 composites adsorbent by dispersing the silica particles into nylon in formic acid. The adsorbents were used for extracting some hormones in bioanalytical samples. Only a few pieces of research have been reported so far for acid dyes adsorption using nylon/silica composite adsorbents. Therefore, in this work nylon/nanosilica composites prepared using a simple method were studied for the adsorption of acid red 1. Nanosilica particles incorporated into nylon were expected to increase the surface area of the material and consequently, increase the adsorption capacity of the adsorbents.

2.5 Reference

Algieri, C., Drioli, E., Guzzo, L., and Donato, L. (2014). Bio-mimetic sensors based on molecularly imprinted membranes. **Sensors**. 14: 13863-13912.

Anbia, M., Hariri, S. A., and Ashrafizadeh, S. N. (2010). Adsorptive removal of anionic dyes by modified nanoporous silica SBA-3. **Applied Surface Science**. 256: 3228-3233.

Chang, Y. S., Ko, T. H., Hsu, T. J., and Syu, M. J. (2009). Synthesis of an imprinted hybrid organic-inorganic polymeric sol-gel matrix toward the specific binding and isotherm kinetics investigation of creatinine. **Analytical Chemistry**. 81: 2098-2105.

Chen, J., Beake, B. D., Bell, G. A., Tait, Y., and Gao, F. (2015). Probing polymer chain constraint and synergistic effects in nylon 6-clay nanocomposites and nylon 6-silica flake sub-micro composites with nanomechanics. **Nanocomposites**. 1(4): 185-194.

Do, D. D. (1998). **Adsorption analysis: Equilibria and kinetic**. World Scientific Publishing Co. Pte. Ltd: Singapore. P.13.

El-Hosiny, F. I., Abdel-Khalek, M. A., Selim, K. A., and Osama, I. (2017). Physicochemical study of dye removal using electro-coagulation-flotation process. **Physicochemical Problems of Mineral Processing**. 54(2): 321-333.

Foguel, M.V., Pedro, N. T. B., Wong, A., Khan, S., Zanoni, M. V. B., and Sotomayor, M. P. T. (2017). Synthesis and evaluation of a molecularly imprinted polymer for selective adsorption and quantification of acid green 16 textile dye in water samples. **Talanta**. 170: 244-251.

Hall, K. R., Eagleton, L. C., Acrivos, A., and Vermeulen, T. (1996). Pore and solid diffusion kinetics in fixed-bed adsorption under constant - pattern conditions**. Industrial and Engineering Chemistry Fundamentals**. 5: 212-223.

Hsu, T. C. (2008). Adsorption of an acid dye onto coal fly ash. **Fuel**. 87: 3040-3045.

Hu, X., Dong, H. Y., Qiu, Z. N., Qian, G. R., Ye, L., Zhu, Z. C., and Ren, Z. M. (2007). The effect of high magnetic field characterized by kinetics: Enhancing the biodegradation of acid red 1 with a strain of *Bacillus* sp. **International Biodeterioration and Biodegradation**. 60: 293-298.

Karim, K., Breton, F., Rouillon, R., Piletska, E. V., Guerreiro, A., Chianella, I., and Piletsky, S. A. (2005). How to find effective functional monomers for effective molecularly imprinted polymers. **Advanced Drug Delivery Reviews**. 57: 1795-1808.

Kayan, B., Akay, S., Kulaksız, E., Gözmen, B., and Kalderis, D. (2017). Acid Red 1 and Acid Red 114 decolorization in H_2O_2-modified subcritical water: process

optimization and application on a textile wastewater. **Desalination and Water Treatment**. 59: 248-261.

Konicki, W., Cendrowski, K., Chen, W., and Mijowska, E. (2013). Application of hollow mesoporous carbon nanospheres as a high effective adsorbent for the fast removal of acid dyes from aqueous solutions. **Chemical Engineering Journal**. 228: 824-833.

Kyzas, G. Z., Bikiaris, D. N., and Lazaridis, N. K. (2009). Selective separation of basic and reactive dyes by molecularly imprinted polymers (MIPs). **Chemical Engineering Journal**. 149: 263-272.

Lee, C. K., Liu, S. S., Juang, L. C., Wang, C. C., Lin, K. S., & Lyu, M. Du. (2007). Application of MCM-41 for dyes removal from wastewater. **Journal of Hazardous Materials**. 147(3): 997-1005.

Lee, J. Y., Chen, C. H., and Cheng, S. (2015). Adsorption of acid dyes by functionalized SBA-15 mesoporous silica of different pore lengths. **Journal of the Chinese Chemical Society**. 62(6): 483-494.

Luo, X., Zhan, Y., Tu, X., Huang, Y., Luo, S., and Yan, L. (2011). Novel molecularly imprinted polymer using 1-(α-methyl acrylate)-3-methylimidazolium bromide as functional monomer for simultaneous extraction and determination of water-soluble acid dyes in wastewater and soft drink by solid phase extraction and high performance liquid chromatography. **Journal of Chromatography A**. 1218: 1115-1121.

Masel, R. I. (1996) **Principles of adsorption and reaction on solid surfaces**. John Wiley & Sons: Canada, pp. 111-112.

Nakada, K., Hasanin, T. H. A., Tanaka, T., Ueda, M., Tsukahara, S., Okamoto, Y., and Fujiwara, T. (2016). Synthesis of Nylon-6.6 using cetyltrimethylammonium chloride reverse micelles immobilized on silica surfaces. **Journal of Molecular Liquids**. 219: 789-794.

Reyes-Gallardo, E. M., Lucena, R. and Cardenas, S. (2017). Silica nanoparticles-Nylon 6 composites: synthesis, characterization and potential use as sorbent. **RSC Advances**. 7: 2308-2314.

Salaskar, N. R., and Sahasrabudhe, A. S. (2003). Development of shades on cellulosic substrates with trichromatic reactive dyes using CCM technique. **The Bombay Textile Research Association. BTRA**.33: 19-26.

Shimizu, Y., Taga, A., and Yamaoka, H. (2003). Synthesis of novel crosslinked chitosans with a higher fatty diacid diglycidyl and their adsorption abilities towards acid dyes. **Adsorption Science and Technology**. 21(5): 439-449.

Su, X., Liu, L., Zhang, Y., Liao, Q., Yu, Q., Meng, R, and Yao, J. (2017). Efficient removal of cationic and anionic dyes from aqueous solution using cellulose-g-p(AA-co-AM) bio-adsorbent. **BioResources**. 12(2): 3413-3424.

Tayebi, H. A., Yazdanshenas, M. E., Rashidi, A., Khajavi, R., and Montazer, M. (2015). The isotherms, kinetics, and thermodynamics of acid dye on Nylon 6 with different amounts of titania and fiber cross sectional shape. **Journal of Engineered Fibers and Fabrics**. 10(1): 97-108.

Thue, P. S., Sophia, A. C., Lima, E. C., Wamba, A. G.N., Alencar, W. S., Reis, G. S., Rodembusch, F. S., and Dias, S. L. P. (2018). Synthesis and characterization of a novel organic-inorganic hybrid clay adsorbent for the removal of acid red

1 and acid green 25 from aqueous solutions. **Journal of Cleaner Production**. 171(10): 30-44.

Tran, H. N., Lee, C. K., Vu, M. T., and Chao, H. P. (2017). Removal of copper, lead, methylene green 5, and acid red 1 by saccharide-derived spherical biochar prepared at low calcination temperatures: adsorption kinetics, isotherms, and thermodynamics. **Water Air and Soil Pollution**. 228(401): 1-16.

Vasapollo, G., Sole, R. Del, Mergola, L., Lazzoi, M. R., Scardino, A., Scorrano, S., and Mele, G. (2011). Molecularly imprinted polymers: Present and future prospective. **International Journal of Molecular Sciences**. 12(9), 5908-5945.

Wayne C., Patrick D., and Peter M. (2005) A comparative study of the potential of acrylic and sol - gel polymers for molecular imprinting. **Analytica Chimica Acta**. 542: 52-60.

Wu, Y., Zhang, M., Zhao, H., Yang, S., and Arkin, A. (2014). Functionalized mesoporous silica material and anionic dye adsorption: mcm-41 incorporated with amine groups for competitive adsorption of acid fuchsine and acid orange II. **RSC Advances**. 106(4): 61256-61267.

Yan, H. and Row, K. H. (2006). Characteristic and synthetic approach of molecularly imprinted polymer. **International Journal of Molecular Sciences**. 7: 155-178.

Yang, X., You, X., Zhang, B., Guo, C., and Yu, C. (2017). Preparation of magnetic imprinted graphene oxide composite for catalytic degradation of congo red under dark ambient condition. **Water Science and Technology**. 76(7): 1676-1686.

Zhao, K., Feng, L., Lin, H., Fu, Y., Lin, B., Cui, W., Li, S., and Wei, J. (2014). Adsorption and photocatalytic degradation of methyl orange imprinted composite membranes using TiO_2/calcium alginate hydrogel as matrix. **Catalysis Today**. 236:127-134.

Zumdahl, S. S., and Zumdahl, S. A. (1989). **Chemistry**, 2nd ed.; D.C. Heath: Lexington, MA. pp. 737-771.
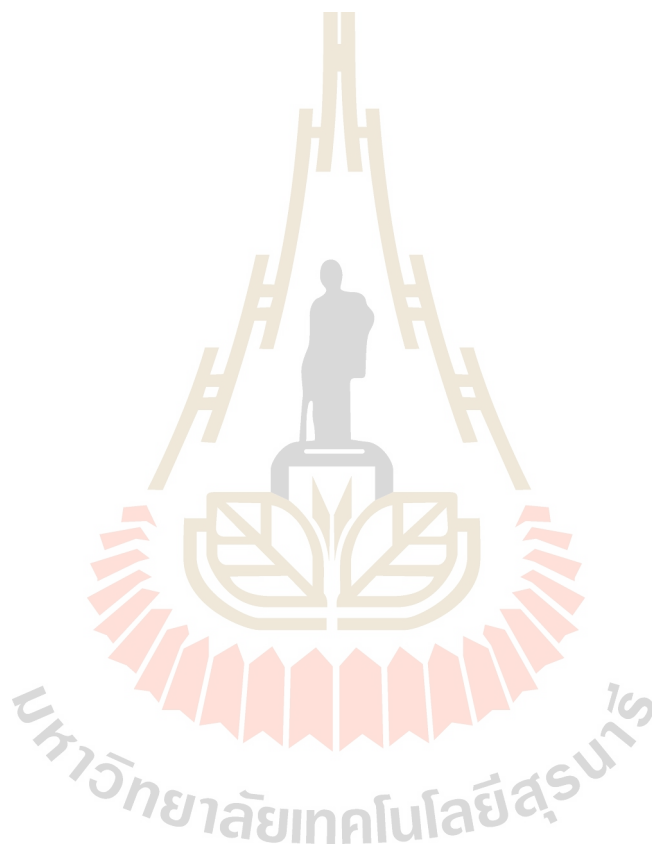
CHAPTER III

AMINO-FUNCTIONALIZED MESOPOROUS SILICA

ADSORBENT FOR THE REMOVAL OF ACID RED 1

3.1 Abstract

Mesoporous silica is well-known to provide high surface area and size selectivity for large molecules for application in adsorption. The surface of the mesoporous silica contains some hydroxyl groups. These groups could be potential adsorption sites for species that could form a hydrogen bond. To improve its adsorption capacity and selectivity for target compounds, the surface of the mesoporous silica could be modified. In this work, adsorbents based on mesoporous silica were synthesized using a sol-gel process and used for the adsorption of acid red 1. Tetraethylorthosilicate (TEOS) was used as a silica source and cetyltrimethylammonium bromide was used to direct the formation of mesoporous structure. 3-aminopropyltriethoxysilane (APTES) was used to functionalize the mesoporous silica. Adsorbents were characterized by transmission electron microscopy (TEM), X-ray diffraction (XRD), nitrogen adsorption-desorption analysis, and Fourier transform infrared (FTIR) spectroscopy.

TEM images show relatively homogeneous size distribution of spherical particles with about 1 μm diameter. Mesoporous structure was confirmed by XRD and N_2 adsorption-desorption analysis. Adsorption experiments were performed using 0.035

g adsorbent. The dye concentration, pH of dye solutions, adsorption time and temperature were varied within the range of 10-260 mg/L, 1.0-10.0, 30-120 min and 25.0-45.0 ^{o}C, respectively. The optimum pH for the adsorption was 2.0. The adsorption capacity of the APTES-functionalized adsorbent at 25.0 ^{o}C was 139.6 mg/g, which was higher than that of the unmodified adsorbent. Adsorption isotherm followed Freundlich model at the lower range of dye concentration and followed Langmuir model at the higher range of dye concentration. The adsorption processes were spontaneous and endothermic. After the equilibrium adsorption, the systems were in a higher state of randomness. Adsorption kinetics followed pseudo-second order model.

3.2 Introduction

Acid red 1 was added into baby food, breakfast sausages and burger meat as a food coloring. Aniline is a product of metabolized acid red 1, which could cause carcinogen (Villa and Conso, 2004) and interfere with blood hemoglobin (González-Vargas et al., 2014). Therefore, the European Food Safety Authority (EFSA) (2007) noted that the maximum level of 20 mg/kg acid red 1 is allowed to add in foodstuffs.

Acid red 1 is one class of dyes that contains sulfonate groups ($-SO_3^-$). In industry, acid red 1 is also used as a dyeing source. The U.S. Environmental Protection Agency (EPA) listed acid red 1 as one of non-biodegradable azo dye (Thomas et al., 2014). The intense color of the dye contaminated in water could cause some environment problems. Therefore, it is important to remove acid red 1 from wastewater before releasing from industrial factories.

Various methods have been used to remove acid dyes contamination in water, for example, degradation by enzyme (Gioia et al., 2018), electro-coagulation-flotation process (El-Hosiny et al., 2017), and catalytic degradation by using H_2O_2 (Kayan et al., 2017). Among these methods, adsorption has some advantages such as high efficiency, simple process, and relatively low cost.

Adsorbents, for example, coal fly ash (Hsu et al., 2008), cellulose grafted polymer based on acrylic acid and acrylamide monomers (Su et al., 2017), chitosan crosslinked with 7-ethyloctadecane diacid diglycidyl (Shimizu et al., 2003), biochars (Tran et al., 2017), and APTES modified clay (Thue et al., 2017) were used for the adsorption of acid red 1. These adsorbents have relatively low surface area which is one of the factors that contributes to the adsorption capacity.

Porous solids with high surface area and large pore volume were reported for the adsorption of acid dyes. MCM-41 (Lee et al., 2007) and SBA-3 (Anbia et al., 2010), were used to remove acid dyes from wastewater. Hollow mesoporous carbon nanospheres (Konicki et al., 2013) was used for the adsorption of acid orange 8 and acid red 88 from aqueous solutions.

To enhance the adsorption performance, mesoporous silica materials were functionalized with organosilanes. MCM-41 functionalized with 3-aminopropyltriethoxysilane (APTES) was used for the adsorption of acid fuchsine and acid orange II. Other organosilanes also have been used to functionalize onto mesoporous materials. Organosilanes including methyltriethoxysilane (MTES), phenyltriethoxysilane (PTES), and APTES were functionalized onto SBA-15 for the adsorption of acid orange 12 and acid red 73 (Lee et al., 2015). The adsorption

capacities of the dye increased with the increase amount of functionalized organosilanes.

In this research, mesoporous silica particles were prepared using tetraethylorthosilicate (TEOS) as a silica source and cetyltrimethylammonium bromide as a template to form a mesoporous structure. Mesoporous silica particles were functionalized by 3-aminopropyltriethoxysilane (APTES). Amino group ($-NH_2$) of an adsorbent can interact with sulfonate group ($-SO_3^-$) of acid red 1.

3.3 Experimental

3.3.1 Chemicals

Chemicals used in this research are listed in Table 3.1.

Table 3.1 Chemicals used in this research.

Chemicals	Formula	Content (%)	Suppliers
3-aminopropyltriethoxy-silane (APTES)	$H_2NC_3H_6Si(OC_2H_5)_3$	99.0	Sigma-Aldrich
acid red 1 dye	$C_{18}H_{13}N_3O_2(SO_3Na)_2$	60.0	Sigma-Aldrich
ammonia	NH_3	99.0	Acros Organics™
cetyltrimethylammonium-bromide (CTAB)	$C_{19}H_{42}BrN$	98.0	Carlo ERBA
ethanol	C_2H_5OH	99.9	Carlo ERBA
hydrochloric acid	HCl	37.0	Carlo ERBA
tetraethyl orthosilicate (TEOS)	$Si(OC_2H_5)_4$	99.0	Acros Organics™

3.3.2 Synthesis of amino-functionalized mesoporous silica adsorbent

3.3.2.1 Preparation of mesoporous silica adsorbent

Mesoporous silica adsorbent was prepared by using a method adapted from Yuan et al. (2014). 80 mL H_2O, 1.2 mL of 28% NH_3 and 0.3 g CTAB were added into 140 mL ethanol under constant stirring. After 6 h, 0.43 mL TEOS was added dropwise into the mixture solution. The mixture solution was stirred for another 6 h. Particles were isolated from the liquid mixture by centrifugation at 3,000 rpm for 10 min and redispersed in 150 mL ethanol under sonication for 1 h to remove CTAB (Jabariyan and Zanjanchi, 2012). After that, the particles were separated by centrifugation at 3,000 rpm for 10 min and dried at 60 °C overnight. The obtained powder, mesoporous silica adsorbent, was denoted as meso-SiO_2.

3.3.2.2 Preparation of amino-functionalized mesoporous silica adsorbent

To prepare amino-functionalized silica particles, meso-SiO_2 was modified by using a method from Liang et al. (2013). 2 mL H_2O, 4 mL of 28% NH_3 and 80 μL APTES were added to 1 g of meso-SiO_2 dispersed in 100 mL ethanol. The mixture solution was stirred for 12 h. The particles were separated by centrifugation at 3,000 rpm for 10 min. The amino modified mesoporous silica particles were washed with H_2O until the pH of the washed solution was close to 7 and after that with ethanol to remove the unreacted APTES. The resulting particles were dried at 60 °C overnight. The amino-functionalized mesoporous silica particles were denoted as NH_2-meso-SiO_2.

3.3.3 Characterizations

3.3.3.1 Transmission electron microscopy (TEM)

TEM was used to obtain very high spatial resolution images of the structures of the adsorbents. TEM analysis was performed on a Tecnai G^2 with an accelerating voltage of 200 kV. For TEM analysis, the adsorbents were suspended in 95% ethanol solution with sonication. The suspension was deposited on a micro grid with a holey carbon copper as a support membrane and dried at 70 °C with a UV lamp.

3.3.3.2 Nitrogen adsorption-desorption analysis

Nitrogen adsorption-desorption analysis was used to determine surface area, average pore size and total pore volume of the adsorbents. Nitrogen adsorption-desorption isotherm was obtained from a BELSORP-mini II. Before analysis, about 0.10 g of each sample was degassed at 200 °C under vacuum for 2 h and left until the pressure was reached to 10^{-2} mPa in order to remove physisorbed gases. The analysis was carried out at -196 ºC at relative pressure (P/P_0) from 0.01 to 0.99. Surface area was calculated by Brunauer-Emmett-Teller (BET) method. The total pore volume was obtained from the nitrogen amount adsorbed in correspondence of P/P_0 equal to 0.99 and the pore size distributions was calculated by Barrett-Joyner-Halenda (BJH) method.

3.3.3.3 X-ray diffraction (XRD)

An X-ray diffractometer (Bruker AXS D8) was used to investigate phases of the adsorbents. An X-ray source with Cu target was operated at a voltage of 40 kV and a current of 40 mA to provide Cu K_α radiation. An X-ray filtered was made of Ni. Diffraction patterns were obtained in 2θ range of 1 to 10º with a step increment

of 0.02° and a step time of 0.5 s. Samples were placed into sample holders. The powder was spread evenly before the measurement.

3.3.3.4 Fourier-transform infrared spectroscopy (FTIR)

Functional groups of adsorbents were studied by Fourier-transform infrared spectroscopy (Bruker, Tensor 27) using attenuated total reflection (ATR) mode. A sample for the measurement was prepared by sprinkling particles on a sample holder. IR spectra were obtained in the wavenumber range of 400-4000 cm^{-1} with the resolution of 4 cm^{-1}.

3.3.4 Adsorption study

3.3.4.1 Effect of pH

Effect of pH on the adsorption of acid red 1 was investigated over the pH range of 1.0-10.0. An adsorbent with the weight of 0.035 g was added into 35 mL of 200 mg/L dye solution contained in a 40-mL vial. The mixture solution was stirred for 60 min at 25.0 °C. After that, the adsorbent was separated from the solution by centrifugation. A concentration of the dye left in the solution was determined using a UV–Vis spectrometer (CHEM4-Vis-fiber spectrometer: USB 4000, Ocean optics). Absorbance measurement was made at 532 nm.

3.3.4.2 Effect of contact time

Adsorption study was conducted in a 40-mL vial contained with 35 mL of 200 mg/L acid red 1 and 0.035 g of an adsorbent. The pH of the dye solutions was controlled at 2.0. The temperature of solutions was controlled at 25.0 °C. Adsorption time was varied in the range of 30 to 120 min. After a given time, the adsorbent was separated from the solution by centrifugation and the dye solution was used for the absorbance measurement to determine the dye concentration.

3.3.4.3 Adsorption isotherm and thermodynamics experiments

Adsorption of acid red 1 at different concentration was carried out with 0.035 g adsorbent in 35 mL solution contained in a 40-mL vial. The dye concentration was varied in the range of 10-260 mg/L and the pH of the solutions was controlled at 2.0. The adsorption temperature was varied in the range of 25.0-45.0 $^{\circ}$C. After 60 min of adsorption, the adsorbent was separated by centrifugation and the dye solutions were used of absorbance measurement at 532 nm for the determination of dye concentration.

3.3.4.4 Kinetic experiment

Kinetic study of the dye onto adsorbent was carried out with 0.035 g adsorbent in 35 mL dye solution with the initial concentration at 80 mg/L. The mixture was contained in a 40-mL vial. The pH of the solutions was fixed at 2.0. Adsorption was carried out at different temperature, 25.0, 35.0, and 45.0 $^{\circ}$C. At each temperature, the dye concentration at different adsorption time,10, 20, 30, 40, 50, and 60 min, was determined by measuring the absorbance of the solutions at 532 nm.

3.4 Results and discussion

3.4.1 Characterization

3.4.1.1 Morphologies of the synthesized adsorbent

Figure 3.1 presents TEM images of NH_2-meso-SiO_2. The particles have spherical shape with a relatively uniform size distribution. The diameter of the particles is approximately 700 nm. The mesoporous structure was not observed due to low resolution of the TEM.
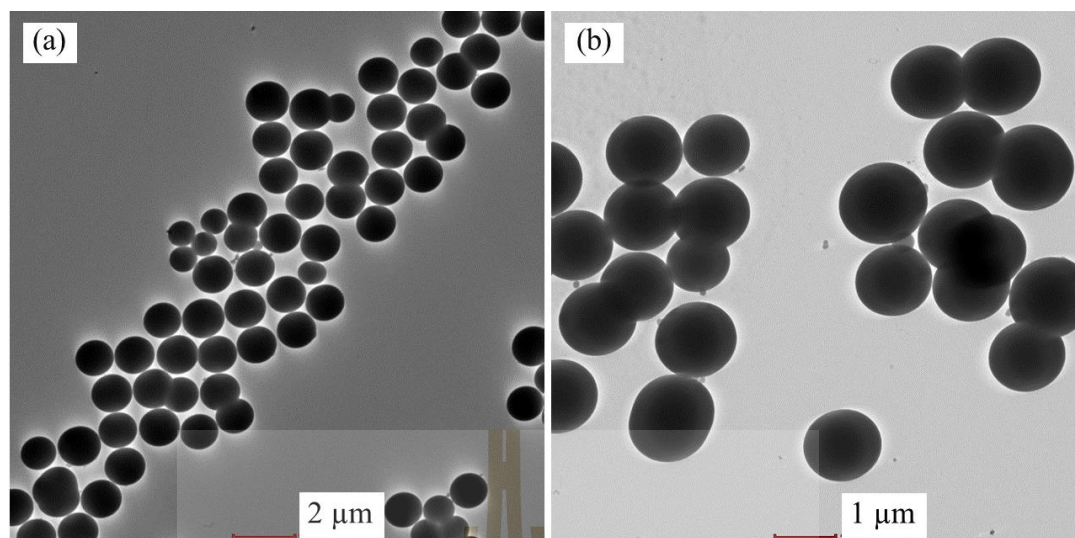
Figure 3.1 TEM images of NH_2-meso-SiO_2 (a) and (b) in different magnification.

To confirm the existence of mesoporous structure, the meso-SiO_2 and NH_2-meso-SiO_2 were investigated using XRD at low angles. XRD patterns are shown in Figure 3.2. A peak was observed at 2.5° in the XRD pattern of the meso-SiO_2, indicating the presence of mesoporous structure. Diffraction peak of NH2-meso-SiO2 was shifted to higher angle after functionalization of amino groups. A similar shift of a diffraction peak was also reported for APTES-functionalized mesoporous silica, which was coated onto magnetic silica particles (Yuan et al., 2014).

3.4.1.2 Nitrogen adsorption-desorption analysis

Nitrogen adsorption-desorption isotherm of NH_2-meso-SiO_2 is shown in Figure 3.3. This isotherm is type IV with H2-type hysteresis loop according to IUPAC classification for mesoporous material with pore size and shape that are not

well defined. The surface area, total pore volume and average pore diameter of the

NH_2-meso-SiO_2 were 192 m^2/g, 0.21 cm^3/g, and 4.5 nm, respectively.
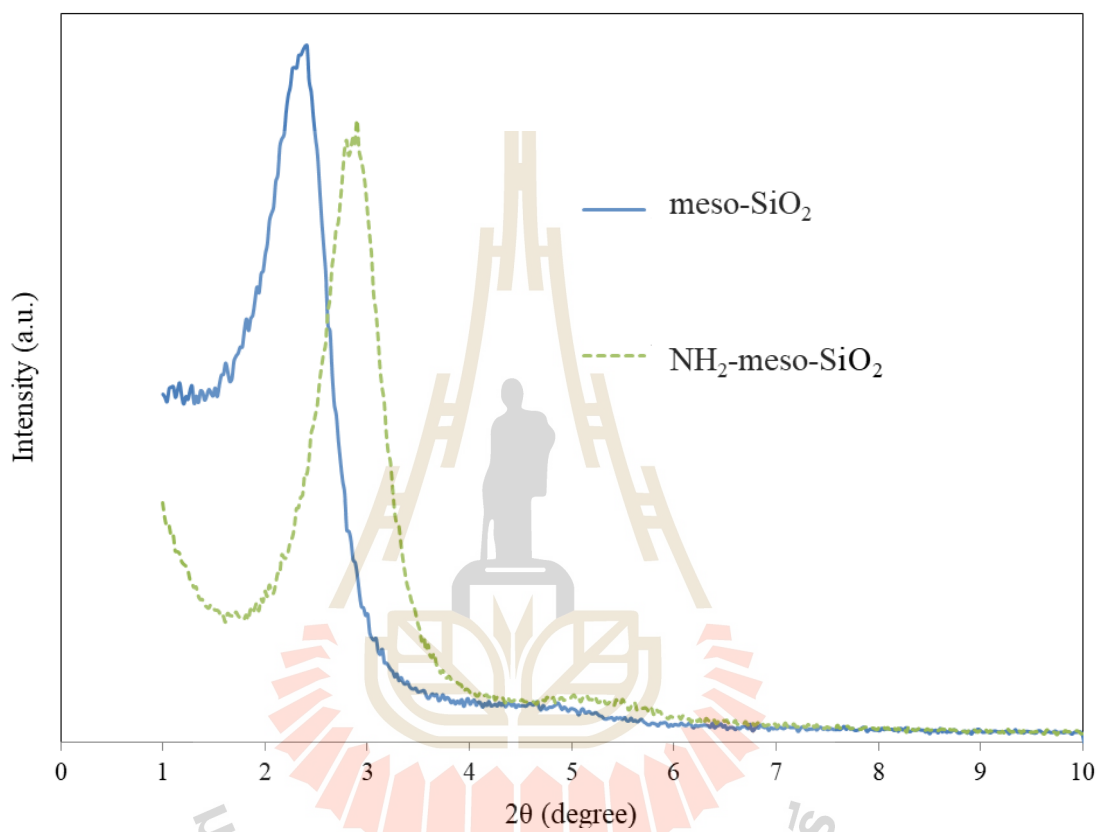
Figure 3.2 XRD patterns of meso-SiO_2 and NH_2-meso-SiO_2.
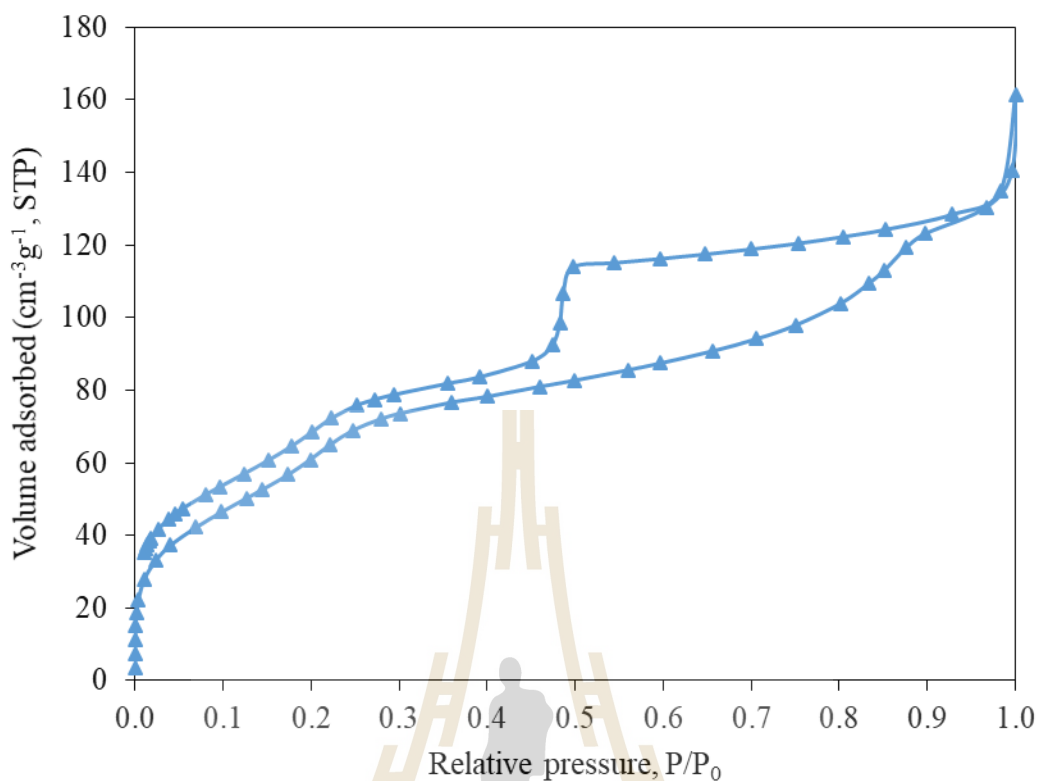
Figure 3.3 Nitrogen adsorption-desorption isotherm of NH_2-meso-SiO_2.

3.4.1.3 Adsorbents characterization by FTIR spectroscopy

The meso-SiO_2 and NH_2-meso-SiO_2 particles were characterized by FTIR to identify functional groups on their structures. FTIR spectra of NH_2-meso-SiO_2 and meso-SiO_2 are shown in Figure 3.4.

For NH_2-meso-SiO_2, the bands at 1,054 cm^{-1} and 790 cm^{-1} were assigned to symmetric Si-O-Si groups (Yuan et al., 2014). The band at 1,612 and 960 cm^{-1} was attributed to Si-OH groups (Yuan et al., 2014). Peaks at around 2,852 and 2,921 cm^{-1} belonged to the vibrations of -CH_2 of animosilane indicating that APTES was functionalized onto meso-SiO_2 (Zhang et al., 2014). The incorporation of the

amino group was verified by symmetric -NH$_2$ bending at new peaks appeared at 1473 cm^{-1} (Yuan et al., 2014).

3.4.2 Adsorption study

3.4.2.1 Effect of pH

The effect of pH on adsorption capacity of acid red 1 onto the adsorbent was investigated in the pH range of 1.0 to 10.0 at a fixed dye concentration of 200 mg/L at 25.0 °C for 60 min. The adsorption capacity was calculated according to equation [3.1];

$$q_e = \frac{V(C_0 - C_e)}{m} \qquad [3.1]$$
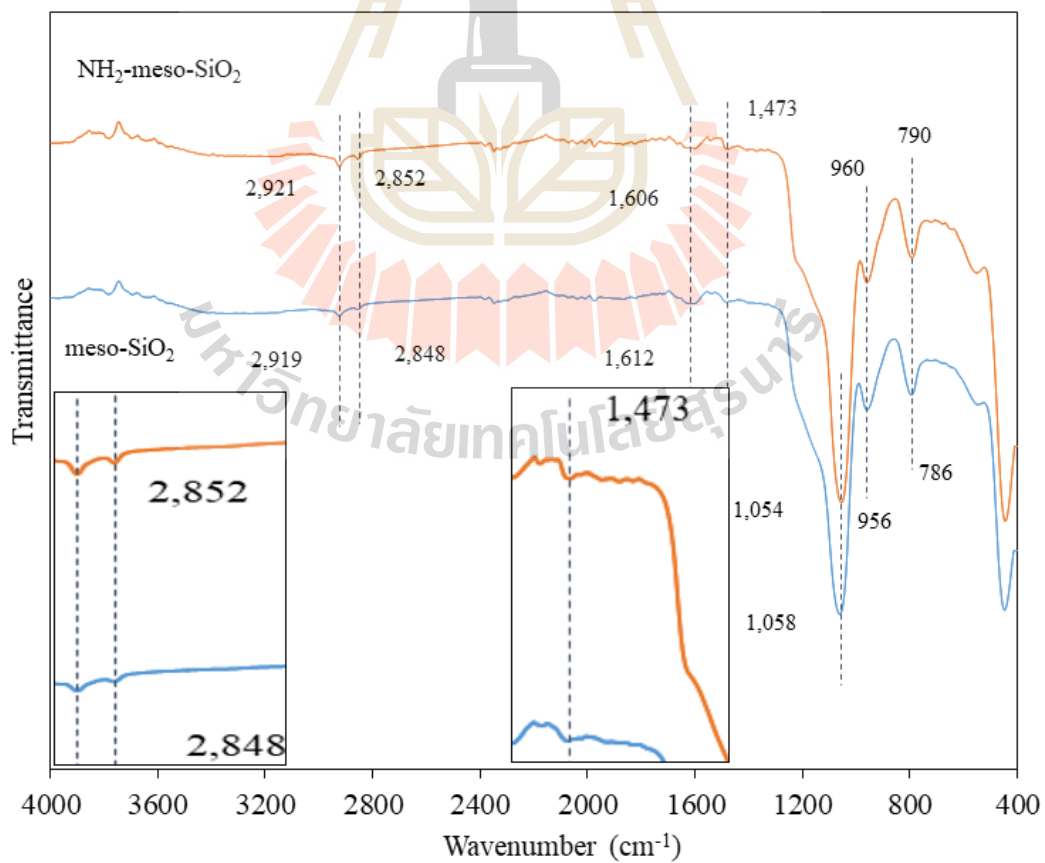
Figure 3.4 FTIR spectra of NH$_2$-meso-SiO$_2$ and meso-SiO$_2$ adsorbent.

where q_e is the equilibrium adsorption capacity (mg/g), V is the volume of the solution (L), C_0 and C_e (mg/L) are the initial and equilibrium concentrations of the acid red 1 in a solution, respectively, and m is the adsorbent mass (g).

Acid red 1 is an anionic azo dye that contains two sulfonic acid groups $[R\text{-}(SO_3Na)_2]$. In aqueous solutions, acid red 1 can be dissociated to sulfonate anion $[R\text{-}(SO_3^-)_2]$ which can interact with the protonated amino groups of $-NH_3^+$ on the adsorbent. Therefore, the pH of the solutions could affect both the anionic form of the dye and the surface charge of the adsorbent.

In Figure 3.5, the optimum adsorption capacity was observed at pH 2.0. The adsorption tended to increase when the pH of the solutions was decreased from 10.0 to 2.0. This can be explained by pH at point of zero charge (pH_{pzc}) which represents the surface charge behavior of the adsorbents. Adsorption of anionic dyes is favored at $pH<pH_{pzc}$ of the adsorbent, where the surface charge of the adsorbent is positive (Konicki et al., 2017). The adsorbent in this work consists of $-NH_2$ group and mesoporous silica. The pH_{pzc} of mesoporous silica was found to be about 3.1 (Velez et al., 2013) and that of the pH_{pzc} of the primary amine groups ($-NH_2$) was about 7.34 (Yang et al., 2013). Therefore, the extent of the positive surface charge of the adsorbent should be increase with the decrease of the pH of the solution. Araghi and Entezari (2005) reported that at pH = 2, the amino groups were fully protonated, and the adsorption could not be further improved by adjusting the initial pH to 1. When the pH of the solution was adjusted to 1.0, the adsorption capacity decreased. This could be resulted from the protonation of $-SO_3^-$ groups on the dye that reduced the amount of the dye in the anionic form.
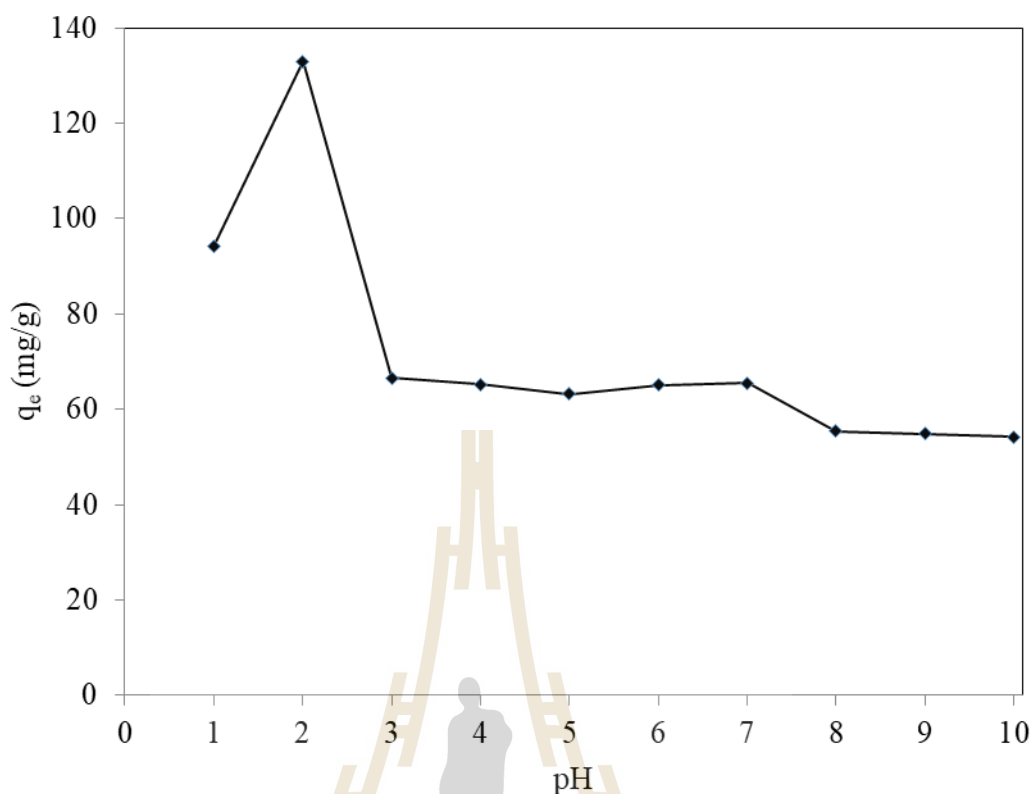
Figure 3.5 Influence of pH on the adsorption capacity of NH_2-meso-SiO_2 for acid red 1.

Sulfonic groups exhibit negative charge even at higher acidic solutions due to their pK_a values lower than zero (Cardoso et al., 2011). The pK_a of the sulfonate groups of the azo dye are in the range 0.7–1.5 (Owusu-Apenten, 2002). Therefore, at the $pH < pK_a$ the fraction of anionic form should be decrease.

3.4.2.2 Effect of contact time

Effect of contact time on the adsorption capacity of the adsorbent was investigated. Figure 3.6 shows time profile adsorption of acid red 1 onto meso-SiO_2 and NH_2-meso-SiO_2. The extent of dye removal by meso-SiO_2 and NH_2-meso-SiO_2 was found to increase with the increase of contact time. The adsorption reached

equilibrium in about 60 min. Therefore, adsorption time at 60 min was selected for further study with NH_2-meso-SiO_2.

The adsorption capacity of NH_2-meso-SiO_2 toward acid red 1 was higher than that of meso-SiO_2. This could be due to functionalization of -NH_2 onto the meso-SiO_2 resulting in high adsorption site for the adsorbent.

3.4.2.3 Adsorption isotherm

Adsorption isotherms are important for explaining the interaction between adsorbate and adsorbent in an equilibrium state. Langmuir and Freundlich isotherms are commonly used to explain adsorption behaviors.

The Langmuir adsorption equation can be represented as equation [3.2];

$$\frac{q_e}{q_m} = \frac{K_A C_e}{1 + K_A C_e} \qquad [3.2]$$

where, q_e (mg/g) is the amount of an adsorbate adsorbed per gram of an adsorbent at equilibrium; q_m (mg/g) is the maximum amount of the adsorbate adsorbed to form a monolayer coverage per gram of the adsorbent; K_A (L/mg) is the Langmuir adsorption equilibrium constant; C_e (mg/L) is the concentration of the adsorbate at equilibrium. Adsorption data can be fitted to the Langmuir isotherm in a linear form as the following equation [3.3];

$$\frac{C_e}{q_e} = \frac{C_e}{q_m} + \frac{1}{K_A q_m} \qquad [3.3]$$

Maximum adsorption capacity (q_m) can be obtained from a linear plot of C_e/q_e against C_e. K_A can be calculated from the intercept value.
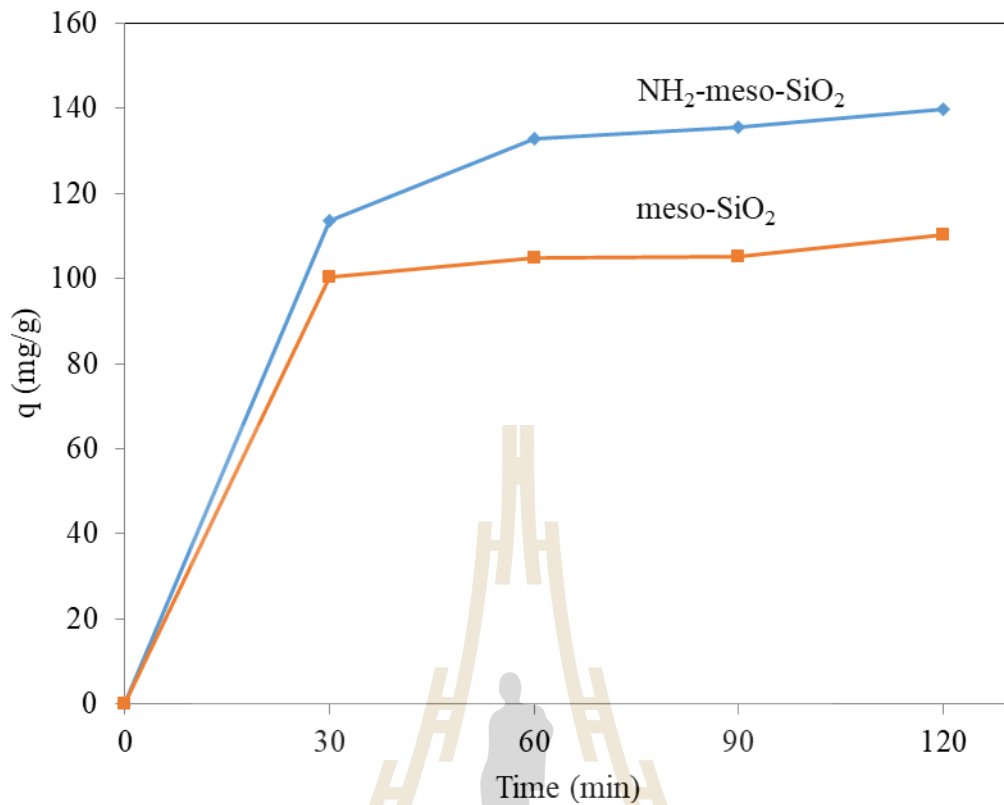
Figure 3.6 Time profile adsorption of acid red 1 on meso-SiO$_2$ vs NH$_2$-meso-SiO$_2$ at pH 2.0.

The Freundlich isotherm is another commonly used model. It has a general form as expressed by equation [3.4];

$$q_e = K_F C_e^{1/n} \tag{3.4}$$

where q$_e$ and C$_e$ are defined as in equation [3.2], K$_F$ is the Freundlich constant, the indicative of the relative adsorption capacity of the adsorbent and 1/n is an empirical constant. A linear form of Freundlich isotherm is shown in equation [3.5];

$$\ln q_e = \ln K_F + \frac{1}{n} \ln C_e \tag{3.5}$$

when ln q_e is plotted against ln C_e and the data are treated by linear regression analysis, K_F and $1/n$ can be obtained from the intercept and the slope of the line, respectively. Freundlich model applies well to solid with heterogeneous surface properties.

A graph plotted between q_e and C_e is shown Figure 3.7. The adsorption data from the study with NH_2-meso-SiO_2 were fitted with Langmuir and Freundlich model and the results are shown in Table 3.2 and 3.3, respectively.
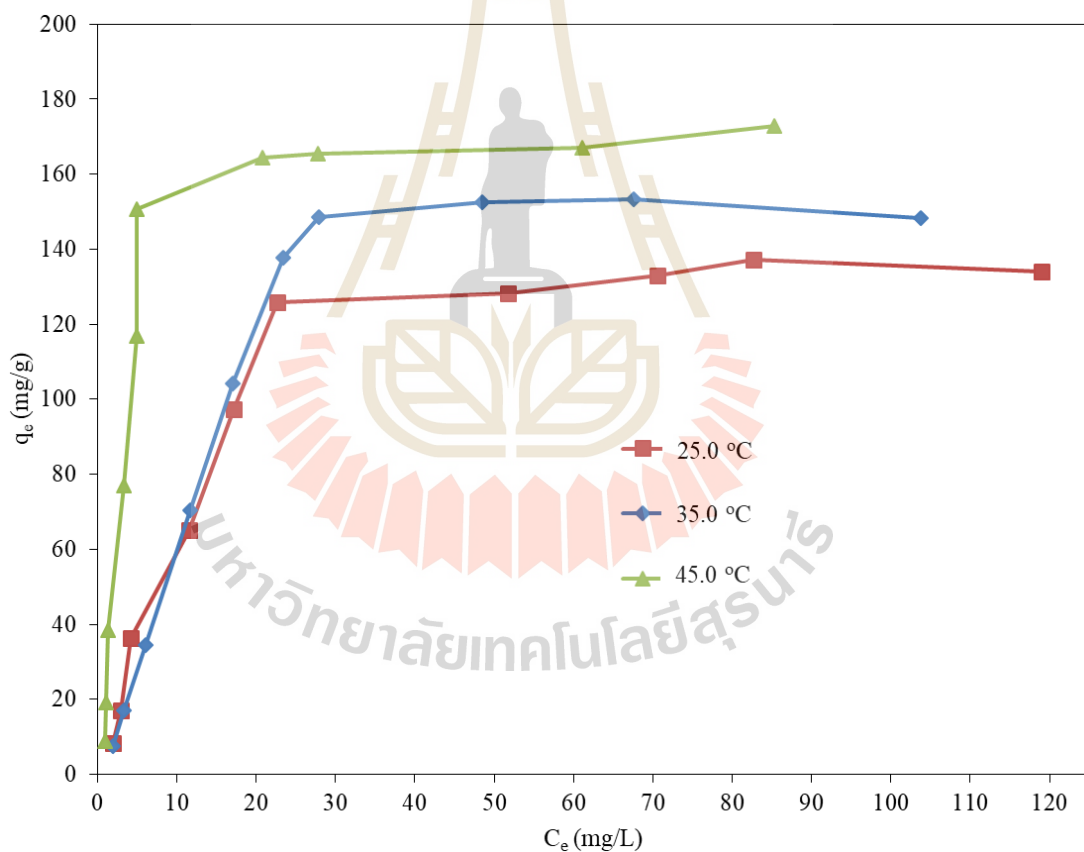
Figure 3.7 Adsorption isotherms of acid red 1 on NH_2-meso-SiO_2 at 25.0, 35.0, and 45.0 $^{\circ}$C at pH 2.

Table 3.2 Isotherm equations for Langmuir model and other derived parameters for the adsorption of acid red 1 in the concentration range 10-260 mg/L onto NH_2-meso-SiO_2 adsorbent.

Temperature (°C)	Fitting equation	R^2	q_m (mg/g)	K_A (L/mg)
25.0	$C_e/q_e = 0.0061\ C_e + 0.114$	0.9565	163.93	0.053
35.0	$C_e/q_e = 0.0049\ C_e + 0.1261$	0.8601	204.08	0.039
45.0	$C_e/q_e = 0.0053\ C_e + 0.0363$	0.9651	188.68	0.146

Table 3.3 Isotherm equations for Freundlich model and other derived parameters for the adsorption of acid red 1 in the concentration range 10-260 mg/L onto NH_2-meso-SiO_2 adsorbent.

Temperature (°C)	Fitting Linear equation	R^2	$1/n$	K_F $[(mg/g)/(mg/L)^{1/n}]$
25.0	$\ln q_e = 0.6257 \ln C_e + 2.3560$	0.8434	1.59	10.55
35.0	$\ln q_e = 0.7699 \ln C_e + 2.0594$	0.8655	1.30	7.84
45.0	$\ln q_e = 0.5307 \ln C_e + 3.2915$	0.6835	1.88	26.88

The values of the correlation coefficients for Langmuir model are (not all) higher than those for Freundlich model. However, the obtained q_m values from Langmuir model are significantly different from those of the experimental values. This suggests that the adsorption did not conform well to Langmuir model. Experimental data were divided into two groups of dye concentration that is group one in the concentration range of 10-160 mg/L and group two in the concentration range of 180-260 mg/L. Both groups of data were fitted again with Langmuir and Freundlich model and the results are in Table 3.4 and 3.5, respectively.

At the concentration range of 10-160 mg/L, the values of the correlation coefficient for Freundlich model are ~0.9. This suggests that the adsorption data at low concentration could be better explained by Freundlich model. Freundlich model applies well to solid with heterogeneous surface properties. Heterogeneous adsorption sites of NH2-meso-SiO2 could result from different orientations of aminopropyl groups on the silica surface. These are aminopropyl groups protruding above the silica surface and aminopropyl groups interacting with silanol groups on the silica surface as explained by Yokoi et al. (2012). In addition, the results from nitrogen adsorption-desorption analysis suggest that the adsorbent has non-uniform pore distribution. This could also contribute to heterogeneous adsorption sites after APTES functionalization.

For the concentration range of 180-260 mg/L, the data fitted well with Langmuir model as the correlation coefficients (R^2) for every studied temperature were greater than 0.99. This suggests homogeneous adsorption sites. It is assumed that the adsorbed dyes on the adsorbent surface could later act as the adsorption sites, which could interact with other dye molecules in the solution.

Table 3.4 Isotherm equations for Freundlich model and other derived parameters for the adsorption of acid red 1 in the concentration range 10-160 mg/L onto NH_2-meso-SiO_2 adsorbent.

Temperature (^{o}C)	Fitting equation	R^2	$1/n$	K_F [(mg/g)/(mg/L)$^{1/n}$]
25.0	$\ln q_e = 1.021 \ln C_e + 1.7161$	0.9511	0.98	5.56
35.0	$\ln q_e = 1.1536 \ln C_e + 1.3748$	0.9937	0.87	3.95
45.0	$\ln q_e = 1.4037 \ln C_e + 2.6917$	0.8956	0.71	14.76

Table 3.5 Isotherm equations for Langmuir model and other derived parameters for the adsorption of acid red 1 in the concentration range 180-260 mg/L onto NH_2-meso-SiO_2 adsorbent.

Temperature (^{o}C)	Fittting equation	R^2	q_m (mg/g)	K_A (L/mg)
25.0	$C_e/q_e = 0.0072 \, C_e + 0.0218$	0.9971	138.89	0.33
35.0	$C_e/q_e = 0.0068 \, C_e - 0.0069$	0.9989	147.06	0.99
45.0	$C_e/q_e = 0.0057 \, C_e + 0.0096$	0.9992	175.44	0.59

3.4.2.4 Thermodynamic study

Thermodynamic parameters including Gibbs free energy change (ΔG), enthalpy change (ΔH) and entropy change (ΔS) were used in providing the information about the adsorption process. Relationship among a distribution coefficient (K_D), ΔH and ΔS can be described by equation [3.6];

$$\ln K_D = \frac{\Delta S}{R} - \frac{\Delta H}{RT} \qquad [3.6]$$

where, R is the universal gas constant ($8.314 \ Jmol^{-1} \ K^{-1}$) and T is the absolute temperature (Kelvin). The values of ΔH and ΔS can be calculated from the slope and the intercept of the plot of $\ln K_D$ against $1/T$. K_D can be calculated from equation [3.7];

$$K_D = \frac{q_e}{C_e} \qquad [3.7]$$

From the adsorption data conducted at different temperatures: a plot of $\ln K_D$ against $1/T$ was constructed. The values of ΔH and ΔS can be calculated from the slope and intercept of the plot.

The ΔG provides information about the process spontaneity, which can be related to ΔH and ΔS as shown in equation [3.8];

$$\Delta G = \Delta H - T\Delta S \qquad [3.8]$$

The results are given in Table 3.6. The values of R^2 are relatively low for the dye concentrations 10-160 mg/L, but > 0.9 for those from 180-260 mg/L. The derived parameters, ΔG, ΔH, and ΔS, obtained from the data with higher values of correlation coefficient suggest that the adsorption process is spontaneous and endothermic with the increased randomness at the solid/liquid interface.

Table 3.6 Thermodynamic parameters for the adsorption of acid red 1 onto NH_2-meso-SiO_2.[a]

C_0 (mg/L)	Equation	R^2	ΔH (kJ/mol)	ΔS (J/mol)	ΔG (kJ/mol) 25 °C	35 °C	45 °C
10	y = -3381.9x + 12.635	0.6457	28.1	105	-3.20	-4.25	-5.30
20	y = -5044.4x + 18.457	0.6540	41.9	153	-3.82	-5.35	-6.88
40	y = -5565.7x + 20.495	0.4847	46.2	170	-4.41	-6.11	-7.81
80	y = -6645.1x + 23.806	0.7707	55.3	198	-3.76	-5.74	-7.72
120	y = -6768.4x + 24.218	0.7769	56.3	201	-3.76	-5.77	-7.78
160	y = -7984.5x + 28.23	0.7579	66.4	235	-3.59	-5.94	-8.29
180	y = -5515.1x + 19.46	0.9736	45.9	162	-2.39	-4.00	-5.62
200	y = -5458.3x + 18.914	0.9934	45.4	157	-1.50	-3.08	-4.65
220	y = -2376.3x + 8.4946	0.9838	19.8	70.6	-1.30	-2.01	-2.71
260	y = -2776.7x + 9.4122	0.9837	23.1	78.3	-0.25	-1.03	-1.81

[a] Data for K_D calculation are shown in Appendix A.

3.4.2.5 Kinetic study

To describe the adsorption behavior with time, several kinetic models were tested. In this work, pseudo-first-order and pseudo-second-order models

were used. These models are commonly used to describe the adsorption of dye on adsorbents.

Pseudo-first order model is written as shown in equation [3.9];

$$\log (q_e - q_t) = \log q_e - (k_1 t / 2.303) \tag{3.9}$$

where q_t is the adsorption capacity at time t (mg/g), k_1 is the pseudo first-order rate constant (min^{-1}), and t is the contact time (min).

Pseudo-second order model is written as shown in equation [3.10];

$$t/q_t = 1/k_2 q_e^2 + (1/q_e)t \tag{3.10}$$

where k_2 is the pseudo second-order rate constant (g/mg.min), and t is the contact time (min).

Figure 3.8 and 3.9 show a plot of log (q_e-q_t) versus t and t/q_t versus t, respectively. Table 3.7 shows derived equations and parameters for both kinetic models. It appears that the data seem to fit well both models because the values of R^2 are greater than 0.9. Besides the high value of R^2, the agreement between experimental and calculated values of q_e was evaluated according to the literature (Montazerolghaem et al., 2017) using equation [3.11];

$$\Delta q_e \, (\%) = \sqrt{\frac{\sum \left[\frac{(q_{e,exp} - q_{e,cal})}{q_{e,exp}} \right]^2}{N-1}} \times 100 \tag{3.11}$$

where $q_{e,exp}$ and $q_{e,cal}$ are the experimental and calculated adsorption capacity, respectively, and N is the total number of experimental points.

From the calculation, Δq_e was < 1.0% indicating that $q_{e,exp}$ and $q_{e,cal}$ are not significantly different. This suggests that pseudo-second order kinetic model

could be used to describe the adsorption behavior of acid red 1 onto the adsorbents. The model suggests that the rate of the adsorption rate is controlled by the diffusion of the dye molecules through the pores of the adsorbent.
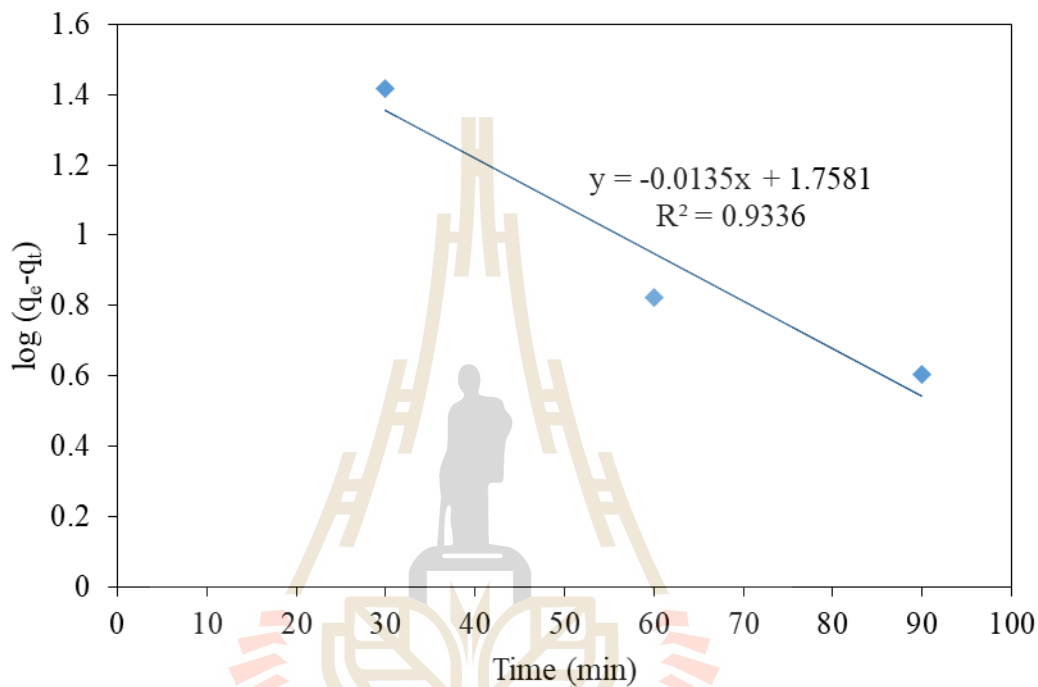
Figure 3.8 Pseudo-first-order kinetic model for the adsorption of 200 mg/L acid red 1 onto 0.035 g NH_2-meso-SiO_2.
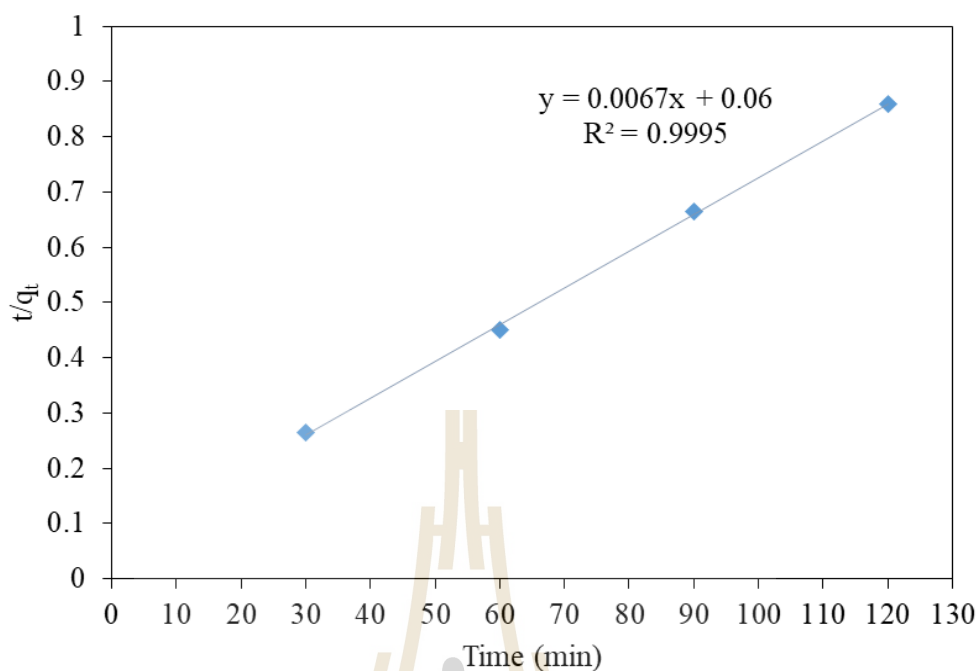
Figure 3.9 Pseudo-second-order kinetic model for the adsorption of 200 mg/L acid red 1 onto 0.035 g NH_2-meso-SiO_2.

Table 3.7 Pseudo-first-order model and Pseudo-second-order model for the adsorption of acid red 1 onto NH_2-meso-SiO_2 at 25.0 °C.[a]

kinetic model	$q_{e,cal}$[b] (mg/g)	Fitting equation	R^2	rate constant
Pseudo-first-order model	57.3	log (q_e - q_t) = -0.0135t + 1.7581	0.9336	0.031 min^{-1}
Pseudo-second-order model	149.3	t/q_t = 0.0067t + 0.06	0.9995	7.0×10^{-4} g/mg·min

[a] Experimental values of adsorption capacity; $q_{e,exp}$ = 139.6 mg/g
[b] Calculated value of adsorption capacity

3.5 Conclusion

The amino-functionalized mesoporous silica adsorbent was successfully prepared and characterized. The adsorbent was applied in aqueous media for adsorption of acid red 1. The adsorption of acid red 1 reached equilibrium state in 60 min at 25.0 ℃. The equilibrium adsorption data fitted to the Freundlich isotherm model at the lower dye concentration range of 10-160 mg/L and to the Langmuir isotherm model at the higher dye concentration range of 180-260 mg/L. The maximum adsorption capacity under the studied experimental conditions found to be 139.6 mg/g at 25.0 ℃. The adsorption processes were spontaneous and endothermic. After the equilibrium adsorption, the systems were in a higher state of randomness. Adsorption kinetics followed pseudo-second order model. Moreover, the APTES functionalized on mesoporous silica particles provided higher adsorption sites leading to higher adsorption capacity for acid red 1.

3.6 References

Anbia, M., Hariri, S. A., and Ashrafizadeh, S. N. (2010). Adsorptive removal of anionic dyes by modified nanoporous silica SBA-3. **Applied Surface Science**. 256: 3228-3233.

Araghi, S, H., and Entezari, M. H. (2015). Amino-functionalized silica magnetite nanoparticles for the simultaneous removal of pollutants from aqueous solution. **Applied Surface Science**. 333: 68-77.

Cardoso, N. F., Lima, E. C., Pinto, I. S., Amavisca, C. V., Royer, B., Pinto, R. B., Alencar, W. S., and Pereira, S. F. P. (2011). Application of cupuassu shell as

biosorbent for the removal of textile dyes from aqueous solution. **Journal of Environmental Management**. 92: 1237-1247.

European Food Safety Authority. (2007). Opinion of the scientific panel on food additives, flavourings, processing aids and materials in contact with food. **The EFSA Journal**. 515: 1-28. Parma, Italy.

Gioia, L., Ovsejevi, K., Manta, C., Míguez, D., and Menéndez, P. (2018). Biodegradation of acid dyes by an immobilized laccase: an ecotoxicological approach. **Environmental Science Water Research & Technology**. 4: 2125-2135.

González-Vargas, C., Salazar, R., and Sirés, I. (2014). Electrochemical treatment of acid red 1 by electro-fenton and photoelectro-fenton processes. **International Journal of Electrochemical Science**. 4(4): 235-245.

Hsu, T. C. (2008). Adsorption of an acid dye onto coal fly ash. **Fuel**. 87: 3040-3045.

Jabariyan, S., and Zanjanchi, M. A. (2012). A simple and fast sonication procedure to remove surfactant templates from mesoporous MCM-41. **Ultrasonics Sonochemistry**. 19: 1087-1093.

Lee, C. K., Liu, S. S., Juang, L. C., Wang, C. C., Lin, K. S., & Lyu, M. Du. (2007). Application of MCM-41 for dyes removal from wastewater. **Journal of Hazardous Materials**. 147(3): 997-1005.

Lee, J. Y., Chen, C. H., and Cheng, S. (2015). Adsorption of acid dyes by functionalized SBA-15 mesoporous silica of different pore lengths. **Journal of the Chinese Chemical Society**. 62(6): 483-494.

Liang, J., Xue, Z., Xu, J., Li, J., Zhang, H., and Yanga, W. (2013). Highly efficient incorporation of amino-reactive dyes into silica particles by a multi-step

approach. **Colloids and Surfaces A: Physicochemical and Engineering Aspects**. 426: 33-38.

Montazerolghaem, M., Aghamiri, S. F., Talaie, M. R., and Tangestaninejad, S. (2017). A comparative investigation of CO_2 adsorption on powder and pellet forms of MIL-101. **Journal of the Taiwan Institute of Chemical Engineers**.72: 45-52.

Owusu-Apenten, R, K. (2002). Food Protein Analysis. **Quantitative Effects on Processing**. Marcel Dekker, Inc., U.S., p.135.

Shimizu, Y., Taga, A., and Yamaoka, H. (2003). Synthesis of novel crosslinked chitosans with a higher fatty diacid diglycidyl and their adsorption abilities towards acid dyes. **Adsorption Science and Technology**. 21(5): 439-449.

Su, X., Liu, L., Zhang, Y., Liao, Q., Yu, Q., Meng, R, and Yao, J. (2017). Efficient removal of cationic and anionic dyes from aqueous solution using cellulose-g-p(AA-co-AM) bio-adsorbent. **BioResources**. 12(2): 3413-3424.

Thomas, S, Sreekanth, R., Sijumon, V. A., Aravind, U. K., and Aravindakumar, C. T. (2014). Oxidative degradation of acid red 1 in aqueous medium. **Chemical Engineering Journal**. 244: 473-482.

Thue, P. S., Sophia, A. C., Lima, E. C., Wamba, A. G.N., Alencar, W. S., Reis, G. S., Rodembusch, F. S., and Dias, S. L. P. (2018). Synthesis and characterization of a novel organic-inorganic hybrid clay adsorbent for the removal of acid red 1 and acid green 25 from aqueous solutions. **Journal of Cleaner Production**. 171(10): 30-44.

Tran, H. N., Lee, C. K., Vu, M. T., and Chao, H. P. (2017). Removal of copper, lead,methylene green 5, and acid red 1 by saccharide-derived spherical

biochar prepared at low calcination temperatures: adsorption kinetics, isotherms, and thermodynamics. **Water Air and Soil Pollution**. 228(401): 1-16.

Villa, A. F. and Conso, F. (2004). Aromatic amines. **EMC - Toxicologie-Pathologie**. 1: 161-177.

Yang, X., Wang, X., Liu, X., Zhang, Y., Song, W., Shu, C., Jiang, L., and Wang, C. (2013). Preparation of graphene-like iron oxide nanofilm/silica composite with enhanced adsorption and efficient photocatalytic properties. **Journal of Materials Chemistry A**. 1: 8332-8337.

Yokoi, T., Kubota, Y., and Tatsumia, T. (2012). Amino-functionalized mesoporous silica as base catalyst and adsorbent. **Applied Catalysis A: General**. 421-422: 14-37.

Yuan, Q., Chi, Y., Yu, N., Zhao, Y., Yan, W., Li, X., and Dong, B. (2014). Amino-functionalized magnetic mesoporous microspheres with good adsorption properties. **Materials Research Bulletin**. 49: 279-284.

Zhang, C., Wang, Y., Zhou, Y., Guo, J., and Liu, Y. (2014). Silica-based surface molecular imprinting for recognition and separation of lysozymes. **Analytical Methods**. 6: 8584-8591.

CHAPTER IV

SYNTHESIS AND CHARACTERIZATION OF AMINO-FUNCTIONALIZED MESOPOROUS SILICA-BASED MOLECULARLY IMPRINTED ADSORBENT TOWARDS SELECTIVE ADSORPTION OF ACID RED 1

4.1 Abstract

Acid dyes are one class of pollutants and difficult to treat due to their high solubility in water and complex molecular structures. Adsorption is one of the effective methods for dye removal. Among many adsorbents, molecularly imprinted adsorbents have attracted considerable attention because of their predetermined recognition ability, high selectivity and reusability. In this work, a sol-gel process using tetraethyl orthosilicate as a silica source was used for the synthesis of molecularly imprinted adsorbent. The adsorbent surface was functionalized with 3-aminopropyltriethoxysilane before using in the imprinting process. Acid red 1 was used as a template. A non-imprinted adsorbent was synthesized using the same procedure except the template. The obtained adsorbents were characterized by X-ray diffraction (XRD), transmission electron microscopy (TEM), Fourier transform infrared (FTIR) spectroscopy, and nitrogen adsorption-desorption technique.

Adsorption experiments were performed using 0.035 g adsorbent. The dye concentration, a pH of dye solutions, adsorption time and temperature were varied within the range of 10-260 mg/L, 1.0-10.0, 30-150 min and 25.0-45.0 $^{\circ}$C, respectively. The adsorption of the imprinted adsorbent followed the Langmuir isotherm model. The adsorption capacities at 25.0 $^{\circ}$C of the imprinted adsorbent and non-imprinted adsorbent were 36.93 and 28.32 mg/g, respectively. The adsorption processes were spontaneous and exothermic. After the equilibrium adsorption, the systems were in a lower state of randomness. Adsorption kinetics followed pseudo-second order model. Values of a separation factor of the imprinted adsorbent for acid red 1 compared to tartrazine, zincon and sulfasalazine were 30.46, 2.22, and 1.78, respectively. The results demonstrate that the imprinted adsorbent can selectively bind the target dye.

4.2 Introduction

Nowadays, various existing treatment processes of removing dyes from wastewater have been investigated. Several techniques such as adsorption (Shan et al., 2015), degradation by enzyme (Gioia et al., 2018), electrocoagulation (El-Hosiny et al., 2017), and catalytic degradation by using H_2O_2 (Kayan et al., 2017) have been used. However, the efficiency of these methods is relatively moderate. Among these methods, adsorption has been found to be superior to other techniques in terms of low cost of operation and simplicity of adsorbents preparation.

Adsorbents are important components in adsorption processes. Their structures have a strong influence on the adsorption of target compounds. Some adsorbents investigated for the adsorption of acid red 1 were coal fly ash (Hsu et al., 2008),

cellulose grafted polymer based on acrylic acid (AA) and acrylamide (AM) as monomers (Su et al., 2017), chitosan crosslinked with 7-ethyloctadecane diacid diglycidyl (Shimizu et al., 2003), biochars (Tran et al., 2017), and APTES modified clay (Thue et al., 2017). These adsorbents, except the biochar, were able to remove acid red 1 from aqueous solutions. However, their adsorption efficiency might be reduced in the presence of other species in the solutions that could also interact with the adsorption sites. Generation of adsorption sites that are selective to target molecules could solve the problem.

Molecularly imprinted adsorbents (MIAs) are alternative adsorbents for the removal of dyes. MIAs have gained some attentions because of several advantages such as high selectivity to target compounds and reusability (Zhang et al., 2014). In a synthesis of an MIA, a target molecule is used as a template. After finishing the synthesis, it is extracted from the adsorbent, leaving sites that provide selectivity in size, shape, and functionality to the target molecule (Vasapollo et al., 2011). In general, MIA prepared by bulk and solution polymerization have been shown to be applicable for the adsorption of the target dyes (Yan and Raw, 2006).

Many MIAs are synthesized by polymerization of organic functional monomers and an organic crosslinking monomer. The synthesized methods could be time-consuming and a moderate amount of imprinted sites could be obtained. Organic MIAs could be unsuitable for their applications in aqueous solutions because interactions between the target species and the polymer could become weaker. To avoid these problems, silica-based MIAs synthesized by a sol-gel method could be used.

The objectives of this work are to synthesize, characterize, and use the silica-based MIA and nonimprinted adsorbent (NIA) in the adsorption study of acid red 1 in aqueous solutions. Acid red 1 as a representative of acid dyes with two sulfonate groups was used as a model template for the synthesis of the molecularly imprinted adsorbent under mild conditions. Figure 4.1 shows acid red 1 and other dyes used in the adsorption study. Preparation of nanosilica particles was based on the sol-gel process. The obtained nanosilica particles were modified with 3-aminopropyltriethoxysilane (APTES) to yield adsorption sites for the dye. The amino-functionalized silica particles were coated with a mesoporous silica layer to form imprinted sites.

Acid red 1

Tartrazine

Zincon
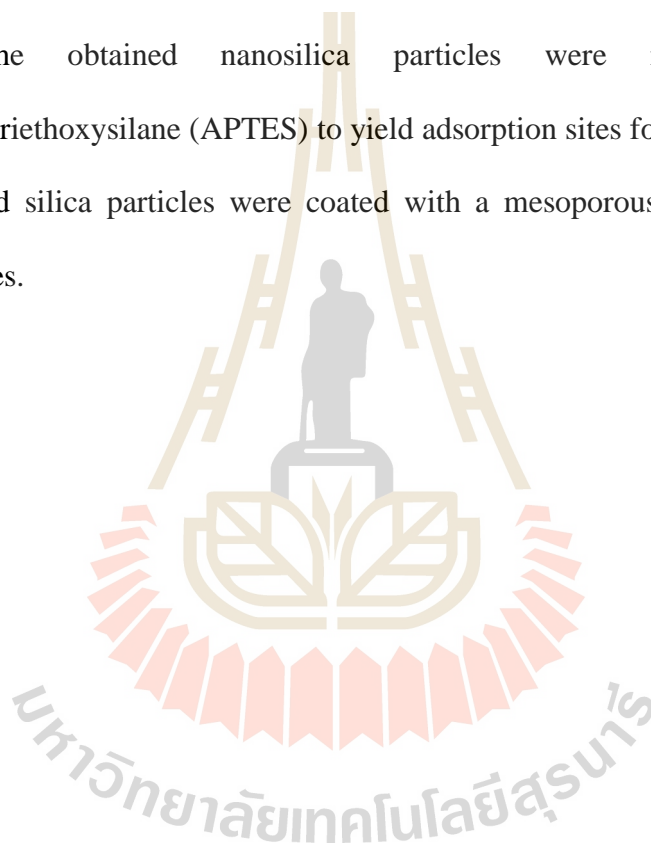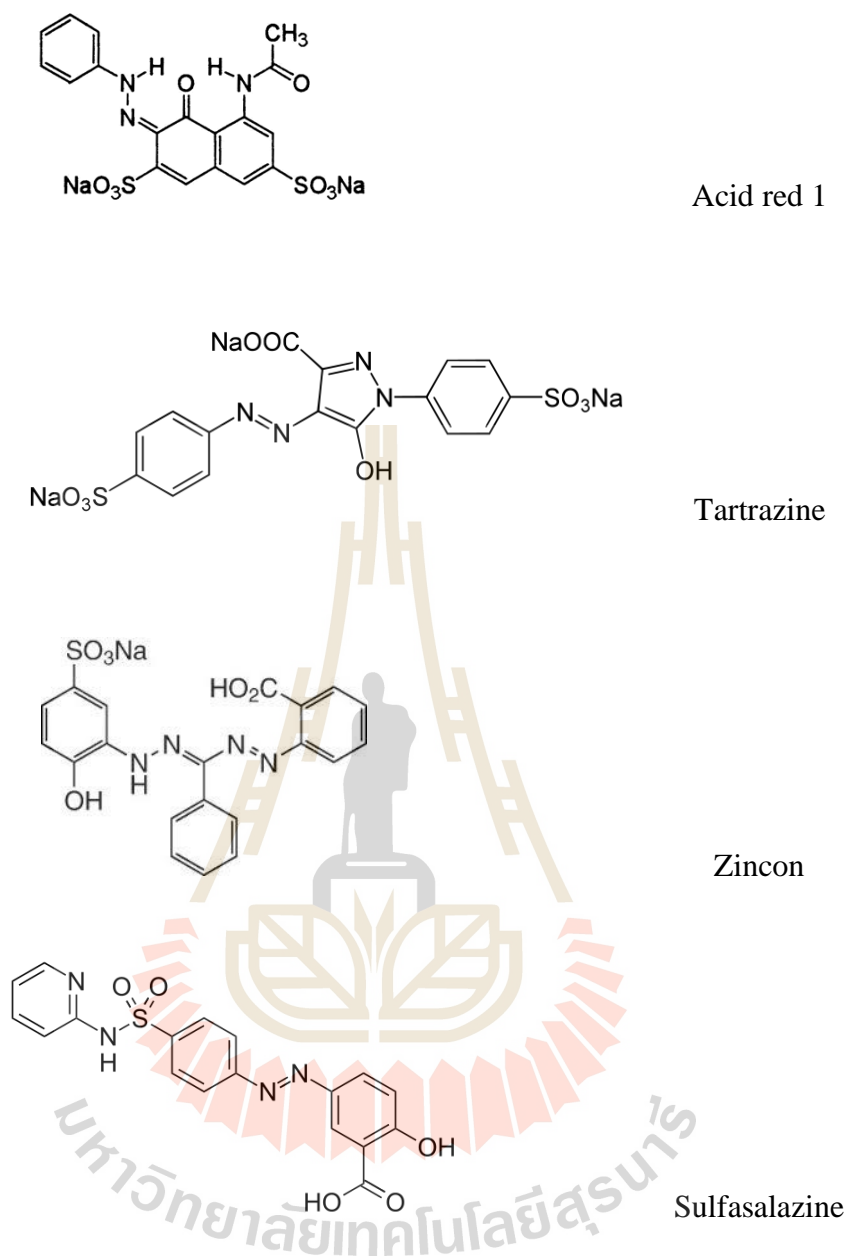
Sulfasalazine

Figure 4.1 Structures of acid red 1, tartrazine, zincon, and sulfasalazine.

4.3 Experimental

4.3.1 Chemicals

Chemicals used in this research are listed in Table 4.1.

Table 4.1 Chemicals used in this research.

Chemicals	Formula	Content (%)	Suppliers
3-aminopropyltriethoxy-silane (APTES)	$H_2NC_3H_6Si(OC_2H_5)_3$	99.0	Sigma-Aldrich
acid red 1	$C_{18}H_{13}N_3O_2(SO_3Na)_2$	60.0	Sigma-Aldrich
ammonia	NH_3	99.0	Acros Organics™
cetyltrimethylammonium-bromide (CTAB)	$C_{19}H_{42}BrN$	98.0	Carlo ERBA
ethanol	C_2H_5OH	99.9	Carlo ERBA
hydrochloric acid	HCl	37.0	Carlo ERBA
sodium hydroxide	$NaOH$	95.0	Carlo ERBA
sulfasalazine	$C_{18}H_{14}N_4O_5S$	95.5	Sigma-Aldrich
tartrazine	$C_{16}H_9N_4O_3Na(SO_3Na)_2$	85.0	Sigma-Aldrich
tetraethyl orthosilicate (TEOS)	$Si(OC_2H_5)_4$	99.0	Acros Organics™
zincon	$C_{20}H_{15}N_4O_3(SO_3Na)$	75.0	Sigma-Aldrich

4.3.2 Preparation of mesoporous silica coated dye-imprinted amino silica adsorbent

4.3.2.1 Preparation of silica nanoparticles

Silica particles were prepared by the Stöber method (Liang et al., 2013). 10 mL H_2O, 24 mL of 28% NH_3 and 17 mL TEOS were added into 500 mL ethanol. The reaction mixture was stirred for 12 h under magnetic stirring. At the reaction time of 3 and 6 h, 12 mL TEOS was added dropwise into the solution. The resulting silica particles were separated by centrifugation at 3,000 rpm for 10 min. The silica particles were washed with H_2O until the pH of the washed solution was close to 7 and after that with ethanol to remove the unreacted TEOS. Finally, the silica particles were kept by dispersing in 100 mL ethanol.

4.3.2.2 Preparation of amino-functionalized silica particles

To prepare amino-functionalized silica particles, silica particles were modified by using a method from Liang et al. (2013). 2 mL H_2O, 4 mL of 28% NH_3 and 80 μL APTES were added to the silica particles dispersed in 100 mL ethanol. The mixture solution was stirred for 12 h. The particles were separated by centrifugation at 3,000 rpm for 10 min. The amino modified silica particles were washed with H_2O until the pH of the washed solution was close to 7 and after that with ethanol to remove the unreacted APTES. The resulting amino-functionalized silica particles were dried at 60 ºC overnight. The particles were denoted as NH_2-SiO_2.

4.3.2.3 Preparation of dye-amino silica particles

NH_2-silica particles with the weight of 1.0 g were dispersed in 100 mL of 100 ppm acid red 1 solution. Acid red 1 was used as a template. The mixture

solution was stirred for 12 h. After that, the particles were isolated by centrifugation at 3,000 rpm for 10 min. The particles were washed with H_2O until the washed solution became colorless. The particles were wash with ethanol to remove the unreacted dye. The particles were dried at 60 ^{o}C overnight and denoted as dye-NH_2-silica particles.

The dye stock solution was prepared by dissolving 1 g of dye in H_2O, which adjusted pH to 2.0 by using 1.0 M HCl. The volume of the solution was brought up to 1,000 mL in a volumetric flask.

4.3.2.4 Preparation of mesoporous silica coated dye-amino silica particles

Mesoporous silica coated amino-silica particles were prepared by using a method, adapted from Yuan et al. (2014). Dye-NH_2-silica particles with the weight of 1.0 g were dispersed in 140 mL ethanol with sonication. 80 mL H_2O, 1.2 mL of 28% NH_3 and 0.3 g CTAB were added into the mixture of the dispersed dye-NH_2-silica particles under constant stirring. After 6 h, 0.43 mL TEOS was added dropwise into the mixture solution. The mixture solution was stirred for another 6 h. The particles were isolated by centrifugation at 3,000 rpm for 10 min and redispersed in 150 mL ethanol under sonication for 1 h to remove CTAB (Jabariyan and Zanjanchi, 2012). After that, the particles were separated by centrifugation at 3,000 rpm for 10 min and dried overnight. The dye template was removed from the particles by stirring in 25 mL 1.0 M NaOH for 30 min. Then the resulting powders were washed with H_2O until the pH of the washed solution was close to 7. Finally, the particles were washed with ethanol. The particles were dried at 60 ^{o}C overnight. The obtained powder, mesoporous silica coated dye-imprinted amino silica adsorbent, was denoted as MIA.

4.3.2.5 Preparation of non-imprinted adsorbent

Synthesis of a non-dye-imprinted mesoporous silica coated amino silica adsorbent (NIA) was done using the similar procedures as those for MIA. However, acid red 1 was not used as the template.

4.3.3 Characterization of synthesized adsorbents

4.3.3.1 Transmission electron microscopy (TEM)

TEM was used to obtain very high spatial resolution images of the structures of the adsorbents. TEM was performed on a Tecnai G^2 with an accelerating voltage of 200 kV. For TEM measurement, the adsorbents were suspended in 95% ethanol solution with sonication. The suspension was deposited on a micro grid with a holey carbon copper as a support membrane and dried at 70 °C with a UV lamp.

4.3.3.2 X-ray diffraction (XRD)

An X-ray diffractometer (Bruker AXS D8) was used to investigate phases of the adsorbents. An X-ray source with Cu target was operated at a voltage of 40 kV and a current of 40 mA to provide Cu K_α radiation. An X-ray filtered was made of Ni. Diffraction patterns were obtained in 2θ range of 1 to 10° with a step increment of 0.02° and a step time of 0.5 s. Samples were placed into sample holders. The powder was spread evenly before the measurement.

4.3.3.3 Nitrogen adsorption-desorption analysis

Nitrogen adsorption-desorption analysis was used to investigate surface area, average pore size and total pore volume of the adsorbents. Nitrogen adsorption-desorption isotherms were obtained from a BELSORP-mini II. Before analysis, about 0.10 g of each sample was degassed at 200 °C under vacuum for 2 h and left until the pressure was reached to 10^{-2} mPa in order to remove physisorbed

gas. The analysis was carried out at -196 $^{\circ}$C at relative pressure (P/P$_0$) from 0.01 to 0.99. Surface area was calculated by Brunauer-Emmett-Teller (BET) method. The total pore volume was obtained from the nitrogen amount adsorbed in correspondence of P/P$_0$ equal to 0.99 and the pore size distribution was calculated by Barrett-Joyner-Halenda (BJH) method.

4.3.3.4 Fourier transform infrared spectroscopy (FTIR)

Functional groups of adsorbents were studied by Fourier transform infrared spectroscopy (Bruker, Tensor 27) using attenuated total reflection (ATR) mode. A sample for the measurement was prepared by sprinkling particles on a sample holder. IR spectra were obtained in the wavenumber range of 400 to 4000 cm^{-1} with the resolution of 4 cm^{-1}.

4.3.4 Adsorption study of acid red 1

4.3.4.1 Effect of pH

Effect of pH on the adsorption of acid red 1 was investigated over the pH range of 1.0-10.0. An adsorbent with the weight of 0.035 g was added into 35 mL of 20 mg/L dye solution contained in a 40-mL vial. The mixture solution was stirred for 60 min at 25.0 $^{\circ}$C. After that, the adsorbent was separated from the solution by centrifugation. A concentration of the dye left in the solution was determined using a UV–Vis spectrometer (CHEM4-Vis-fiber spectrometer: USB 4000, Ocean Optics). Absorbance measurement was made at 532 nm.

4.3.4.2 Effect of contact time

Adsorption study was conducted in a 40-mL vial contained with 35 mL of 20 mg/L acid red 1 and 0.035 g of an adsorbent. The pH of the dye solutions was controlled at 2.0. The temperature of solutions was controlled at 25.0 $^{\circ}$C.

Adsorption time was varied in the range of 30 to 150 min. After a given time, the adsorbent was separated from the solution by centrifugation and the dye solution was used for the absorbance measurement to determine the dye concentration.

4.3.4.3 Adsorption isotherm and thermodynamics experiments

Adsorption of acid red 1 at different concentrations was carried out with 0.035 g adsorbent in 35 mL solution contained in a 40-mL vial. The dye concentration was varied in the range of 10-260 mg/L and the pH of the solutions was controlled at 2.0. The adsorption temperature was varied in the range of 25.0-45.0 ºC. After 60 min of adsorption, the adsorbent was separated by centrifugation and the dye solutions were used for absorbance measurement at 532 nm for the determination of dye concentration.

4.3.4.4 Kinetic experiment

The kinetic of adsorption of dye onto adsorbent was carried out with 0.035 g adsorbent in 35 mL dye solution with the initial concentration at 80 mg/L. The mixture was contained in a 40-mL vial. The pH of the solutions was fixed at 2.0. Adsorption was carried out at different temperature, 25.0, 35.0, and 45.0 ºC. At each temperature, the dye concentration at different adsorption time,10, 20, 30, 40, 50, and 60 min, was determined by measuring the absorbance of the solutions at 532 nm.

4.3.4.5 Determination of separation factor and imprinting factor

In order to investigate the selectivity of the adsorbents toward the target dye and to compare the adsorption efficiency between MIA and NIA, separation factor and imprinting factor were determined. The optimized adsorption condition for the target dye was used in this study.

To determine a separation factor, adsorption experiments were carried out with MIA. Solutions of acid red 1 and dyes with analogous structures such as tartrazine, zincon, and sulfasalazine at the concentration of 1.57×10^{-4} mol/L with the pH of 2.0 were used in the study. Adsorption of each dye solution was done separately on MIA. Similar adsorption procedures as previously described were used. The absorbance of tartrazine, zincon, and sulfasalazine was measured at 442, 520, and 359 nm, respectively.

To determine an imprinting factor, adsorption of acid red 1 on MIA and NIA was conducted at the dye concentration of 80 mg/L and the pH of solutions was fixed at 2.0. The adsorption was done at 25.0 $^{\circ}$C for 60 min. The concentration of the dye left in the solution was determined spectrometrically.

4.3.4.6 Desorption and reusability

Regeneration of MIA after the adsorption of acid red 1 was investigated. The adsorption of acid red 1 in the concentration range of 10-80 mg/L was done for 60 min at 25.0 $^{\circ}$C. Adsorbents obtained after the adsorption of the dye were used repeatedly in the adsorption-desorption study. Desorption of the adsorbed dye from the adsorbents was performed by stirring the adsorbents in 25 mL of 1.0 M NaOH for 30 min. The weight of the adsorbent was 0.035 g. The desorption was done at 25.0 $^{\circ}$C. After 30 min, the adsorbent was separated by centrifugation and was washed several times with H$_2$O until the pH of the washed solution was close to 7. The adsorbent was dried at 60 $^{\circ}$C overnight before used for the next cycle of adsorption.

4.4 Results and discussion

4.4.1 Characterization of the synthesized adsorbents

4.4.1.1 Morphologies of the synthesized adsorbents

Morphologies of the synthesized adsorbents are shown in Figure 4.2. The synthesized adsorbents have spherical nanostructure with diameter of about 100 nm and relatively narrow particle size distributions. Chemical modification of NH_2-SiO_2 seems not to drastically affect the size of the particles. A thin layer of mesoporous silica coating was observed on both MIA and NIA as shown in Figure 4.1(c) and 4.1(e), although the mesoporous structures are not clearly seen.
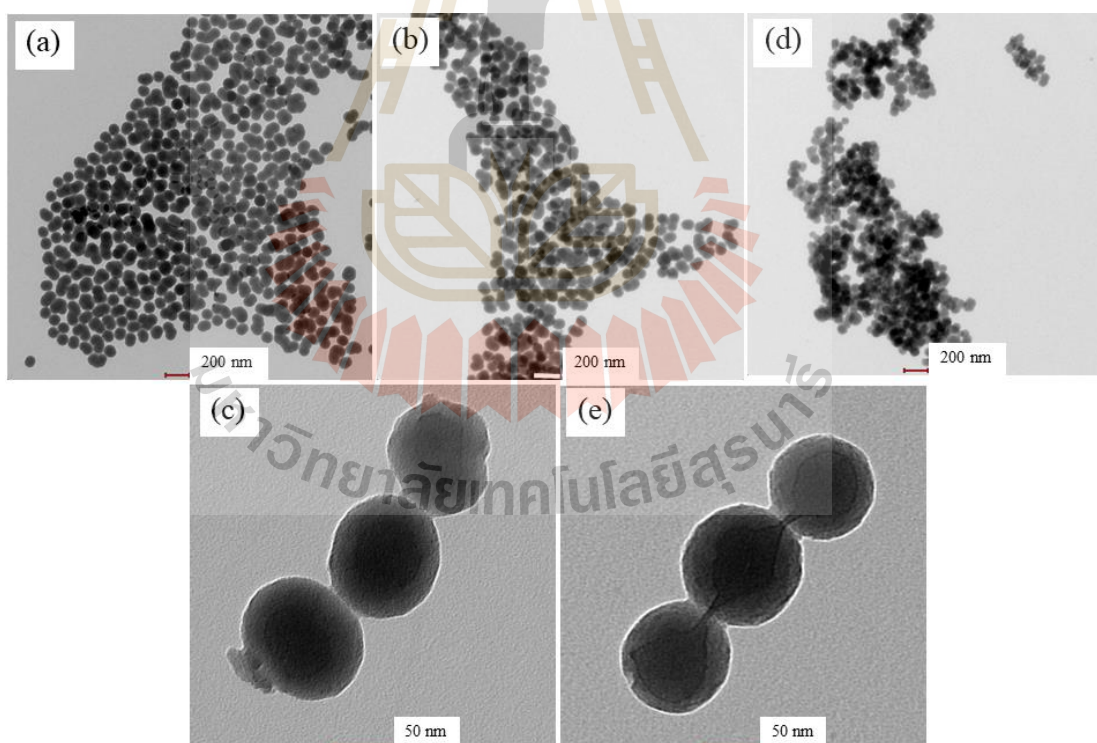
Figure 4.2 TEM images of NH_2-SiO_2 (a), MIA (b)-(c), and NIA (d)-(e).

To confirm the existence of mesoporous structures on MIA and NIA, XRD analysis at low diffraction angles was conducted. XRD patterns of MIA and NIA in Figure 4.3 show a single diffraction peak around 2.5°. This peak indicates the presence of mesoporous structure on both adsorbents (Yuan et al., 2014).

4.4.1.2 Nitrogen adsorption-desorption analysis

Nitrogen adsorption-desorption isotherms of the adsorbents were obtained using a BELSORP-mini II and are shown in Figure 4.4. A type isotherm, according to the IUPAC classification, was observed for both adsorbents. Hysteresis loops indicate the presence of mesopores on both adsorbents.
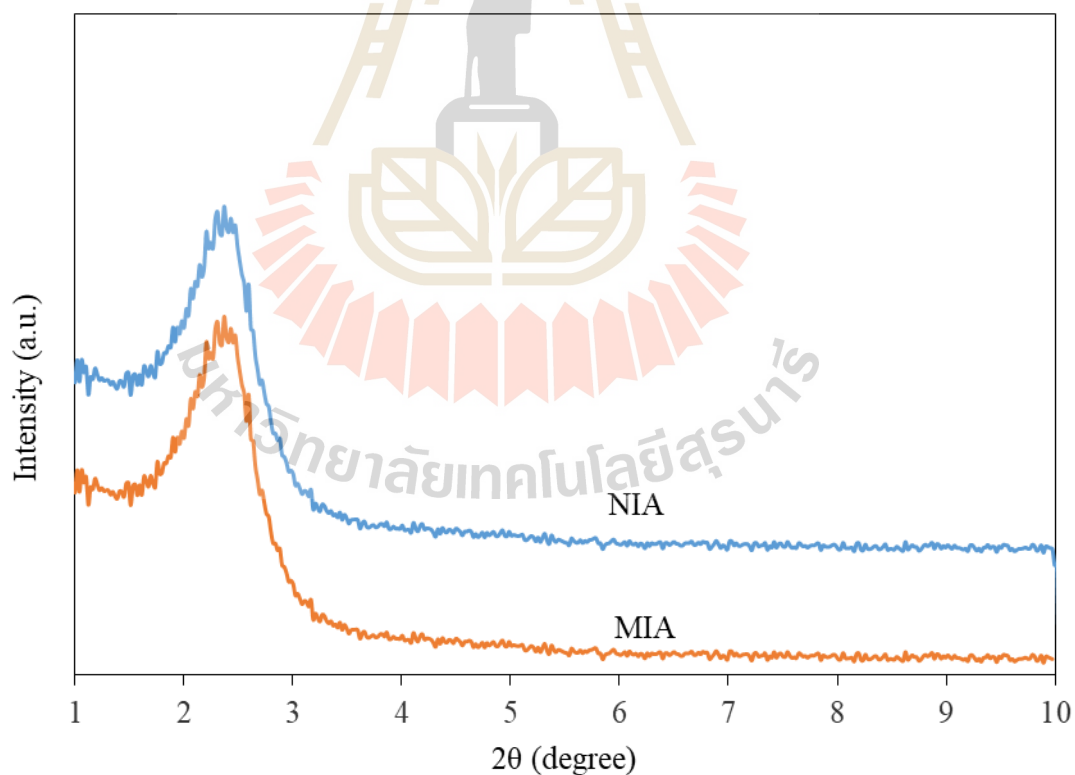
Figure 4.3 XRD patterns of MIA and NIA.
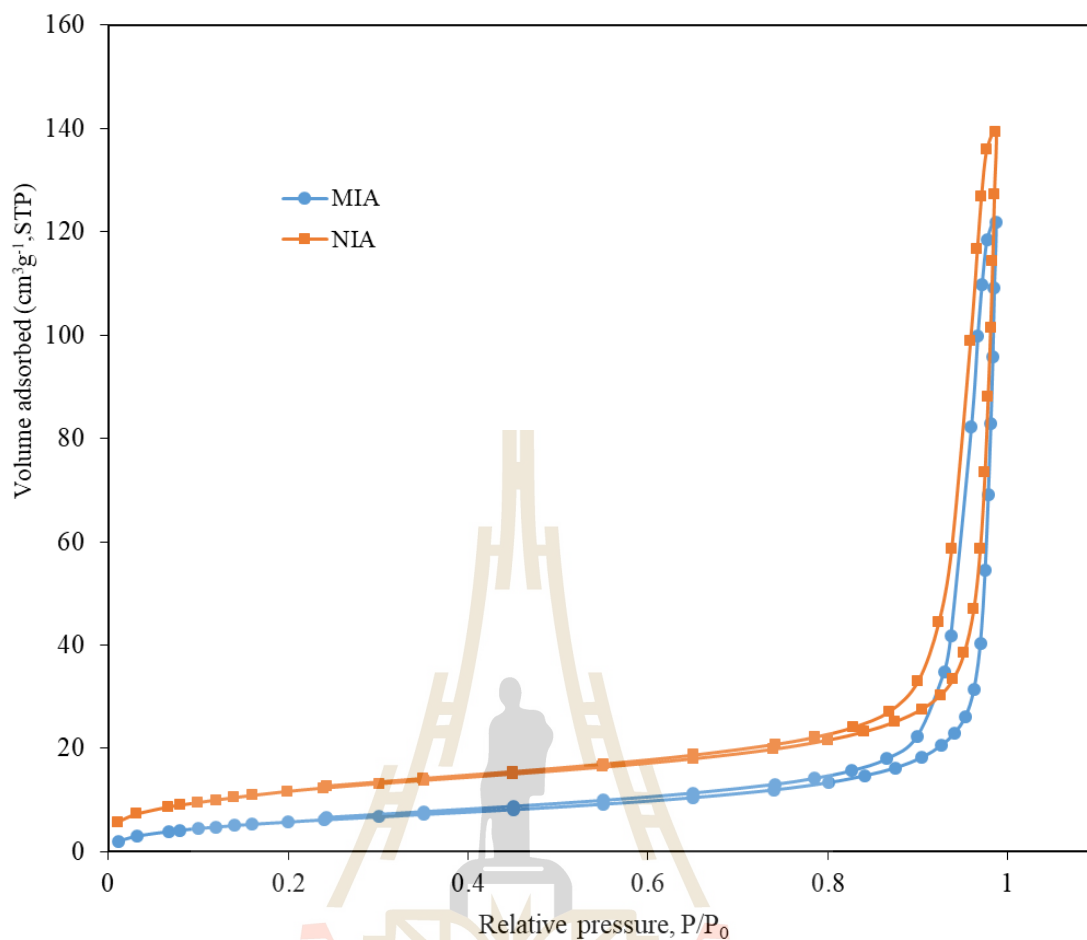
Figure 4.4 Nitrogen adsorption-desorption isotherms of MIA and NIA adsorbents.

        Specific surface area, total pore volumes, average pore diameters, and pore size distributions of MIA and NIA adsorbents are shown in Table 4.2. The specific surface area of MIA is smaller than that of NIA. This could be from that in the MIA synthesis method, the dye molecules on the dye-NH2-SiO_2 particles could hinder some sites to be used in formation the mesoporous structure.

Table 4.2 Textural properties of MIA and NIA from N_2-analysis.

Adsorbents	BET surface area (m^2/g)	Total pore volume (cm^3/g)	Average pore diameter (nm)
MIA	22	0.19	40
NIA	42	0.21	34

4.4.1.3 Adsorbents characterization by FTIR spectroscopy

The adsorbents were characterized by FTIR to identify functional groups on their structures. The measurements in the wavenumber range of 400-4,000 cm^{-1} with the resolution of 4 cm^{-1} were carried out. FTIR spectra of MIA and NIA are shown in Figure 4.5. The spectra provide evidence for the presence of functional moieties in the MIA adsorbent. The bands in the range 1,056 cm^{-1} and 790 cm^{-1} were assigned to Si-O-Si groups. The band at 958 cm^{-1} was attributed to Si-OH groups. In addition, peaks at around 2,883 and 2,987 cm^{-1} represent the vibrations of -CH_2 indicating that APTES was functionalized onto MIA (Zhang et al., 2014). Peak at 3,373 cm^{-1} could be from stretching vibrations of -OH and -NH. The incorporation of the amino group was verified by symmetric -NH_2 bending at 1,602-1,631 cm^{-1}. These peak assignments are similar to those reported in literature (Yuan et al., 2014) which the researchers studied amino-functionalized magnetic mesoporous silica microspheres. Similar FTIR peaks were also observed in the NIA adsorbent. The peaks of NIA were shifted slightly compared to those of MIA. This could be attributed to the dye template used in the synthesis of MIA, but not in the synthesis of NIA (Zhang et al., 2014).
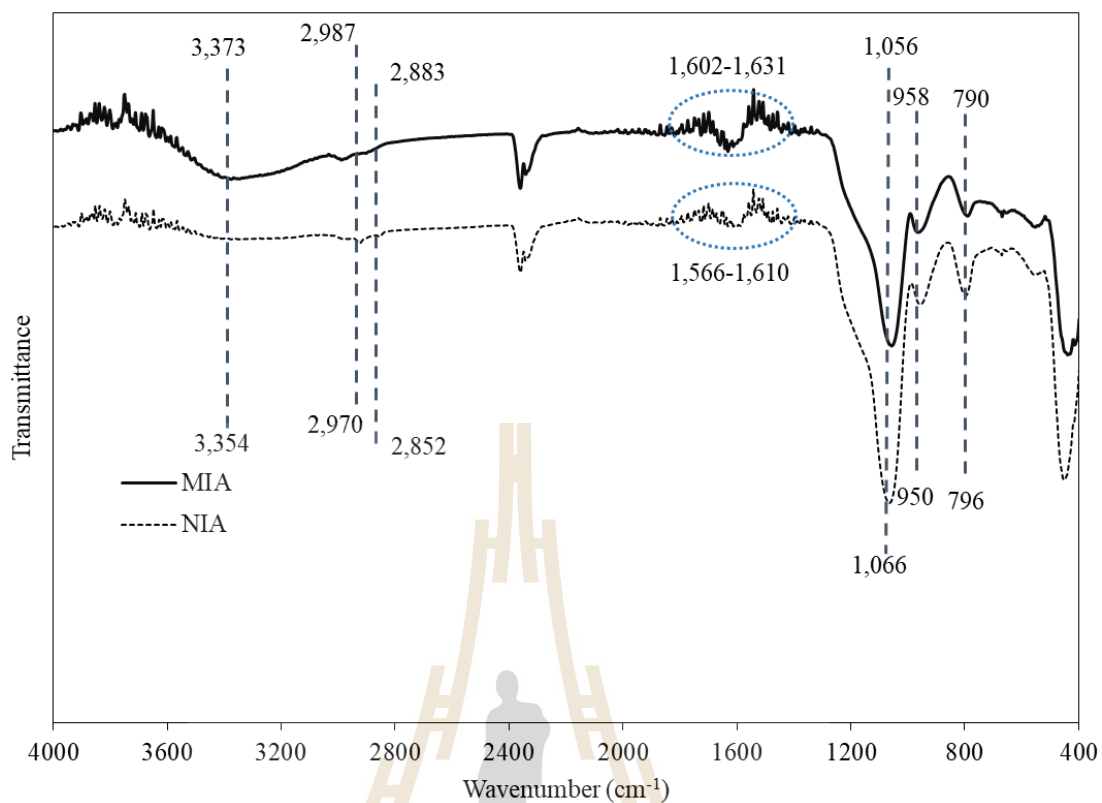
Figure 4.5 FTIR spectra of MIA and NIA.

4.4.2 Adsorption of MIA for acid red 1

4.4.2.1 Effect of pH on adsorption capacity of acid red 1 onto MIA

The effect of pH on adsorption capacity of acid red 1 onto MIA was investigated in the pH range of 1.0 to 10.0 at a fixed dye concentration of 20 mg/L at 25.0 °C. The adsorption time was 60 min. The adsorption capacity was calculated according to equation [4.1];

$$q_e = \frac{V(C_0 - C_e)}{m} \tag{4.1}$$

where q_e is the equilibrium adsorption capacity (mg/g), V is the volume of the solution (L), C_0 and C_e (mg/L) are the initial and equilibrium concentrations of the acid red 1 in a solution, respectively, and m is the adsorbent mass (g).

Acid red 1 is an anionic azo dye that contains two sulfonic acid groups $[R\text{-}(SO_3Na)_2]$. In aqueous solutions, acid red 1 can be dissociated to sulfonate anion $[R\text{-}(SO_3^-)_2]$ which can interact with the protonated amino groups, $\text{-}NH_3^+$, on the adsorbent. The pH of the solutions has strong influence on the surface charge of the adsorbent and the anionic form of the dye.

In Figure 4.6, the optimum adsorption capacity was observed at pH 2.0. The adsorption tended to increase when the pH of the solutions was decreased from 10.0 to 2.0. This can be explained by pH at point of zero charge (pH_{pzc}) which represents the surface charge behavior of the adsorbents. MIA consists of $NH_2\text{-}SiO_2$ and mesoporous silica. The pH_{pzc} of mesoporous silica was reported to be about 3.1 (Velez et al., 2013) and for that of the primary amine groups ($\text{-}NH_2$) on silica was about 7.34 (Yang et al., 2013). The amino groups were fully protonated at pH 2.0 (Araghi and Entezari, 2005). Therefore, adsorption of anionic dyes are favored at $pH < pH_{pzc}$ of the adsorbent, where the surface charge of the adsorbent is positive (Konicki et al., 2017).

The adsorption capacity decreased when the pH of the solution was adjusted to 1.0. This could be resulted from the protonation of $\text{-}SO_3^-$ groups on the dye that reduced the amount of the dye in the anionic form. The pK_a values of azo dyes are in the range 0.7–1.5 (Owusu-Apenten, 2002) which means that there is a lower percentage of the dye molecule in the anionic form (deprotonated form) at pH < pK_a.
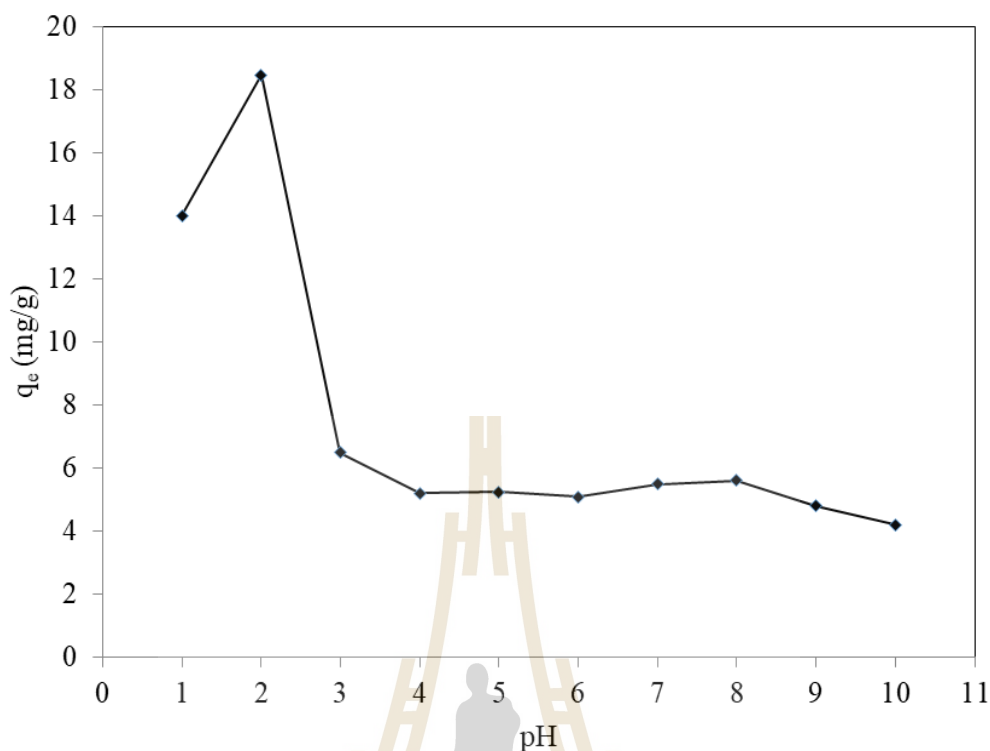
Figure 4.6 Influence of pH on the adsorption capacity of MIA for acid red 1.

4.4.2.2 Effect of contact time

Effect of contact time on the adsorption capacity of the adsorbent was investigated. The adsorption was carried out at 25.0 °C with the initial dye concentration of 20 mg/L, the pH of the solution of 2.0, and the adsorbent weight of 0.035 g. Figure 4.7 shows time profile adsorption of acid red 1 onto MIA and NIA. The extent of dye removal by MIA and NIA was found to increase with the increase of contact time. The adsorption reached equilibrium in about 60 min for MIA and about 120 min for NIA. Adsorption time at 60 min was selected for further study with MIA.
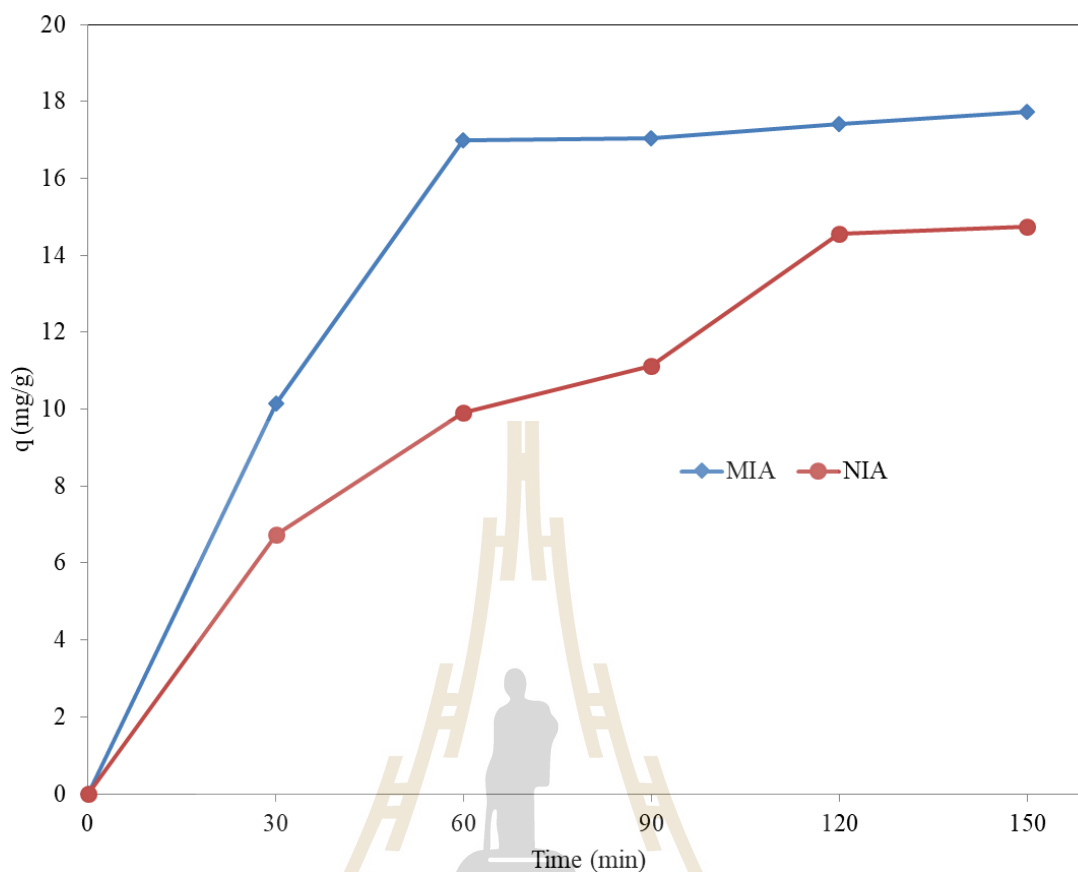
Figure 4.7 Time profile adsorption of acid red 1 onto MIA and NIA.

The adsorption capacity of MIA toward acid red 1 was higher than that of NIA. This could be due to that during the molecular imprinting process adsorption sites were retained by the dye template while the mesoporous layer coating was forming around the dye-NH_2-silica particles. After the removal of the dye template, specific recognition cavities were formed. For NIA, however, adsorption sites for acid red 1 could be hindered to some extent during the mesoporous layer coating on NH_2-silica particles. It is noted that the rate of adsorption is higher for MIA. This could be from the molecular imprinting process that resulted in cavities appropriate for acid red 1 diffusion into the particles.

4.4.2.3 Adsorption isotherm study

Adsorption isotherms are important for explaining the interaction between adsorbate and adsorbent in an equilibrium state. Langmuir and Freundlich isotherms are commonly used to explain adsorption behaviors.

The Langmuir adsorption equation can be represented as equation [4.2];

$$\frac{q_e}{q_m} = \frac{K_A C_e}{1 + K_A C_e} \qquad [4.2]$$

where, q_e (mg/g) is the amount of an adsorbate adsorbed per gram of an adsorbent at equilibrium; q_m (mg/g) is the maximum amount of the adsorbate adsorbed to form a monolayer coverage per gram of the adsorbent; K_A (L/mg) is the Langmuir adsorption equilibrium constant; C_e (mg/L) is the concentration of the adsorbate at equilibrium. Adsorption data can be fitted to the Langmuir isotherm in a linear form as the following equation [4.3];

$$\frac{C_e}{q_e} = \frac{C_e}{q_m} + \frac{1}{K_A q_m} \qquad [4.3]$$

Maximum adsorption capacity (q_m) can be obtained from a linear plot of C_e/q_e against C_e. K_A can be calculated from the intercept value.

The Freundlich isotherm is another commonly used model. It has a general form as expressed by equation [4.4];

$$q_e = K_F C_e^{1/n} \qquad [4.4]$$

where q_e and C_e are defined as in equation [4.2], K_F is the Freundlich constant, the indicative of the relative adsorption capacity of the adsorbent and $1/n$ is an empirical constant. A linear form of Freundlich isotherm is shown in equation [4.5];

$$\ln q_e = \ln K_F + \frac{1}{n} \ln C_e \qquad\qquad [4.5]$$

When $\ln q_e$ is plotted against $\ln C_e$ and the data are treated by linear regression analysis, K_F and $1/n$ can be obtained from the intercept and the slope of the line, respectively. Freundlich model applies well to solid with heterogeneous surface properties.

Figure 4.8 shows adsorption isotherms of acid red 1 on MIA at different temperature. The adsorption data from the study were fitted with Langmuir and Freundlich model. Isotherm equations and derived parameters for Langmuir and Freundlich model are shown in Table 4.3 and 4.4, respectively. The adsorption data were better fitted with the Langmuir model because the obtained fitted equations have correlation coefficients (R^2) >0.99 at every adsorption temperature. From the assumption of Langmuir model, it can be concluded that the imprinted sites on MIA are uniform with monolayer adsorption of the dye molecules onto the adsorbent.

In Table 4.3, it can be seen that the K_A value decreases as the temperature is increased. This means that less amount of dye is absorbed when the temperature is increased. In addition, the maximum adsorption capacity decreases with increase temperature. This suggests that the adsorption of acid red 1 on MIA is an exothermic process.

4.4.2.4 Thermodynamic study

Thermodynamic parameters including Gibbs free energy change (ΔG), enthalpy change (ΔH) and entropy change (ΔS) were used in providing the information about the adsorption process.
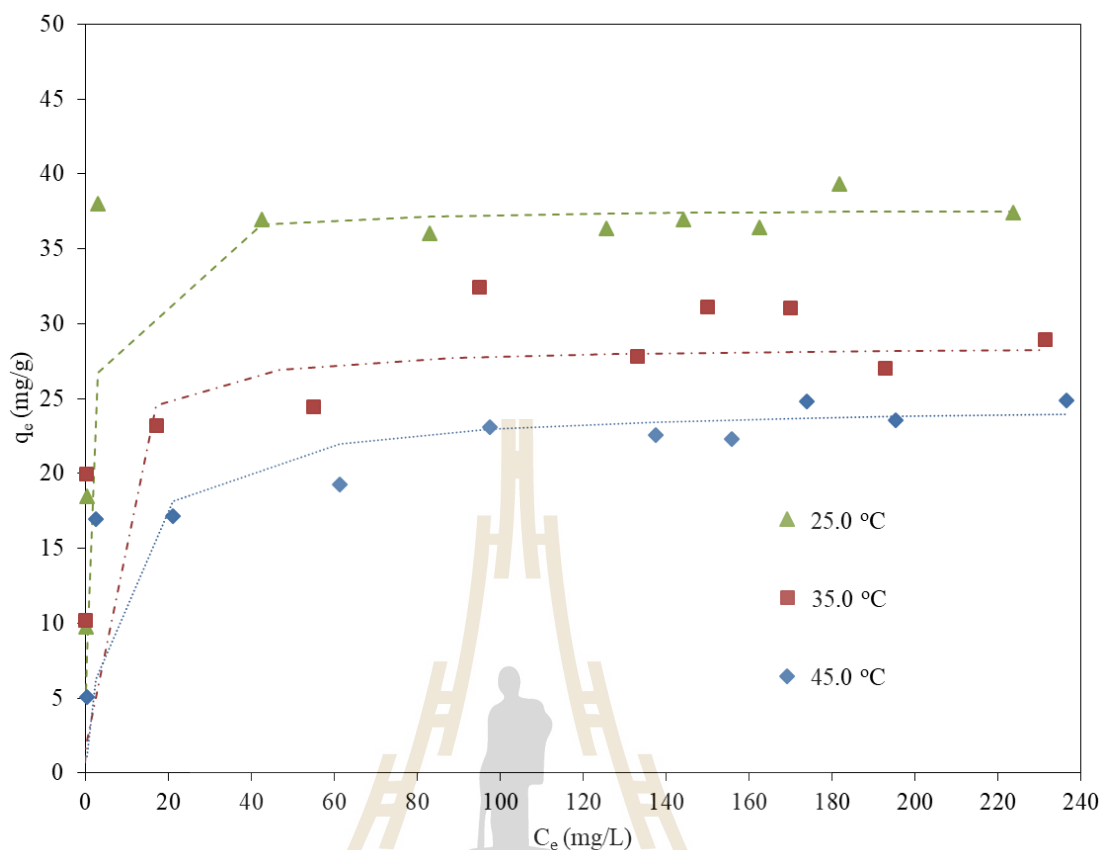
Figure 4.8 Adsorption isotherms of acid red 1 on MIA at 25.0, 35.0, and 45.0 °C.

Table 4.3 Isotherm equations for Langmuir model and other derived parameters for the adsorption of acid red 1 onto MIA.

Temperature (°C)	Fitting equation	R^2	q_m (mg/g)	K_A (L/mg)
25.0	$C_e/q_e = 0.0265C_e + 0.0343$	0.9981	37.7	0.773
35.0	$C_e/q_e = 0.0350C_e - 0.0986$	0.9933	28.6	0.355
45.0	$C_e/q_e = 0.0404C_e + 0.3097$	0.9930	24.8	0.130

Table 4.4 Isotherm equations for Freundlich model and other derived parameters for the adsorption of acid red 1 onto MIA.

Temperature (°C)	Fitting equation	R^2	1/n	K_F [(mg/g)/(mg/L)$^{1/n}$]
25.0	$\ln q_e = 0.1435 \ln C_e + 2.9494$	0.7133	0.1435	19.10
35.0	$\ln q_e = 0.0995 \ln C_e + 2.9722$	0.6394	0.0995	19.53
45.0	$\ln q_e = 0.1324 \ln C_e + 2.4821$	0.9017	0.1324	11.96

From the data conducted at different temperature, relationship among a distribution coefficient (K_D), ΔH and ΔS can be described by equation [4.6];

$$\ln K_D = \frac{\Delta S}{R} - \frac{\Delta H}{RT} \qquad [4.6]$$

where R is the universal gas constant (8.314 Jmol^{-1} K^{-1}) and T is the absolute temperature (Kelvin). The values of ΔH and ΔS can be calculated from a slope and an intercept of a plot of ln K_D against 1/T. K_D can be calculated from equation [4.7];

$$K_D = \frac{q_e}{C_e} \qquad [4.7]$$

where q_e and C_e, defined as in equation [4.2], can be obtained from adsorption of acid red 1 in the range of 10-260 mg/L on MIA. The adsorption temperature was varied in the range of 25.0-45.0 °C. The adsorption time was 60 min.

ΔG provides information about the process spontaneity, which can be related to ΔH and ΔS as shown in equation [4.8];

$$\Delta G = \Delta H - T\Delta S \qquad [4.8]$$

The results are given in Table 4.5. Negative ΔG suggests that the process is spontaneous. In addition, for each initial dye concentration the negative values of the free energy decrease upon increasing the temperature, this suggests that the process is favored at low temperatures. Negative ΔH suggests the exothermic nature of the process, which was demonstrated by the decrease in the adsorption capacity and the equilibrium constant at a higher temperatures. Negative ΔS suggests the decrease randomness at the solid/liquid interface. This could be due to release of water molecules before acid red 1 adsorption on the surface of the adsorbent. The driving force for acid red 1 adsorption onto the adsorbent would be both of enthalpy effect and entropy effect, but the adsorption process would be controlled by an enthalpy effect rather than an entropy change (Leite et al., 2017).

4.4.2.5 Kinetic study

To describe the adsorption behavior with time, adsorption of acid red 1 on MIA was conducted with 80 mg/L dye solution at different time and temperature.

The obtained adsorption data were fitted with pseudo-first-order and pseudo-second-order models. These models are the most commonly used to describe the adsorption of dyes on adsorbents.

Pseudo-first order model is written as shown in equation [4.9];

$$\log (q_e - q_t) = \log q_e - (k_1 t / 2.303) \qquad [4.9]$$

where q_e is the equilibrium adsorption capacity (mg/g), q_t is the adsorption capacity at time t (mg/g), k_1 is the pseudo first-order rate constant (min^{-1}), and t is the contact time (min).

Table 4.5 Thermodynamic parameters for the adsorption of acid red 1 onto MIA.[a]

C_0 (mg/L)	Fitting equation	R^2	ΔH (kJ/mol)	ΔS (J/mol)	ΔG (kJ/mol) 25 °C	35 °C	45 °C
10	y = 8070.5x - 22.243	0.9705	- 67.10	-184.92	-11.96	-10.12	-8.27
20	y = 13110x - 39.065	0.9038	- 109.00	-324.79	-12.16	-8.91	-5.66
40	y = 12756x - 40.034	0.8981	-106.05	-332.84	- 6.82	- 3.49	-0.16

[a] Data for K_D calculation are shown in Appendix B.

Pseudo-second order model is written as shown in equation [4.10];

$$t/q_t = 1/k_2q_e^2 + (1/q_e)t \qquad\qquad [4.10]$$

where k_2 is the pseudo second-order rate constant (g/mg.min), and t is the contact time (min).

Graphs obtained from plotting log $(q_e\text{-}q_t)$ versus t are shown in Figure 4.9 and model equations are shown in Table 4.6. The data seem to fit well with pseudo-first order model because the values of R^2 are > 0.9. However, the model derived q_e values are significantly different from those obtained from the experiment. This suggests that pseudo first-order model could not be used to describe the adsorption kinetic. Graphs obtained from plotting t/q_t versus t are shown in Figure 4.10 and model equations are shown in Table 4.7. The data fitted well with the model with R^2 > 0.99. In addition, the values of adsorption capacity from the models and that from the experiments are about the same. This suggests that pseudo-second-order kinetics provide better correlation of the experimental data. The model suggests that

the rate of the adsorption rate is controlled by the diffusion of the dye molecules through the pores of the adsorbent.

4.4.2.6 Separation factor and imprinting factor

4.4.2.6.1 Separation factor

Separation factor (α) is a measure of the strength of interaction of MIA towards the template molecule compared to another molecule. It is calculated using equation [4.11];

$$\alpha = K_{D1}/ K_{D2} \qquad [4.11]$$
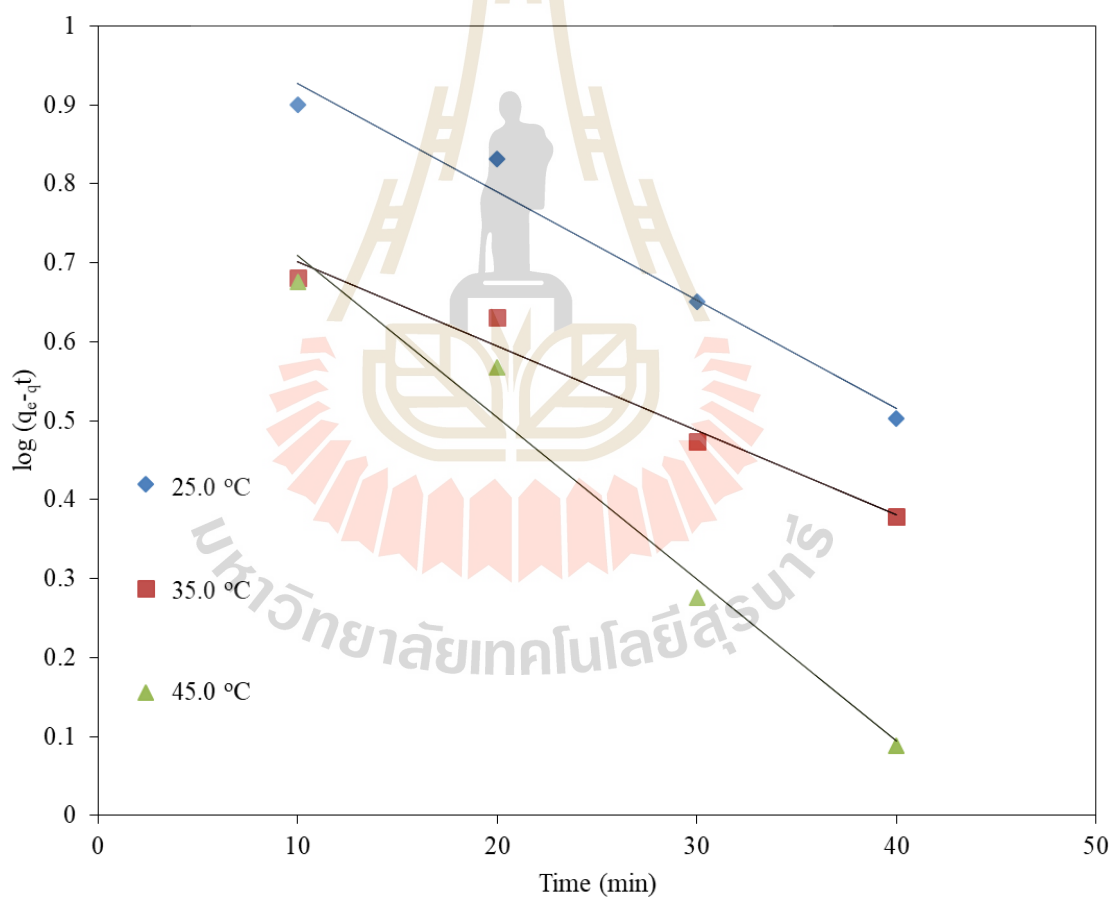
Figure 4.9 Pseudo-first-order kinetics for the adsorption of 80 mg/L acid red 1 onto 0.035 g MIA.

Table 4.6 Pseudo-first-order model for the adsorption of acid red 1 onto MIA.

T (°C)	Fitting equation	R^2	k_1 (min^{-1})	$q_{e, cal}$[a] (mg/g)	$q_{e, exp}$[b] (mg/g)
25.0	log (q$_e$ - q$_t$) = -0.0205t + 0.9147	0.9734	0.0472	8.2	36.8
35.0	log (q$_e$ - q$_t$) = -0.0107t + 0.8075	0.9668	0.0246	6.4	27.3
45.0	log (q$_e$ - q$_t$) = -0.0137t + 1.0641	0.9729	0.0315	11.5	25.7

[a] Calculated values obtained from plots of t/q_t against t.
[b] Experimental values.
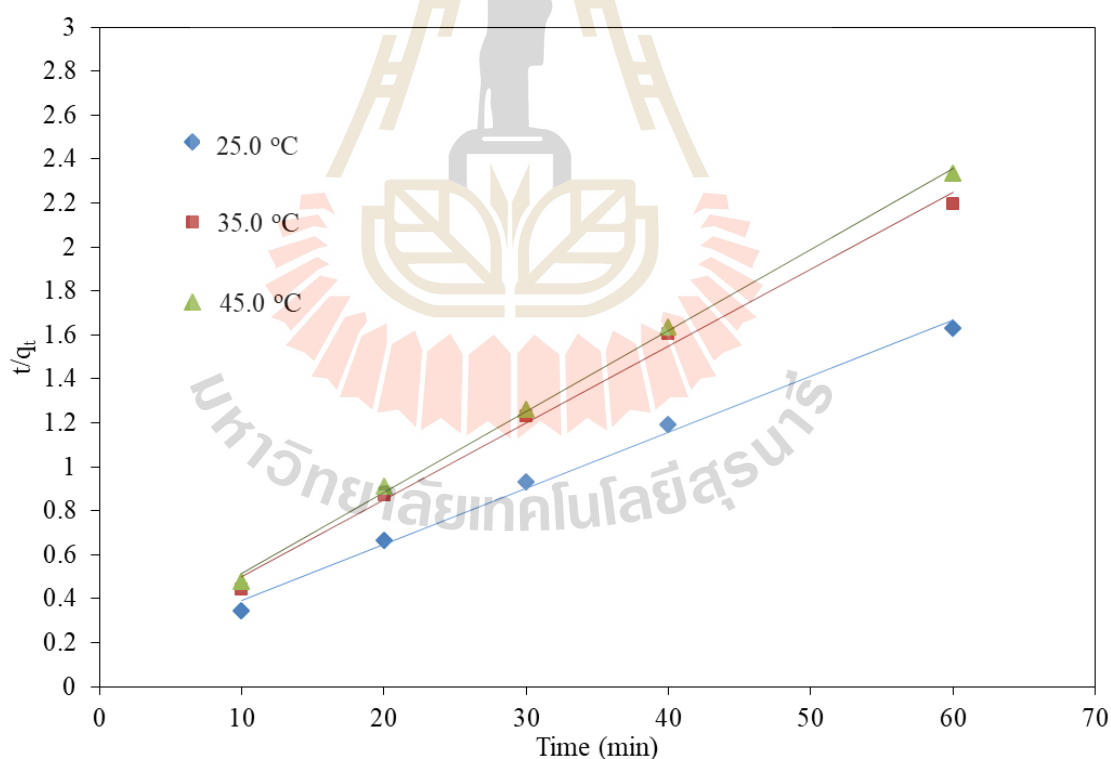
Figure 4.10 Pseudo-second-order kinetics for the adsorption of 80 mg/L acid red 1 onto 0.035 g MIA.

Table 4.7 Pseudo-second-order model for the adsorption of acid red 1 onto MIA.

T (°C)	Fitting equation	R^2	k_2 (g/mg.min)	$q_{e, cal}$[a] (mg/g)	$q_{e, exp}$[b] (mg/g)
25.0	$t/q_t = 0.0255t + 0.1377$	0.9942	0.0047	39.2	36.8
35.0	$t/q_t = 0.035t + 0.1513$	0.9944	0.0081	28.6	27.3
45.0	$t/q_t = 0.0369t + 0.1442$	0.9986	0.0094	27.1	25.7

[a] Calculated values obtained from plots of t/q_t against t.
[b] Experimental values.

where K_{D1} and K_{D2} are distribution coefficients for dyes 1 and 2 over the same adsorbent. K_D value is calculated according to equation [4.12];

$$K_D = \frac{q_e}{C_e} \qquad [4.12]$$

In the calculation of the value, K_{D1} is assigned to the dye with higher K_D value. Therefore, the value is ≥ 1. When α is close to 1 it is suggested that the adsorbent has no selectivity over the investigated dye. However, when α is greater than 1 the adsorbent tends to selectively adsorb the target dye over the other.

Table 4.8 shows values of separation factor of MIA on acid red 1 compared with tartarzine, zincon, and sulfasalazine. The values are higher than 1 suggesting that MIA favored the selective separation of acid red 1 than the other investigated dyes. Selective adsorption of MIA toward acid red 1 could be attributed to the memory effect from the adsorption sites generated using the dyes as the template during the synthesis of the adsorbent. Tartarzine and zincon have $-SO_3^-$

groups and sulfasalazine has carboxylate group on the structure as shown in Figure 4.1. These groups can interact with the $-NH_3^+$ on the adsorbent. However, with different molecular structures compared to acid red 1 and the preformed adsorption sites, lower adsorption capacity of these dyes is expected. Moreover, pH of the solutions is also influence the adsorption of the dyes. The pK_a of acid red 1, tartrazine, zincon and sulfasalazine were found to be 0.7-1.5 (Owusu-Apenten, 2002), 9.4 (El-Sheikh and Al-Degs, 2013), 4 - 4.5 (Oehme et al., 1998), and 11 (Buoro et al., 2014), respectively. The fraction of the anionic form of the dyes would be increase when the pH of the solution is $> pK_a$. This could contribute to the larger K_D for acid red 1 compared to the other dyes.

Table 4.8 Values of separation factor of MIA on acid red 1 toward analogous dyes at pH 2.0 at 25.0 ^{o}C.[a]

Dyes	C_e (mol/L)	q_e (mol/g)	K_D	α
Acid red 1	7.3×10^{-5}	7.87×10^{-5}	1.005	-
Tartrazine	1.52×10^{-4}	5.00×10^{-6}	0.033	30.46
Zincon	1.08×10^{-4}	4.90×10^{-5}	0.453	2.22
Sulfasalazine	1.02×10^{-4}	5.50×10^{-5}	0.559	1.78

[a] The initial concentration of the dyes was 1.57×10^{-4} mol/L

4.4.2.6.2 Imprinting factor

Imprinting factor (β) is a measure of the strength of interaction of MIA towards the template molecule compared with that of the NIA. The imprinting factor (β) can be represented as equation [4.13];

$$\beta = K_{D\,(MIA)}/K_{D\,(NIA)} \qquad [4.13]$$

where $K_{D\,(MIA)}$ and $K_{D\,(NIA)}$ are the distribution coefficients of the template molecule for MIA and NIA, respectively. Higher value of β corresponds to greater difference in the interaction upon the template molecule between the two adsorbents. When β is equal to 1.0, it means that there is no difference in the adsorption character between MIA and NIA.

Table 4.9 shows data used for the calculation of the imprinting factor and the obtained value of the imprinting factor. The value of the imprinting factor is greater than 1. The prepared MIA has higher adsorption capacity than the NIA in aqueous environment, which might result from the imprinting effect. During the preparation of the imprinted adsorbent, the -NH$_2$ interacted with the -SO$_3^-$ of acid red 1 and the cavities were formed around the dye molecules. After removal of the acid red 1, the imprinted cavities and specific binding sites were formed in a predetermined orientation. However, the NIA had no such imprinted cavities and specific binding sites.

4.4.2.7 Regeneration of MIA

Reusability of MIA was evaluated by alternatively adsorbing the dye and then desorbing by soaking MIA in 1.0 M NaOH. The experiment was carried out for 3 cycles. The results are shown in Figure 4.11. The adsorption capacity of the

adsorbent is about the same suggesting that the adsorbent has good stability and could be reused.

Table 4.9 Value of imprinting factor for acid red 1 for the adsorption using MIA and NIA at pH 2.0 at 25.0 $^{\circ}$C.[a]

Adsorbents	C_e (mg/L)	q_e (mg/g)	K_D	β
MIA	42.64	36.93	0.87	-
NIA	51.68	28.32	0.54	1.61

[a] The initial concentration of the dye solution was 80 mg/L.
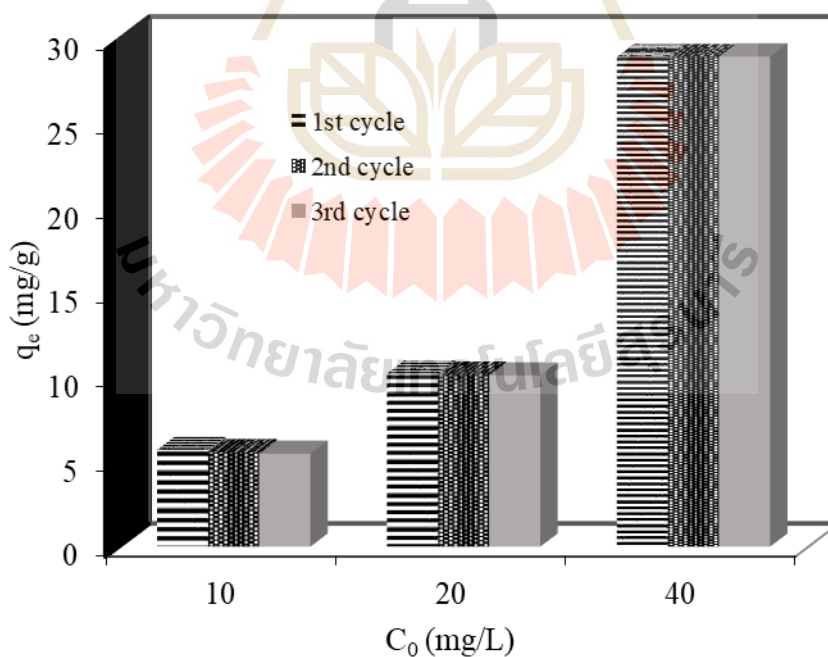
Figure 4.11 Reusability of MIA after treated with 1.0 M NaOH.

4.5 Conclusion

The mesoporous silica coated amino-silane imprinted adsorbent was successfully prepared and characterized. The adsorbent was applied in aqueous media for the adsorption of acid red 1. Equilibrium adsorption was reached in 60 min. The equilibrium adsorption data was successfully fitted to the Langmuir isotherm. The maximum adsorption capacity under the studied experimental conditions was about 37.73 mg/g at 25.0 °C. The adsorption processes were spontaneous and exothermic. After the equilibrium adsorption, the systems were in a lower state of randomness. Adsorption kinetics followed pseudo-second order model. The adsorbent was selective for acid red 1 compared with the dyes of analogous structures. The adsorbent could be used for 3 cycles with no significant decrease in their binding affinity.

4.6 References

Araghi, S, H. and Entezari, M. H. (2015). Amino-functionalized silica magnetite nanoparticles for the simultaneous removal of pollutants from aqueous solution. **Applied Surface Science**. 333: 68-77.

Buoro, R. M., Diculescu, V. C., Lopes, I. C. Serrano, S. H. P., Oliveira-Brett, A .M. (2014). Electrochemical oxidation of sulfasalazine at a glassy carbon electrode. **Electroanalysis**. 26: 924-930.

El-Hosiny, F. I., Abdel-Khalek, M. A., Selim, K. A., and Osama, I. (2017). Physicochemical study of dye removal using electro-coagulation-flotation process. **Physicochemical Problems of Mineral Processing**. 54(2): 321-333.

El-Sheikh, A. H. and Al-Degs, Y. H. (2013). Spectrophotometric determination of food dyes in soft drinks by second order multivariate calibration of the absorbance spectra-pH data matrices. **Dyes and Pigments**. 97: 330-339.

European Food Safety Authority. (2007). Opinion of the scientific panel on food additives, flavourings, processing aids and materials in contact with food. **The EFSA Journal**. 515: 1-28. Parma, Italy.

Gioia, L., Ovsejevi, K., Manta, C., Míguez, D., and Menéndez, P. (2018). Biodegradation of acid dyes by an immobilized laccase: an ecotoxicological approach. **Environmental Science Water Research & Technology**. 4: 2125-2135.

González-Vargas, C., Salazar, R., and Sirés, I. (2014). Electrochemical treatment of acid red 1 by electro-fenton and photoelectro-fenton processes. **International Journal of Electrochemical Science**. 4(4): 235-245.

Hsu, T. C. (2008). Adsorption of an acid dye onto coal fly ash. **Fuel**. 87: 3040-3045.

Jabariyan, S., and Zanjanchi, M. A. (2012). A simple and fast sonication procedure to remove surfactant templates from mesoporous MCM-41. **Ultrasonics Sonochemistry**. 19: 1087-1093.

Kayan, B., Akay, S., Kulaksız, E., Gözmen, B., and Kalderis, D. (2017). Acid Red 1 and Acid Red 114 decolorization in H_2O_2-modified subcritical water: process optimization and application on a textile wastewater. **Desalination and Water Treatment**. 59: 248-261.

Konicki, W., Sibera, D., and Narkiewicz, U. (2017). Adsorption of acid red 88 anionic dye from aqueous solution onto $ZnO/ZnMn_2O_4$ nanocomposite: equilibrium,

kinetics, and thermodynamics. **Journal of Environmental Studies**. 26(6): 1-9.

Lee, C. K., Liu, S. S., Juang, L. C., Wang, C. C., Lin, K. S., & Lyu, M. Du. (2007). Application of MCM-41 for dyes removal from wastewater. **Journal of Hazardous Materials**. 147(3): 997-1005.

Lee, J. Y., Chen, C. H., and Cheng, S. (2015). Adsorption of acid dyes by functionalized SBA-15 mesoporous silica of different pore lengths. **Journal of the Chinese Chemical Society**. 62(6): 483-494.

Leite, A. J. B., Lima, E. C., Reis, S. G., Thue, P. S., Saucier, C., Rodembusch, F. S., Dias, S. L. P., Umpierres, C. S., and Dotto, G. L. (2017). Hybrid adsorbents of tannin and APTES (3-aminopropyltriethoxysilane) and their application for the highly   efficient removal of acid red 1 dye from aqueous solutions. **Journal of Environmental Chemical Engineering**. 5(5): 4307-4318.

Liang, J., Xue, Z., Xu, J., Li, J., Zhang, H., and Yang, W. (2013). Highly efficient incorporation of amino-reactive dyes into silica particles by a multi-step approach. **Colloids and Surfaces A: Physicochemical and Engineering Aspects**. 426: 33- 38.

Oehme, I., Prattes, S., Wolfbeis, O.S., and Mohr, G. J. (1998). The effect of polymeric supports and methods of immobilization on the performance of an optical copper(II)-sensitive membrane based on the colourimetric reagent zincon. **Talanta**. 47: 595-604.

Owusu-Apenten, R, K. (2002). Food Protein Analysis. **Quantitative Effects on Processing**. Marcel Dekker, Inc., U.S., p.135.

Shan, R. R., Yan, L. G., Yang, Y. M., Yang, K., Yu, S. J., Yu, H. Q., Zhu, B. C., and Du, B. (2015). Highly efficient removal of three red dyes by adsorption onto Mg–Al-layered double hydroxide. **Journal of Industrial and Engineering Chemistry**. 21: 561-568.

Shimizu, Y., Taga, A., and Yamaoka, H. (2003). Synthesis of novel crosslinked chitosans with a higher fatty diacid diglycidyl and their adsorption abilities towards acid dyes. **Adsorption Science and Technology**. 21(5): 439-449.

Su, X., Liu, L., Zhang, Y., Liao, Q., Yu, Q., Meng, R, and Yao, J. (2017). Efficient removal of cationic and anionic dyes from aqueous solution using cellulose-g-p(AA-co-AM) bio-adsorbent. **BioResources**. 12(2): 3413-3424.

Thue, P. S., Sophia, A. C., Lima, E. C., Wamba, A. G.N., Alencar, W. S., Reis, G. S., Rodembusch, F. S., and Dias, S. L. P. (2018). Synthesis and characterization of a novel organic-inorganic hybrid clay adsorbent for the removal of acid red 1 and acid green 25 from aqueous solutions. **Journal of Cleaner Production**. 171(10): 30-44.

Tran, H. N., Lee, C. K., Vu, M. T., and Chao, H. P. (2017). Removal of copper, lead,methylene green 5, and acid red 1 by saccharide-derived spherical biochar prepared at low calcination temperatures: adsorption kinetics, isotherms, and thermodynamics. **Water Air and Soil Pollution**. 228(401): 1-16.

Vasapollo, G., Del Sole, R., Mergola, L., Lazzoi M. R., Scardino, A., Scorrano, S., and Mele, G. (2011). Molecularly imprinted polymers: present and future prospective. **International Journal of Molecular Sciences**. 12: 5908-5945.

Velez, J., Arce, R., Alburquenque, D., Gautier, J. L., Zuñiga, C., and Herrera, F. (2013). Simple steps for synthesis of silicon oxide mesoporous materials used as template. **Journal of the Chilean Chemical Society**. 58(4): 1998-2000.

Wu, Y., Zhang, M., Zhao, H., Yang, S., and Arkin, A. (2014). Functionalized mesoporous silica material and anionic dye adsorption: mcm-41 incorporated with amine groups for competitive adsorption of acid fuchsine and acid orange II. **RSC Advances**. 106(4): 61256-61267.

Yang, X., Wang, X., Liu, X., Zhang, Y., Song, W., Shu, C., Jiang, L., and Wang, C. (2013). Preparation of graphene-like iron oxide nanofilm/silica composite with enhanced adsorption and efficient photocatalytic properties. **Journal of Materials Chemistry A**. 1: 8332-8337.

Yuan, Q., Chi, Y., Yu, N., Zhao, Y., Yan, W., Li, X., and Dong, B. (2014). Amino-functionalized magnetic mesoporous microspheres with good adsorption properties. **Materials Research Bulletin**. 49: 279-284.

Zhang, C., Wang, Y., Zhou, Y., Guo, J., and Liu, Y. (2014). Silica-based surface molecular imprinting for recognition and separation of lysozymes. **Analytical Methods**. 6: 8584-8591.

CHAPTER V

PREPARATION OF NYLON/SILICA COMPOSITE ADSORBENTS FOR ADSORPTION OF ACID RED 1

5.1 Abstract

Composite materials consisting of polymer and nanoparticles are of interest due to serval advantages related to their properties. In this work, a simple procedure was used to prepare nylon/nanosilica composite to use as an adsorbent for acid red 1. Adsorbents were prepared by mixing nylon with nanosilica with or without acid red 1 added into the synthesis mixtures. Influence of hydrolysis time of nylon and mixing time of silica with nylon on the adsorption were studied. The optimum hydrolysis time and mixing time was 2 and 16 h, respectively. The obtained adsorbents were characterized by scanning electron microscopy (SEM) and Fourier transform infrared (FTIR) spectroscopy. Micrographs revealed that nanosilica particles were coated with nylon but were not totally separated from each other.

Adsorption performance of the adsorbents was evaluated in solutions containing single dye component and those containing two dyes which were acid red 1 mixed with tartrazine and acid red 1 mixed with nitroso-R. The adsorption capacity for acid red 1 of nylon/silica composite synthesized with the template was 23.4 mg/g and that of nylon/silica composite synthesized without template was 16.0 mg/g at 25.0 ºC. The adsorption in mixed dye solutions showed that the adsorbent synthesized

with the template favored the adsorption of acid red 1 over the other dye. However, the values of imprinting factor suggested that imprinting sites were not achieved.

5.2 Introduction

Adsorption is widely used to remove dyes from wastewater. Polymer- and silica-based adsorbents have been reported for acid dyes removal. nylon (polyamide) is one of synthetic polymer materials that could potentially be used as an adsorbent. nylon is typified by amide groups ($-CONH_2$) which can interact with sulfonate groups (SO_3^-) of acid dyes. However, nylon membrane has low surface area; therefore, modification of the polymer would be required to improve adsorption capacity for a target compound. One of several options is polymer/nanoparticles composite adsorbents. Nanoparticles incorporated into the polymer could enhance the porosity of the polymer composite and the nanoparticles could act as adsorbents. nylon/silica flake sub-micro composite was produced and tested for its surface mechanical properties (Chen et al., 2015). It was found that the silica nanoparticle with a uniform shape and well distribution in size have been used in different polymers as reinforcement material and could improve the properties of nylon. nylon/nanosilica composites were studied for their ability to extract some hormones in bioanalytical samples (Reyes-Gallardo et al., 2017). In this work, nylon/nanosilica composite adsorbents were synthesized, characterized, and used as adsorbents for acid red 1. Adsorption study was carried out in solutions of acid red 1, acid red 1 mixed with tartrazine, and acid red 1 mixed with nitroso-R.

5.3 Experimental

5.3.1 Chemicals

Chemicals used in this research are listed in Table 5.1

Table 5.1 Chemicals used in this research.

Chemicals	Formula	Content (%)	Suppliers
acid red 1	$C_{18}H_{13}N_3O_2(SO_3Na)_2$	60.0	Sigma-Aldrich
ammonia	NH_3	99.0	Acros Organics™
ammonium acetate	CH_3COONH_4	99.0	Sigma-Aldrich
ethanol	CH_3CH_2OH	99.9	Carlo ERBA
formic acid	$HCOOH$	95-97	Sigma-Aldrich
hydrochloric acid	HCl	37.0	Carlo ERBA
methanol	CH_3OH	99.9	Carlo ERBA
nitroso-R	$C_{10}H_5NO_2(SO_3Na)_2$	90.0	Fluka
nylon 6	$[-NH(CH_2)_5CO-]_n$	99.9	Sigma-Aldrich
tartrazine	$C_{16}H_9N_4O_3Na(SO_3Na)_2$	85.0	Sigma-Aldrich
tetraethyl orthosilicate (TEOS)	$SiC_8H_{20}O_4$	99.0	Acros Organics™

5.3.2 Preparation of Nylon/silica composite adsorbents

5.3.2.1 Preparation of silica nanoparticles

Silica nanoparticles were prepared by the Stöber method (Liang et al., 2013). 10 mL H_2O, 24 mL of 28% NH_3 and 17 mL TEOS were added into 500 mL ethanol. The reaction mixture was magnetically stirred for 12 h. At the reaction

time of 3 and 6 h, 12 mL TEOS was added dropwise into the solution. The resulting silica particles were separated by centrifugation at 3,000 rpm for 10 min. The silica particles were washed with H_2O until the pH of the washed solution was close to 7 and after that with ethanol to remove the unreacted TEOS. Finally, the silica particles were dried at 60 ^{o}C overnight.

5.3.2.2 Preparation of Nylon/silica composite adsorbent using acid red 1 as a template

nylon/silica composite adsorbent were prepared by using a method adapted from Reyes-Gallardo et al. (2017). Nylon 6 with a weight of 0.1 g was dissolved in 10 mL of concentrated formic acid. The mixture was sonicated for 2, 16, and 24 h in order to hydrolyze nylon. After that, acid red 1 with a weight of 0.0500 g was added into the mixture solution. Silica particles with a weight of 0.4 g were added. The mixture was sonicated until silica particles were well dispersed. 10 mL H_2O was added dropwise into the mixture. The reaction mixture was magnetically stirred for 4, 16, and 24 h in order to coat the Nylon onto silica particles. The resulting nylon/silica composite particles were filtered under vacuum by using a filter membrane No. 5 and Büchner flask kit. The particles were washed with acetone and methanol. The dye template was removed from the particles by washing with 1.0 M NaOH. Then the resulting powders were washed with H_2O until the pH of the washed solution was close to 7. The particles were dried at 80 ^{o}C overnight. The obtained powder, nylon/silica composite synthesized with the dye template, was denoted as NST.

5.3.2.3 Preparation of Nylon/silica composite adsorbent without acid red 1 as a template

Synthesis of nylon/silica composite adsorbent without acid red 1 as a template (NS) was done using similar procedures as that of NST. However, acid red 1 was not used in the synthesis.

5.3.3 Characterization of synthesized adsorbents

5.3.3.1 Scanning electron microscopy (SEM)

Morphology of synthesized adsorbents were analyzed by scanning electron microscopy (JEOL model JSM-6400) running with an electron beam accelerating voltage of 20 kV under vacuum pressure of 10^{-4} Pa. Adsorbents specimens were prepared by dispersing particles on carbon tape and after that were coated with gold in an ion sputtering device for 10 min at 10 mA current output. The scanning electron microscope was operated at 15 kV and a working distance of 10 mm. Areas of interest were focused and micrographs were taken.

5.3.3.2 Fourier-transform infrared spectroscopy (FTIR)

Functional groups of adsorbents were studied by Fourier-transform infrared spectroscopy (Bruker, Tensor 27) using attenuated total reflection (ATR) mode. A sample for the measurement was prepared by sprinkling particles on a sample holder. IR spectra were obtained in the wavenumber range of 400 to 4000 cm^{-1} with the resolution of 4 cm^{-1}.

5.3.4 Adsorption study

5.3.4.1 Effect of pH

Effect of pH on the adsorption of acid red 1 was investigated at pH 2.0, 7.0, and 10.0. MA adsorbent with the weight of 0.035 g was added into 35 mL of

40 mg/L dye solution contained in a 40-mL vial. The mixture solution was stirred for 60 min at 25.0 $^{\circ}$C. After that, the adsorbent was separated from the solution by centrifugation. A concentration of the dye left in the solution was determined using a UV–Vis spectrometer (CHEM4-Vis-fiber spectrometer: USB 4000, Ocean Optics). Absorbance measurement was made at 532 nm.

5.3.4.2 Adsorption of acid red 1 using SiO$_2$, Nylon, Nylon/SiO$_2$ composite, and NST as adsorbents

Adsorptions of acid red 1 was carried out with 0.035 g adsorbent in 35 mL solution contained in a 40-mL vial. The dye concentrations were 40, 80, and 120 mg/L and the pH of the solutions was controlled at 2.0. The adsorption temperature was 25 $^{\circ}$C. After 60 min of adsorption, the adsorbent was separated by centrifugation. A concentration of the dye left in the solution was determined using a UV–Vis spectrometer by measuring the absorbance at 532 nm.

5.3.4.3 Effect of hydrolysis time and mixing time

Adsorption of acid red 1 with NST was carried out with 0.035 g adsorbent in 35 mL solution contained in a 40-mL vial. The dye concentration was 40 mg/L and the pH of the solution was controlled at 2.0. The adsorption temperature was 25.0 $^{\circ}$C. After 60 min of adsorption, the adsorbent was separated by centrifugation. A concentration of the dye left in the solution was determined using a UV-Vis spectrometer by measuring the absorbance at 532 nm.

5.3.4.4 Effect of the amount of the adsorbent

Effect of the amount of the adsorbent on the adsorption of acid red 1 was investigated by varying the weight of adsorbent at 0.035, 0.1, and 0.2 g, respectively in 35 mL dye solution contained in a 40-mL vial. The dye concentration

was 40 mg/L and the pH of the solutions was controlled at 2.0. The adsorption temperature was 25 $^\circ$C. Adsorption was carried out for 60 min of adsorption, the adsorbent was separated by centrifugation. A concentration of the dye left in the solution was determined using a UV–Vis spectrometer by measuring the absorbance at 532 nm.

5.3.4.5 Effect of contact time

Adsorption study was conducted in a 40-mL vial contained with 35 mL of 40 mg/L acid red 1 and 0.035 g of an adsorbent. The pH of the dye solutions was controlled at 2.0. The temperature of solutions was controlled at 25.0 $^\circ$C. Adsorption time was varied in the range of 30 to 120 min. After a given time, adsorbent was separated from the solution by centrifugation and the dye solution was used for the absorbance measurement to determine the dye concentration.

5.3.4.6 Adsorption in mixed dyes solutions

Adsorption performance of the synthesized adsorbents was investigated in mixed dyes solutions of acid red 1 mixed with nitroso-R and acid red 1 mixed with tartrazine. The adsorption was carried out with 0.035 g adsorbent in 35 mL solution contained in a 40-mL vial. The dye concentrations were 3.93×10^{-5} and 7.85×10^{-5} mol/L and the pH of the solutions was controlled at 2.0. The adsorption temperature was 25.0 $^\circ$C. After 60 min of adsorption, the adsorbent was separated by centrifugation and the dye solutions were used for the determination of dye concentration by high performance liquid chromatography (HPLC).

A HPLC equipped with standard autosampler (G1315D) with a diode array detector (1260, Agilent Technology) was used for the determination of acid dyes. A reversed phase Zorbax SB C-18 column (4.6×250 mm, 3.5 µm) was used

for separation of acid dyes. A mobile phase consisted of 70:30 volume ratio of methanol: 5 mM ammonium acetate (pH = 2). The flow rate of the mobile phase was 0.5 mL/min. A liquid injection volume was 20 µL. A column temperature was controlled at 30 °C. The absorbance of the eluate was monitored at 254 nm.

5.3.4.7 Determination of separation factor and imprinting factor

In order to investigate the selectivity of the adsorbents toward the target dye and to compare the adsorption efficiency between the adsorbents synthesized with and without the template (NST and NS, respectively), separation factor and an imprinting factor were determined. The optimized adsorption condition for the target dye was used in this study.

To determine a separation factor, adsorption experiments were carried out with NST. Solutions of the dye template and dyes with analogous structures at the concentration of 3.93×10^{-5} and 7.85×10^{-5} mol/L with the pH of 2.0 were used in the study. Adsorption of each dye solution was done separately on the adsorbent. Similar adsorption procedures as previously described were used. The concentration of the dyes were determined by HPLC.

To determine an imprinting factor, adsorption of acid red 1 on NST and NS were conducted at the dyes concentration of 3.93×10^{-5} and 7.85×10^{-5} mol/L and the pH of solutions was fixed at 2.0. The adsorption was done at 25 °C for 60 min. The concentration of the dye left in the solution was determined by HPLC.

5.4 Results and discussion

5.4.1 Characterization of synthesized adsorbents

5.4.1.1 SEM

Morphologies of the synthesized adsorbents are shown in Figure 5.1. Silica particles were coated with Nylon. The material appeared like bulk particles with rough surface. The silica particles were dispersed in nylon through hydrogen bonding between silanol groups (-OH) of silica and amide groups of nylon (Ren et al., 2009).
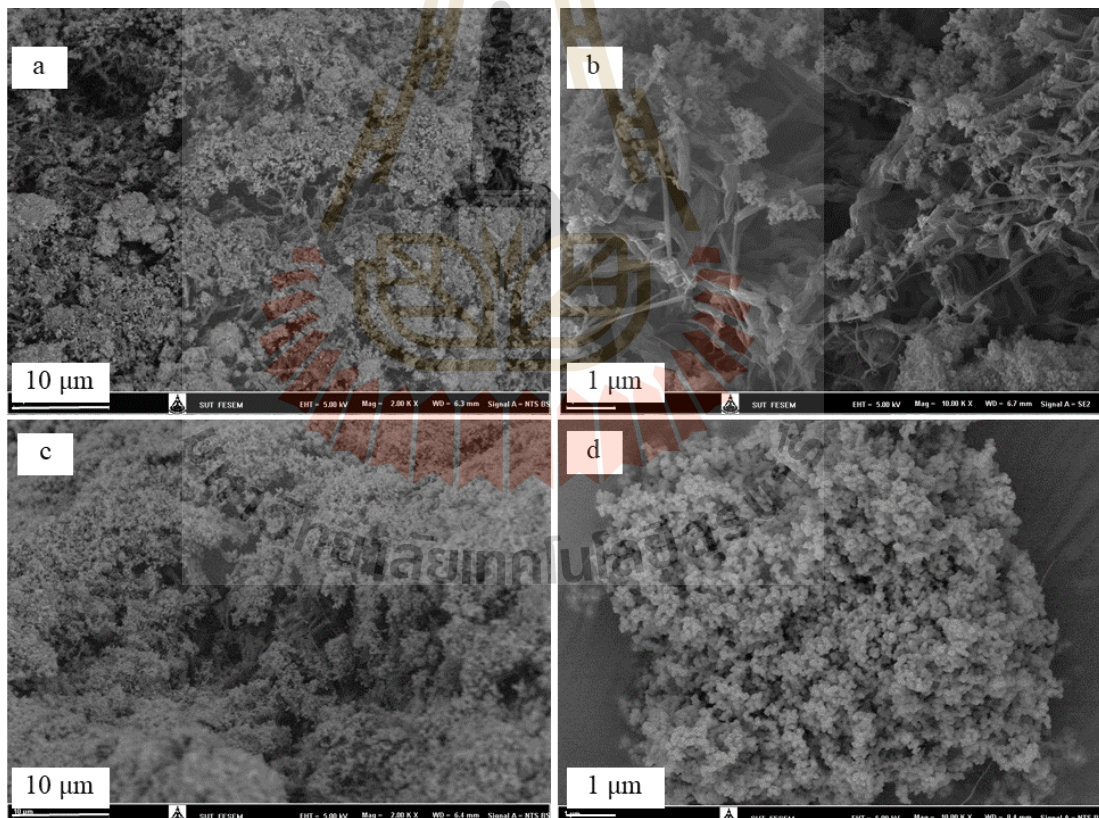
Figure 5.1 SEM images of NST (a-b) and NS (c-d).

5.4.1.2 Adsorbents characterization by FTIR spectroscopy

The adsorbents were characterized by FTIR to identify functional groups on their structures. The measurements in the wavenumber range of 400-4,000 cm^{-1} with the resolution of 4 cm^{-1} were carried out. FTIR spectra of NST and NS are shown in Figure 5.2. In the SNT spectrum, a strong absorbing region at 983-1,271 cm^{-1} were assigned to Si-O-H and Si-O-Si bonds. Peak at around 1,637 cm^{-1} represent the stretching C=O of the amide group. Furthermore, another band around 1,539 cm^{-1} is observed, which can be assigned to the N-H deformation band of the amide (Reyes-Gallardo et al., 2017).

Similar FTIR peaks were also observed in the NS adsorbent. The peaks of NS were shifted slightly compared to those of NST. This could be attributed to the dye template used in the synthesis of NST, but not in the synthesis of NS.

5.4.2 Adsorption study

5.4.2.1 Effect of pH

The effect of pH on adsorption capacity of acid red 1 onto NST was investigated at pH 2.0, 7.0, and 10.0 at a fixed dye concentration of 20 mg/L at 25.0 ℃. The adsorption time was 60 min. The adsorption capacity was calculated according to equation [5.1];

$$q_e = \frac{V(C_0 - C_e)}{m} \qquad [5.1]$$

where q_e is the equilibrium adsorption capacity (mg/g), V is the volume of the solution (L), C_0 and C_e (mg/L) are the initial and equilibrium concentrations of the acid red 1 in a solution, respectively, and m is the adsorbent mass (g).
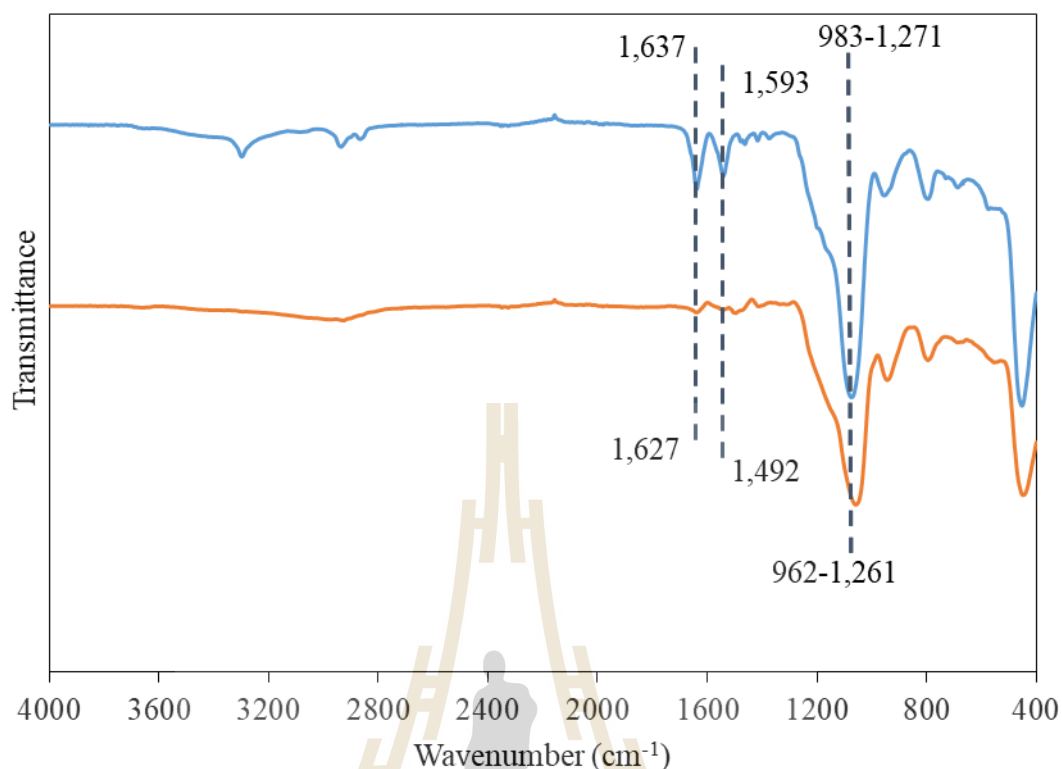
Figure 5.2 FTIR spectra of NST and NS.

Acid red 1 is an anionic azo dye that contains two sulfonic acid groups [R-(SO$_3$Na)$_2$]. In aqueous solutions, acid red 1 can be dissociated to sulfonate anion [R-(SO$_3^-$)$_2$] which can interact with the protonated amide groups, -NH$_3^+$, on the adsorbent. The pH of the solutions has strong influence on the surface charge of the adsorbent and the anionic form of the dye. In Figure 5.3, the optimum adsorption capacity was observed at pH 2.0. The adsorption tended to increase when the pH of the solutions was decreased from 10.0 to 2.0. This can be explained by pH at point of zero charge (pH$_{pzc}$) which represents the surface charge behavior of the adsorbents. NST consists of Nylon and SiO$_2$ and mesoporous silica. The pH$_{pzc}$ of on silica was about 7.34 (Yang et al., 2013). Therefore, adsorption of anionic dyes are favored at

pH<pH$_{pzc}$ of the adsorbent, where the surface charge of the adsorbent is positive (Konicki et al., 2017).
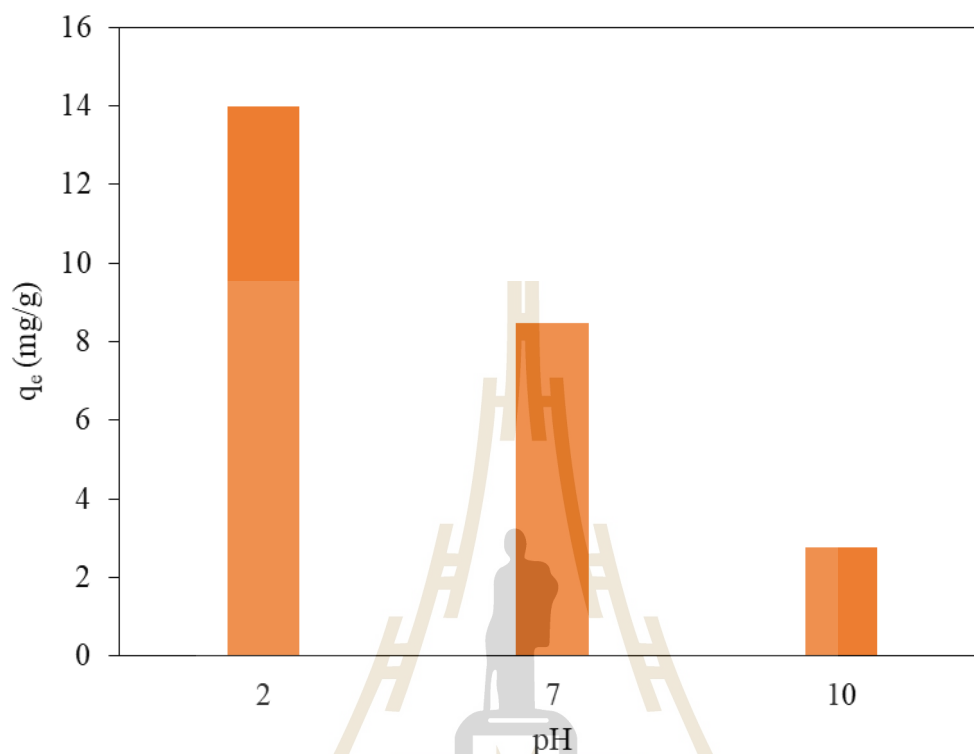
Figure 5.3 Influence of pH on the adsorption capacity of NST for acid red 1.

 5.4.2.2 Adsorption of acid red 1 on SiO$_2$, Nylon, Nylon/SiO$_2$ composite, and NST as adsorbents

 Figure 5.4 shows the adsorption capacity of the studied adsorbents. It was found that the adsorption capacity of nylon/SiO$_2$ composite and NST toward acid red 1 were higher than that of SiO$_2$ and nylon alone. For nylon/SiO$_2$ composite, this could be due to that SiO$_2$ particles enhanced the surface area of nylon to increase the adsorption sites. For NST, this could be due to the preformed sites of the dye and the adsorbent was retained after the synthesis.
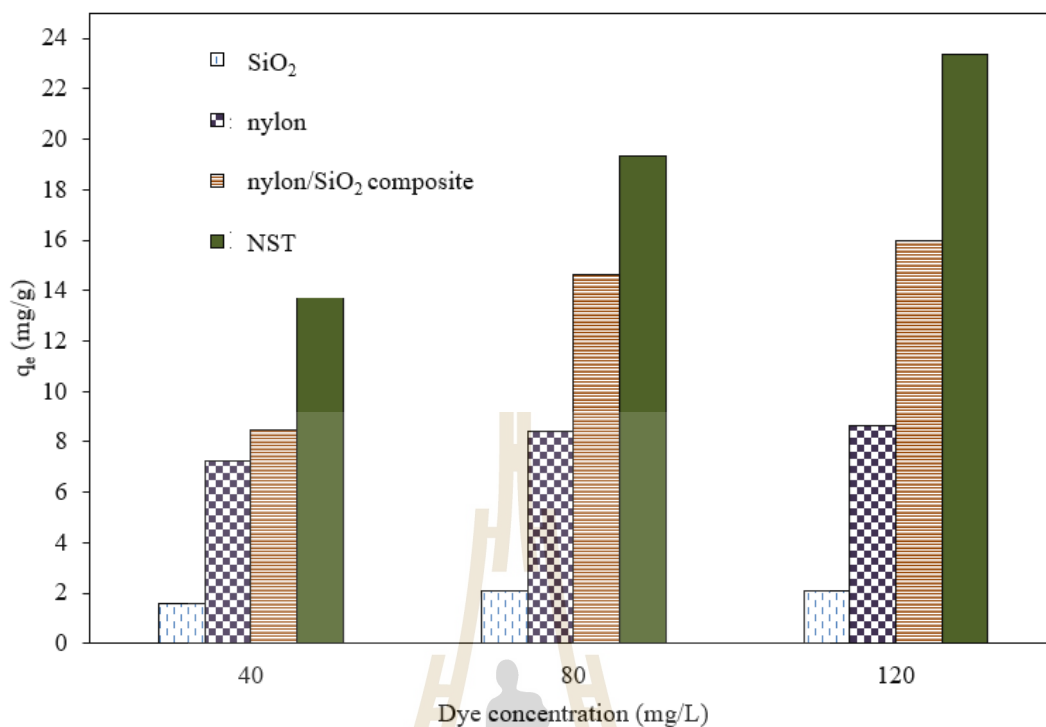
Figure 5.4 Adsorption capacity for acid red 1 by using SiO_2, nylon, nylon/SiO_2 composite, and NST.

5.4.2.3 Effect of hydrolysis time and mixing time

Nylon was hydrolyzed in formic acid at 2, 16, and 24 h and the derived adsorbents at different time were used in the adsorption of acid red 1. Hydrolysis of nylon in formic acid can break the amide bond to form NH_3^+ groups which is responsible for the dye adsorption.

The results are shown in Figure 5.5. It was found that the adsorption capacity was not changed significantly with different hydrolysis time. Therefore, the optimum hydrolysis time at 2 h was used in further synthesis of the adsorbents. Mixing time was varied at 4, 16, and 24 h in order to coat the nylon onto SiO_2 particles.
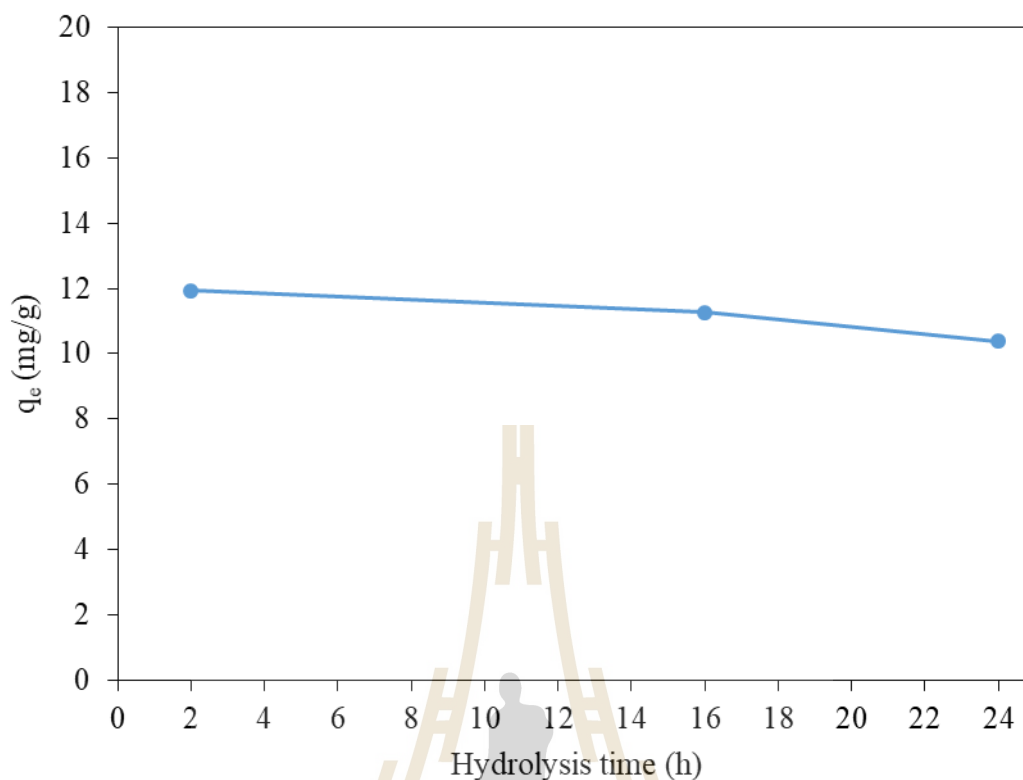
Figure 5.5 Effect of hydrolysis time on adsorption capacity.

Figure 5.6 shows mixing time on the adsorption of acid red 1 onto NST. It was found that the adsorption capacities are about the same at different mixing time. However, mixing time at 16 h was chosen for further synthesis in order to obtain well coated particles.

5.4.2.4 Effect of the amount of the adsorbent

Effect of the amount of the adsorbent on the adsorption of acid red 1 was investigated by varying weight of adsorbent at 0.035, 0.1, and 0.2 g, respectively in 35 mL dye solution contained in a 40-mL vial. The dye concentration was 40 mg/L and the pH of the solutions was controlled at 2.0. The adsorption temperature was 25.0 $^{\circ}$C. Adsorption was carried out for 60 min.
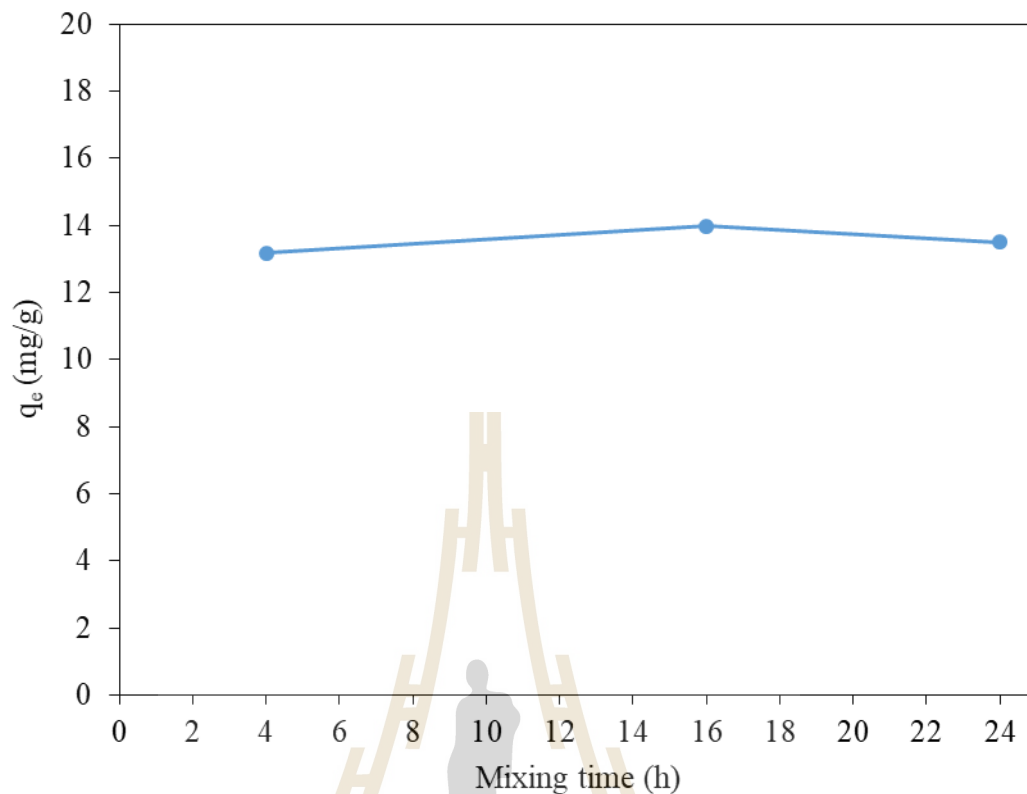
Figure 5.6 Effect of mixing time on adsorpotion capacity.

In general, when the amount of the adsorbent increases, more adsorption would be expected. Increasing the adsorbent weight resulting in increased surface area and adsorption sites. In addition, larger amount of the adsorbent in solutions of fixed dyes concentration resulting in higher % removal as shown in Figure 5.7. However, larger amount of adsorbent in solutions of fixed dyes concentration, more dye was removed from the solution. This leads to the decrease in adsorption capacity. Therefore, weight of adsorbent at 0.035 g was chosen for further adsorption study.
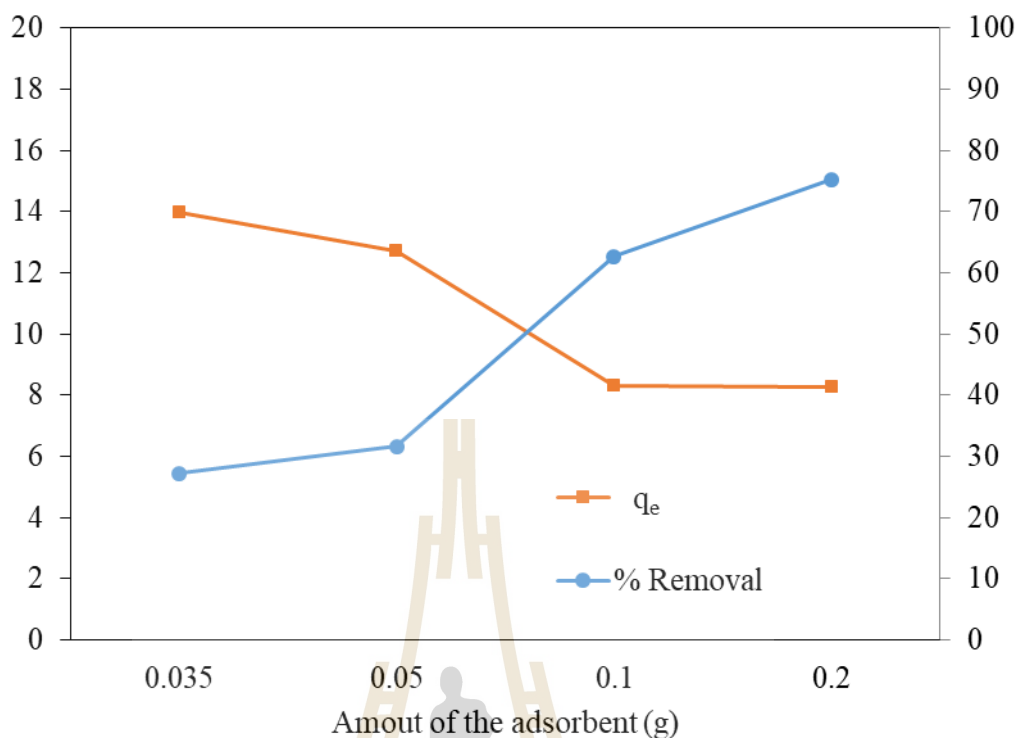
Figure 5.7 Effect of amount of adsorbent on the adsorption of acid red 1.

5.4.2.5 Effect of contact time

Effect of contact time on the adsorption capacity of the adsorbent was investigated. The adsorption was carried out at 25.0 ℃ with the initial dye concentration of 40 mg/L, the pH of the solution of 2.0, and the adsorbent weight of 0.035 g. Figure 5.8 shows the time profile adsorption of acid red 1 onto NST. The adsorption increased with time and reach the equilibrium in 60 min. Therefore, adsorption time at 60 min was selected for further study with NST.

5.4.2.6 Study of adsorption in mixed dye solutions

Adsorption in mixed dye solutions was studied using HPLC for the determination of dyes concentration. Figure 5.9 shows chromatograms of dyes used in
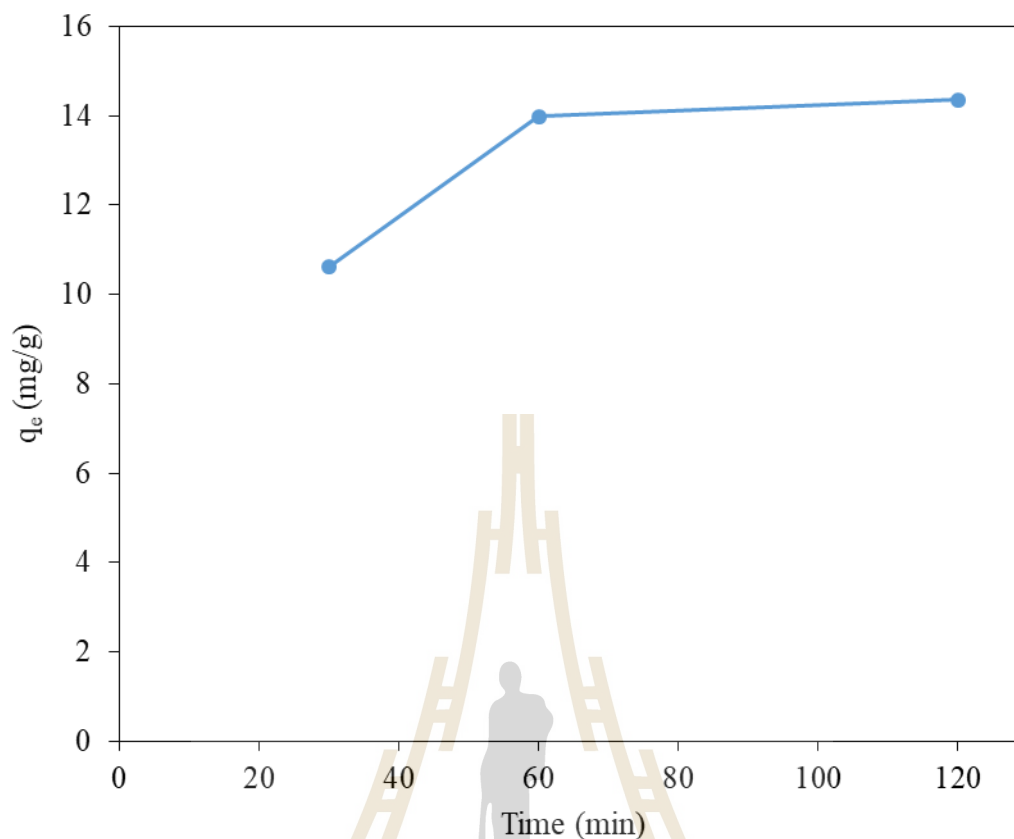
Figure 5.8 Time profile adsorption of acid red 1 onto NST.

the study. The retention times of nitroso-R, tartrazine, and acid red 1 were 4.1, 4.2, and 7.4 min, respectively. Figure 5.10 (a) and (b) show chromatograms of a solution of tartrazine mixed with acid red 1 and a solution of nitroso-R mixed with acid red 1, respectively. Two peaks of two dyes in the solutions were well resolved and the retention time of each dye was about the same as that in the solutions with only one dye. This allows simultaneous determination of the dyes concentration in the adsorption of mixed dyes solutions.
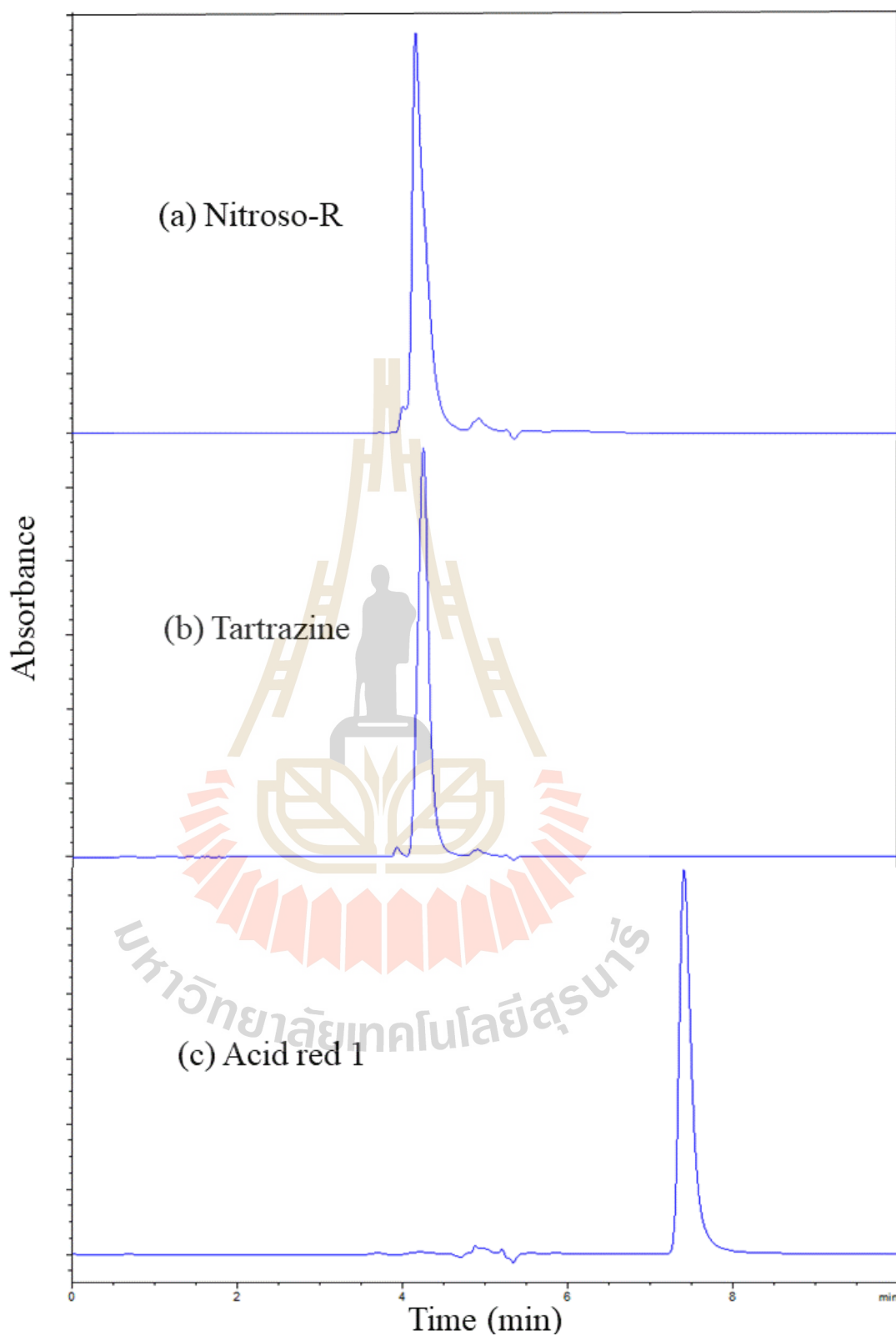
Figure 5.9 Chromatograms of 5.89 $\times 10^{-5}$ M nitroso-R (a), tartrazine (b), and acid red

1 (c).
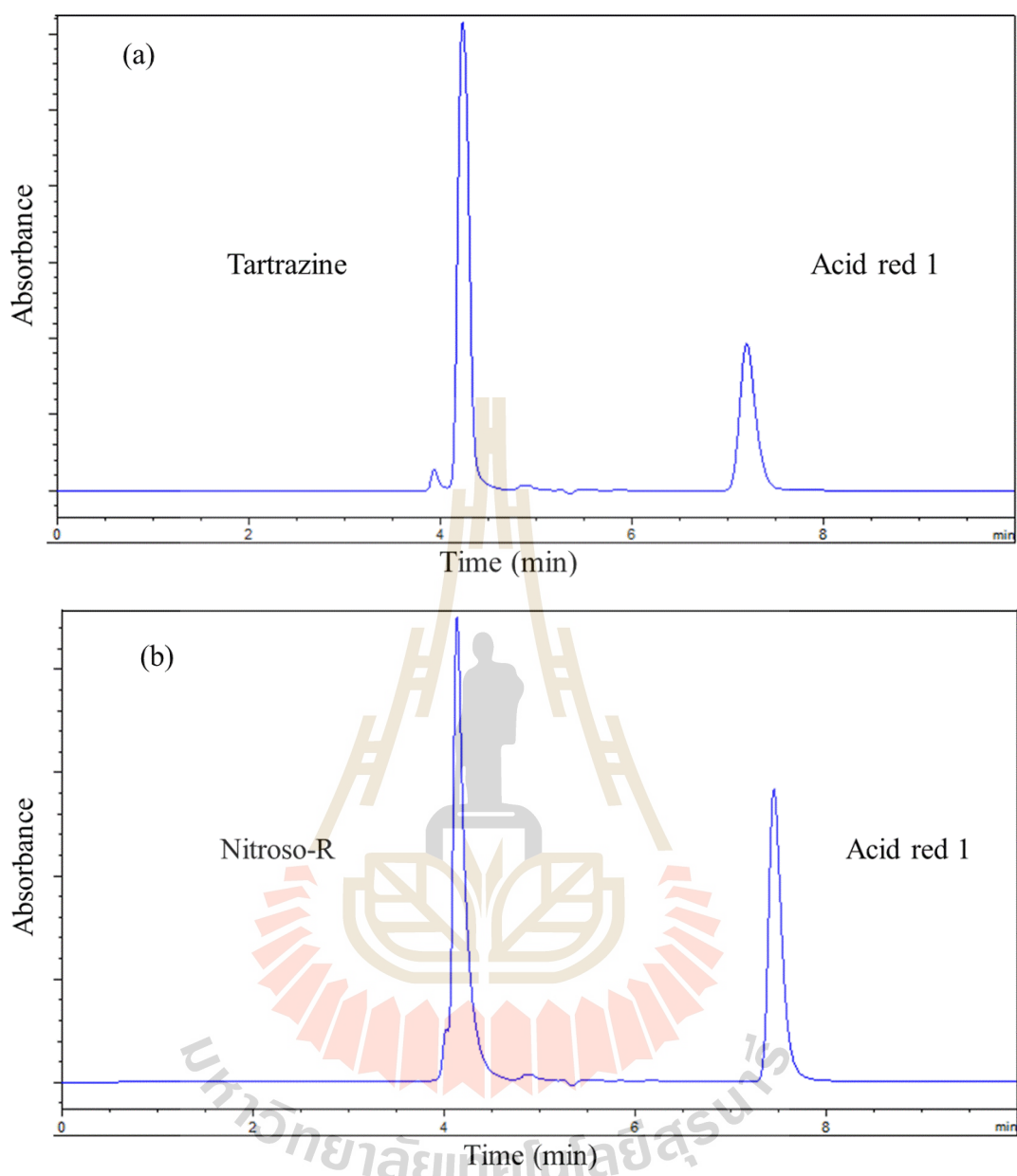
Figure 5.10 Chromatograms of a solution of tartrazine mixed with acid red 1 (a) and a solution of nitroso-R mixed with acid red 1 (b). The concentration of the dyes in the solution was 5.89×10^{-5} M.

The concentration of dye after adsorption was calculated from a calibration graph obtained from peak area of the dye in the chromatograms. The adsorption capacity was calculated according to equation [5.1].

Separation factor (α) is a measure of the strength of interaction of NST towards the template molecule compared to another molecule. It is calculated using by equation [5.2];

$$\alpha = K_{D1}/ K_{D2} \qquad\qquad [5.2]$$

where K_{D1} and K_{D2} are distribution coefficients for dyes 1 and 2 over the same adsorbent. K_D value is calculated according to equation [5.3];

$$K_D = \frac{q_e}{C_e} \qquad\qquad [5.3]$$

In the calculation of the α value, K_{D1} is assigned to the dye with higher K_D value. Therefore, the α value is ≥ 1. When α is close to 1 it is suggested that the adsorbent has no selectivity over investigated dyes. However, when α is greater than 1 the adsorbent tents to selectively adsorb the target dye over the other.

Imprinting factor (β) is a measure of the strength of interaction of NST towards the template molecule compared with that of the NS. The imprinting factor (β) can be represented as equation [5.4];

$$\beta = K_{D\,(NST)}/K_{D\,(NS)} \qquad\qquad [5.4]$$

where $K_{D\,(NST)}$ and $K_{D\,(NS)}$ are the distribution coefficients of the template molecule for NST and NS, respectively. Higher value of β corresponds to greater difference in the interaction upon the template molecule between the two adsorbents. When β is equal to 1.0, it means that there is no difference in the adsorption character between NST and NS.

Table 5.2 and Table 5.3 show parameters derived from the study using NST and NS for the adsorption in solutions contained either single dye or two dyes with the same concentration. For NST, the trend in the adsorption capacity is in the following order; acid red 1 > tartrazine > nitroso-R for both studies in the solutions with one and two dyes. NST could adsorb both dyes in the mixed dye solutions, but it appears to favorably adsorb acid red 1 as suggested by $\alpha > 1$. However, when considering β values which compared the adsorption of the same dye over NST and NS, β is < 1. This indicates that the imprinting process was not succeeded or randomly occurred.
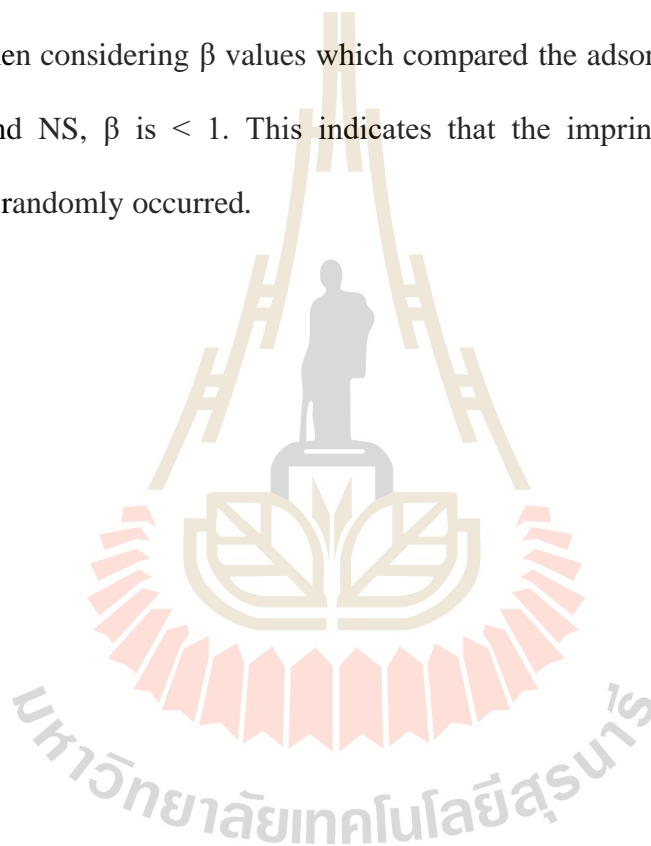
Table 5.2 Adsorption study using NST and NS in solutions with single dye or two dyes at the same concentration of 3.93×10^{-5} mol/L.

Adsorbents	dyes	C_e (mol/L)	q_e (mol/g)	K_D	α	β
NST	acid red 1 (S)	2.95×10^{-5}	9.21×10^{-6}	0.31	-	-
	tartrazine (S)	3.48×10^{-5}	4.49×10^{-6}	0.13	2.38	-
	nitroso-R (S)	3.52×10^{-5}	3.81×10^{-6}	0.11	2.82	-
	acid red 1 (A+T)	3.10×10^{-5}	8.92×10^{-6}	0.29	-	-
	tartrazine (A+T)	3.47×10^{-5}	5.15×10^{-6}	0.15	1.93	-
	acid red 1 (A+N)	2.56×10^{-5}	1.34×10^{-5}	0.52	-	-
	nitroso-R (A+N)	2.90×10^{-5}	1.02×10^{-5}	0.35	1.49	-
NS	acid red 1 (S)	2.86×10^{-5}	1.10×10^{-5}	0.39	-	0.79
	tartrazine (S)	3.37×10^{-5}	5.92×10^{-6}	0.18	-	0.72
	nitroso-R (S)	3.58×10^{-5}	3.83×10^{-6}	0.11	-	1.00
	acid red 1 (A+T)	2.51×10^{-5}	1.37×10^{-5}	0.55	-	0.53
	tartrazine (A+T)	2.89×10^{-5}	1.01×10^{-5}	0.35	-	0.43
	acid red 1 (A+N)	2.30×10^{-5}	1.65×10^{-5}	0.72	-	0.72
	nitroso-R (A+N)	2.92×10^{-5}	9.96×10^{-6}	0.34	-	1.03

S: The solutions contained one dye.
A+T: The solution contained acid red 1 and tratrazine.
A+N: The solution contained acid red 1 and nitroso-R.

Table 5.3 Adsorption study using NST and NS in solutions with single dye or two dyes at the same concentration of 7.85×10^{-5} mol/L.

Adsorbents	dyes	C_e (mol/L)	q_e (mol/g)	K_D	α	β
NST	acid red 1 (S)	6.16×10^{-5}	1.65×10^{-5}	0.27	-	-
	tartrazine (S)	7.02×10^{-5}	8.16×10^{-6}	0.12	2.25	-
	nitroso-R (S)	7.29×10^{-5}	5.61×10^{-6}	0.08	3.38	-
	acid red 1 (A+T)	6.78×10^{-5}	1.36×10^{-5}	0.20	-	-
	tartrazine (A+T)	9.62×10^{-5}	9.65×10^{-6}	0.10	2.00	-
	acid red 1 (A+N)	6.84×10^{-5}	1.01×10^{-5}	0.19	-	-
	nitroso-R (A+N)	6.54×10^{-5}	1.33×10^{-5}	0.20	0.95	-
NS	acid red 1 (S)	5.52×10^{-5}	2.30×10^{-5}	0.42	-	0.64
	tartrazine (S)	7.06×10^{-5}	8.24×10^{-6}	0.12	-	1.00
	nitroso-R (S)	7.28×10^{-5}	5.68×10^{-6}	0.08	-	1.00
	acid red 1 (A+T)	6.12×10^{-5}	1.75×10^{-5}	0.27	-	0.74
	tartrazine (A+T)	6.42×10^{-5}	1.42×10^{-5}	0.22	-	0.45
	acid red 1 (A+N)	6.04×10^{-5}	1.83×10^{-5}	0.30	-	0.67
	nitroso-R (A+N)	6.27×10^{-5}	1.65×10^{-5}	0.26	-	0.77

S: The solutions contained one dye.
A+T: The solution contained acid red 1 and tratrazine.
A+N: The solution contained acid red 1 and nitroso-R.

5.5 Conclusion

The nylon/SiO$_2$ composite adsorbents were prepared and characterized. The composite of nylon and nanosilica enhanced high adsorption sites and increase in adsorption capacity for acid red 1. The adsorbent was used in aqueous media for adsorption of acid red 1. Equilibrium adsorption was reached in 60 min. Adsorbents was applied in the removal of dye solutions containing single dye component and those containing two dyes. The adsorption capacity for acid red 1 of nylon/silica composite synthesized with the template was 23.37 mg/g and that of nylon/silica composite synthesized without template was 15.97 mg/g at 25.0 $^{\circ}$C. For nylon/silica composite synthesized with the template, the trend in the adsorption capacity is in the following order; acid red 1 > tartrazine > nitroso-R for both studies in the solutions with one and two dyes. The adsorption in mixed dye solutions showed that the adsorbent synthesized with the template favored the adsorption of acid red 1 over the other dye as suggested by $\alpha > 1$. However, the values of imprinting factor suggested that imprinting sites were not achieved as suggested by β is < 1. This indicates that the imprinting process was not succeeded or randomly occurred.

5.6 References

Chen, J., Beake, B. D., Bell, G. A., Tait, Y., and Gao, F. (2015). Probing polymer chain constraint and synergistic effects in Nylon 6-clay nanocomposites and Nylon 6-silica flake sub-micro composites with nanomechanics. **Nanocomposites**. 1(4): 185-194.

European Food Safety Authority. (2007). Opinion of the scientific panel on food additives, flavourings, processing aids and materials in contact with food. **The EFSA Journal**. 515: 1-28. Parma, Italy.

González-Vargas, C., Salazar, R., and Sirés, I. (2014). Electrochemical treatment of acid red 1 by electro-fenton and photoelectro-fenton processes. **International Journal of Electrochemical Science**. 4(4): 235-245.

Konicki, W., Sibera, D., and Narkiewicz, U. (2017). Adsorption of acid red 88 anionic dye from aqueous solution onto $ZnO/ZnMn_2O_4$ nanocomposite: equilibrium, kinetics, and thermodynamics. **Journal of Environmental Studies**. 26(6): 1-9.

Liang, J., Xue, Z., Xu, J., Li, J., Zhang, H., and Yanga, W. (2013). Highly efficient incorporation of amino-reactive dyes into silica particles by a multi-step approach. **Colloids and Surfaces A: Physicochemical and Engineering Aspects**. 426: 33-38.

Ren, J., Wang, J., Wang, H., Zhang, J., and Yang, S. (2009). Study on the morphological and mechanical properties of Nylon 6/abs/nano-SiO_2 composites. **Journal of Macromolecular Science, Part B: Physics**. 48: 1069-1080.

Reyes-Gallardo, E. M., Lucena, R. and Cardenas, S. (2017). Silica nanoparticles-Nylon 6 composites: synthesis, characterization and potential use as sorbent. **RSC Advances**. 7: 2308-2314.

Salaskar, N. R., and Sahasrabudhe, A. S. (2003). Development of shades on cellulosic substrates with trichromatic reactive dyes using CCM technique. **The Bombay Textile Research Association. BTRA**. 33: 19-26.

Thomas, S., Sreekanth, R., Sijumon, V. A., Aravind, U. K., and Aravindakumar, C. T. (2014). Oxidative degradation of acid red 1 in aqueous medium. **Chemical Engineering Journal**. 244: 473-482.

Villa, A. F. and Conso, F. (2004). Aromatic amines. **EMC - Toxicologie-Pathologie**. 1: 161-177.

Wang, G. X., Liu, P., Zhang, W., Zhen, Zh. Ch., Wang, X. W., Lu, B., Wang, P. L., and Ji, J. H. (2018). Preparation and characterization of novel PA6/SiO$_2$ composite microsphere applied for selective laser sintering. **eXPRESS Polymer Letters**. 12(1): 13-23.

Yang, X., Wang, X., Liu, X., Zhang, Y., Song, W., Shu, C., Jiang, L., and Wang, C. (2013). Preparation of graphene-like iron oxide nanofilm/silica composite with enhanced adsorption and efficient photocatalytic properties. **Journal of Materials Chemistry A**. 1: 8332-8337.

Yang, X., You, X., Zhang, B., Guo, C., and Yu, C. (2017). Preparation of magnetic imprinted graphene oxide composite for catalytic degradation of Congo red under dark ambient condition. **Water Science and Technology**. 76(7): 1676- 1686.

Zhao, K., Feng, L., Lin, H., Fu, Y., Lin, B., Cui, W., Li, S., and Wei, J. (2014). Adsorption and photocatalytic degradation of methyl orange imprinted composite membranes using TiO$_2$/calcium alginate hydrogel as matrix. **Catalysis Today**. 236:127-134.

CHAPTER VI

CONCLUSIONS

In this thesis, various adsorbents based on silica and Nylon/silica composite were synthesized and investigated in the adsorption of acid red 1 in aqueous solutions. Amino-functionalized mesoporous silica adsorbent was synthesized and characterized. 3-aminopropyltriethoxysilane functionalized onto mesoporous silica provided adsorption sites and enhanced adsorption capacity for acid red 1 compared to the unmodified mesoporous silica. The equilibrium adsorption data was successfully fitted to the Langmuir and Freundlich isotherms. The adsorption processes were spontaneous and endothermic. After the equilibrium adsorption, the systems were in a higher state of randomness. Adsorption kinetics followed pseudo-second order model. The maximum adsorption capacity was 163.93 mg/g. Although, the adsorbent provided high adsorption capacity, further investigation on selective adsorption of the target dye is recommended.

One of the methods to achieve selective adsorption is to use molecularly imprinted adsorbents. In this research, amino-functionalized mesoporous silica-based molecularly imprinted adsorbent was synthesized and characterized. The maximum adsorption capacity of the adsorbent was 37.73 mg/g. The adsorbent selectively adsorbed acid red 1 over the dyes of analogous structures. The adsorbent could be reused for 3 cycles with no significant decrease in their binding affinity. The equilibrium adsorption data was successfully fitted to the Langmuir isotherm. The

adsorption processes were spontaneous and exothermic. After the equilibrium adsorption, the systems were in a lower state of randomness. Adsorption kinetics followed pseudo-second order model.

The Nylon/Silica composite adsorbents were prepared and characterized. The composite of Nylon and nanosilica enhanced adsorption sites and adsorption capacity for acid red 1. The adsorbent was used in aqueous media for adsorption of acid red 1. The adsorption capacity for acid red 1 of Nylon/silica composite synthesized with the template was 23.37 mg/g and that of Nylon/silica composite synthesized without the template was 15.97 mg/g. For Nylon/silica composite synthesized with the template, the trend in the adsorption capacity is in the following order; acid red 1 > tartrazine > nitroso-R for both studies in the solutions with one and two dyes. The adsorption in mixed dye solutions showed that the adsorbent synthesized with the template favored the adsorption of acid red 1 over the other dye as suggested by $\alpha > 1$. However, the formation of imprinting sites on the adsorbent synthesized with the template was not successful. To improve adsorption capacity and selectivity toward the target dye, further study could be done on molecularly imprinted individually polymer-coated silica
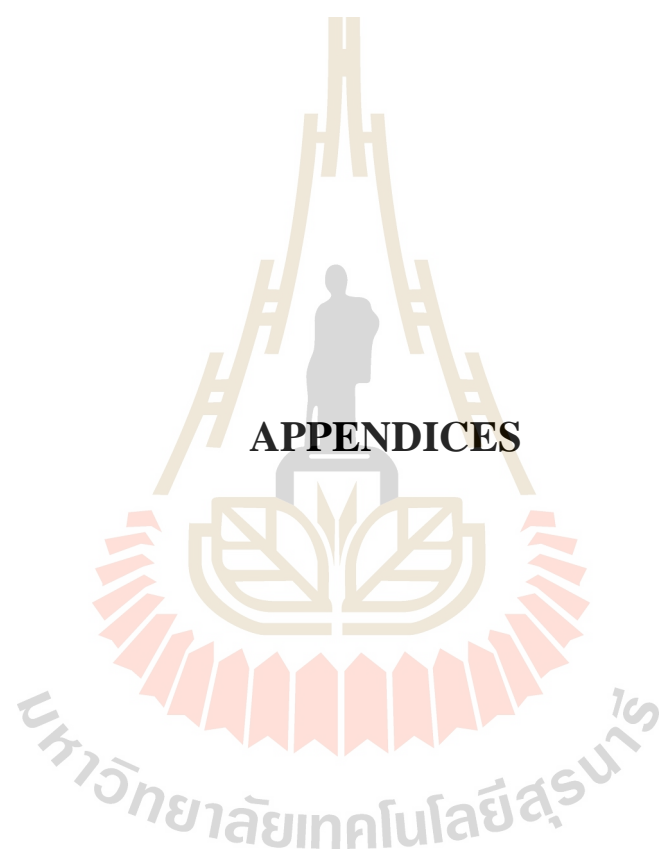
APPENDICES

APPENDIX A

K_D VALUES FOR THE ADSORPTION OF ACID RED 1

USING AMINO-MESO -SILICA

K_D can be calculated from the following equation;

$$K_D = \frac{q_e}{C_e}$$

where q_e is the equilibrium adsorption capacity (mg/g) and C_e (mg/L) is the equilibrium concentration of the acid red 1 in a solution.

Table A-1 Adsorption parameters for the adsorption of acid red 1 using NH_2-meso-

SiO_2 at 25.0 °C.

C_0 (mg/L)	C_e (mg/L)	q_e (mg/g)	K_D	ln K_D
10	1.95	8.24	4.21	1.43
20	2.97	17.17	5.77	1.75
40	4.15	36.25	8.71	2.16
80	11.54	65.19	5.64	1.73
120	17.22	97.21	5.64	1.73
160	22.66	125.9	5.55	1.71
180	51.71	128.2	2.48	0.90
200	70.63	132.9	1.88	0.63
220	82.72	137.2	1.65	0.50
260	118.9	134.1	1.12	0.12

Table A-2 Adsorption parameters for the adsorption of acid red 1 using NH_2-meso-

SiO_2 at 35.0 °C.

C_0 (mg/L)	C_e (mg/L)	q_e (mg/g)	K_D	ln K_D
10	1.97	7.63	3.87	1.35
20	3.29	16.97	5.15	1.64
40	6.10	34.59	5.66	1.73
80	11.65	70.46	6.04	1.79
120	17.01	104.1	6.12	1.81
160	23.47	137.7	5.86	1.76
180	27.91	148.6	5.32	1.67
200	48.45	152.4	3.14	1.14
220	67.52	153.3	2.27	0.82
260	103.8	148.3	1.42	0.35

Table A-3 Adsorption parameters for the adsorption of acid red 1 using NH_2-meso-

SiO_2 at 45.0 °C.

C_0 (mg/L)	C_e (mg/L)	q_e (mg/g)	K_D	ln K_D
10	1.01	8.79	8.69	2.16
20	1.13	19.25	16.98	2.83
40	1.33	38.39	28.83	3.36
80	3.30	76.91	23.25	3.14
120	4.90	116.9	23.85	3.17
160	4.94	150.7	30.46	3.41
180	20.79	164.3	7.90	2.06
200	27.78	165.5	5.96	1.78
220	61.06	167.0	2.73	1.00
260	85.30	172.9	2.02	0.70

APPENDIX B

K_D VALUES FOR THE ADSORPTION OF ACID RED 1 USING AMINO-FUNCTIONALIZED MESOPOROUS SILICA-BASED MOLECULARLY IMPRINTED ADSORBENT

Table B-1 Adsorption parameters for the adsorption of acid red 1 using amino-functionalized mesoporous silica-based molecularly imprinted adsorbent at 25.0 $^{\circ}$C.

C_0 (mg/L)	C_e (mg/L)	q_e (mg/g)	K_D	$\ln K_D$
10	0.22	9.76	43.64	3.77
20	0.33	18.47	54.52	3.99
40	3.13	38.00	12.12	2.49

Table B-2 Adsorption parameters for the adsorption of acid red 1 using amino-functionalized mesoporous silica-based molecularly imprinted adsorbent at 35.0 °C.

C_0 (mg/L)	C_e (mg/L)	q_e (mg/g)	K_D	$\ln K_D$
10	0.075	10.24	135.4	4.90
20	0.19	20.00	104.8	4.65
40	17.16	23.20	1.35	0.30

Table B-3 Adsorption parameters for the adsorption of acid red 1 using amino-functionalized mesoporous silica-based molecularly imprinted adsorbent at 45.0 °C.

C_0 (mg/L)	C_e (mg/L)	q_e (mg/g)	K_D	$\ln K_D$
10	0.37	9.23	24.83	3.21
20	2.60	16.95	6.49	1.87
40	21.21	17.17	0.80	-0.21

CURRICULUM VITAE

Name   Kanlayanee Kajsanthia

Place of birth Nakhon Ratchasima, Thailand

Education:

2005-2008   B. Sc. Chemistry

                    Mahasarakham University,   Mahasarakham, Thailand

2009-2012   M. Sc. Chemistry

                    Suranaree University of Technology, Nakhon Ratchasima,

                    Thailand

2013-Present   Ph.D. candidate (Chemistry)

                    Suranaree University of Technology, Nakhon Ratchasima,

                    Thailand

Scholarship

2005-Present   Science Achievement Scholarship of Thailand (SAST, Ministry

                    of Education Thailand)

Publications

Narachai, B., **Kajsanthia, K**., Osakoo, N., Wittayakun, J., and Prayoonpokarach, S. (2018). Adsorption of oleic acid using MCM-41synthesized from rice husk silica. **Suranaree Journal of Science and Technology**. 25(1):37-48.